

5-2016

## Regulation Of The Escrt Function Of Alix

Sheng Sun

Follow this and additional works at: [https://digitalcommons.library.tmc.edu/utgsbs\\_dissertations](https://digitalcommons.library.tmc.edu/utgsbs_dissertations)



Part of the [Life Sciences Commons](#), and the [Medicine and Health Sciences Commons](#)

---

### Recommended Citation

Sun, Sheng, "Regulation Of The Escrt Function Of Alix" (2016). *Dissertations and Theses (Open Access)*. 656.

[https://digitalcommons.library.tmc.edu/utgsbs\\_dissertations/656](https://digitalcommons.library.tmc.edu/utgsbs_dissertations/656)

This Dissertation (PhD) is brought to you for free and open access by the MD Anderson UTHealth Houston Graduate School at DigitalCommons@TMC. It has been accepted for inclusion in Dissertations and Theses (Open Access) by an authorized administrator of DigitalCommons@TMC. For more information, please contact [digcommons@library.tmc.edu](mailto:digcommons@library.tmc.edu).

# REGULATION OF THE ESCRT FUNCTION OF ALIX

by

Sheng Sun, M.S.

APPROVED:

---

Jian Kuang, Ph.D.  
Advisory Professor

---

Gary E. Gallick, Ph.D.

---

Sue-Hwa Lin, Ph.D.

---

Pierre D. McCrea, Ph.D.

---

Zahid H. Siddik, Ph.D.

---

APPROVED:

---

Dean, The University of Texas  
Graduate School of Biomedical Sciences at Houston

# REGULATION OF THE ESCRT FUNCTION OF ALIX

A

DISSERTATION

Presented to the Faculty of

The University of Texas

Health Science Center at Houston

and

The University of Texas

MD Anderson Cancer Center

Graduate School of Biomedical Sciences

in Partial Fulfillment

of the Requirements

for the Degree of

DOCTOR OF PHILOSOPHY

by

Sheng Sun, M.S.

Houston, Texas

May, 2016

## **DEDICATION**

To my grandmother, who was a tremendous source of will power of the family and  
always supported me.

## **ACKNOWLEDGEMENTS**

I would like to thank my advisor, Dr. Jian Kuang for offering me the great opportunity to pursue graduate training in her laboratory. Dr. Kuang is not only a great mentor, who is willing to take time to supervise her student, but also my role model, who teaches me how to be a real scientist. Her excitement for science inspires me during my PhD study and will continue inspiring me in my future career. She encourages me to challenge myself and improve the abilities required to be a scientist, not only experimental techniques, but also independent thinking, scientific writing and presentation. I am lucky to have Dr. Kuang as the mentor. Without her support and supervision, I would not have today's accomplishments.

I also would like to thank the excellent committee members: Dr. Gary Gallick, Dr. Sue-Hwa Lin, Dr. Pierre McCrea, Dr. Zahid Siddik, Dr. Bryant Darnay, and Dr. Jinsong Liu. They provide constructive suggestions on my projects, presentation and writing, helping me progress during my PhD study. They also provide strong support for my career.

I am also lucky to work with talented and great colleagues in Dr. Kuang's laboratory. I would like thank all of them: Dr. Chuanfen Wu, Dr. Zhehui Feng, Tan Tan and Tianhai Lin. Especially, Dr. Chuanfen Wu helps me a lot with the experimental techniques. She also supports the whole group and maintains a cooperative environment in the laboratory.

Also, I would like to thank Dr. Walter Hittelman and Dr. Khoi Chu. I broaden my knowledge from the joint journal club with Dr. Hittelman's group. He gives me

constructive guidance and helps me significantly improve my presentation skills. I am also very lucky to work with Dr. Chu. Anytime I have questions, he is willing to help.

Last but not least, I would like to thank my parents and my wife for their unconditional love and support.

# **REGULATION OF THE ESCRT FUNCTION OF ALIX**

**Sheng Sun, M.S.**

**Advisory Professor: Jian Kuang, Ph.D.**

The ESCRT (endosomal sorting complex required for transport) is an evolutionary conserved membrane remodeling machinery that performs membrane invagination and abscission. ALIX is a widely expressed adaptor protein that is critically involved in three classical ESCRT-mediated processes, including MVB (multivesicular body) sorting, cytokinetic abscission and retroviral budding. Previous studies have demonstrated that ALIX involvement in these ESCRT-mediated processes requires ALIX interaction with the ESCRT-III component CHMP4 as well as a cargo protein. However, the native form of ALIX contains a default intramolecular interaction between N-terminal Bro1 domain and C-terminal PRD (proline-rich domain), leading to a closed conformation of ALIX that cannot interact with CHMP4. This predicts that ALIX involvement in ESCRT-mediated processes requires an activation step that relieves the intramolecular interaction of ALIX.

The objective of my dissertation research is to identify the regulatory mechanisms that activate the ESCRT function of ALIX in the three classical ESCRT-mediated processes. Whether ALIX is critically involved in MVB sorting of ubiquitinated receptors has been controversial. By examining the effects of ALIX on the level of activated EGFR in the lumen of MVB and the level of EGF-induced phosphorylated ERK1/2, which is the downstream signaling of activated EGFR, I showed that CHMP4-

bound ALIX dimer plays an essential role in MVB sorting and silencing of activated EGFR. However, MVB sorting of activated EGFR is not required for its degradation. My studies thus identify ALIX as an important regulator for signaling output of the activated EGFR. I further demonstrated that ALG-2 (apoptosis-linked gene 2 product) is responsible for generating ALIX in open conformation that supports MVB sorting and timely silencing of activated EGFR. My studies thus identify ALG-2 as a potential negative regulator for the signaling transduction of activated EGFR and provide a new understanding for the role of ALG-2 in apoptotic induction.

While ALG-2 is important for ALIX-mediated MVB sorting, I found that ALG-2 is not important for ALIX-mediated cytokinetic abscission or retroviral budding. Thus, I further identified mechanism that activates ALIX in these two ESCRT-mediated processes. By studying mitotic phosphorylation of ALIX, I found that phosphorylation at S718 and S721 residues in the PRD domain of ALIX relieves the intramolecular interaction of ALIX. This mechanism is required for generating ALIX in open conformation that supports cytokinetic abscission and retroviral budding. These findings provide a new understanding for the regulation of cytokinesis and retroviral budding and may provide new strategies for inhibiting cell division and retroviral budding.

In summary, my dissertation studies have identified two regulatory mechanisms that relieve the intramolecular interaction of ALIX in the three classical ESCRT-mediated membrane remodeling processes. These studies provide insights into the regulation of ESCRT-mediated membrane remodeling processes and suggest that ALIX may be a potential target for anti-cancer and anti-viral therapy.



## Table of contents

Approvals .....	i
Title .....	ii
Dedication .....	iii
Acknowledgements .....	iv
Abstract .....	vi
Table of Contents .....	viii
List of Figures.....	xii
List of Tables .....	xv
Chapter 1: Introduction .....	1
1.1 Endolysosomal trafficking of cell surface receptors.....	1
1.2 Discovery of ESCRT and its MVB sorting function.....	4
1.3 MVB sorting-related functions of ESCRT.....	6
1.4 ESCRT-associated protein: ALIX.....	12
1.5 Diverse cellular functions of ALIX.....	16
1.6 The default intramolecular interaction of ALIX.....	16
1.7 The objective of the dissertation.....	19

Chapter 2: ALIX plays an essential role in MVB sorting of activated EGFR .....	21
Background.....	21
Results.....	23
2.1 ALIX interacts with activated and ubiquitinated EGFR through the V domain.....	23
2.2 EGF-induced EGFR activated promotes ALIX interaction with membrane-bound CHMP4.....	27
2.3 ALIX plays a pivotal role in MVB sorting of activated EGFR.....	31
2.4 ALIX plays an important role in terminating the downstream signaling of activated EGFR.....	36
2.5 Depleting the CHMP4-bound ALIX dimer retards EGF-induced degradation of activated EGFR.....	42
Discussion.....	48
Chapter 3: The mechanism that activates ESCRT function of ALIX in MVB sorting of activated EGFR.....	50
Background.....	50
Results.....	52
3.1 Calcium-dependent ALG-2 interaction with ALIX transforms ALIX from closed conformation to open conformation.....	53
3.2 Calcium-dependent ALG-2 interaction with ALIX is essential for CHMP4-dependent ALIX membrane association.....	58

3.3 EGF-induced EGFR activation increases ALIX association with the membrane through ALG-2 interaction with ALIX.....	62
3.4 Membrane-associated ALIX is in an open conformation.....	66
3.5 ALG-2-induced activation of ALIX plays an essential role in MVB sorting of activated EGFR at early endosome.....	70
3.6 ALG-2-induced activation of ALIX plays an important role in EGF-induced EGFR activation.....	77
3.7 ALG-2 is not required for supporting ALIX to function in cytokinetic abscission or retroviral budding.....	80
Discussion.....	83
Chapter 4: The mechanism that activates ESCRT function of ALIX in cytokinetic abscission and retroviral budding.....	85
Background.....	85
Results.....	88
4.1 The intramolecular interaction of cytosolic ALIX is relieved in a phosphorylation-dependent manner during M phase entry.....	88
4.2 Phosphorylation of ALIX <sub>nPRD</sub> disrupts the intramolecular interaction between ALIX <sub>Bro1</sub> and ALIX <sub>nPRD</sub> .....	93
4.3 Phosphorylation of both S718 and S721 residues disrupts the interaction between ALIX <sub>Bro1</sub> and ALIX <sub>nPRD</sub> .....	96
4.4 Phosphorylation of both S718 and S721 residues transforms ALIX from closed conformation to open conformation in mitotic cells.....	101

4.5 The activating phosphorylation of ALIX is required for ALIX to recruit CHMP4 to the midbody.....	107
4.6 The activating phosphorylation of ALIX is required for ALIX to support cytokinetic abscission.....	111
4.7 The activating phosphorylation of ALIX is required for ALIX to support EIAV budding.....	113
4.8 The activating phosphorylation of ALIX is not important for ALIX to support MVB sorting of activated EGFR.....	117
Discussion.....	121
Chapter 5: Discussion, perspective and future directions.....	124
5.1 The regulation of ALIX in ESCRT-mediated processes.....	124
5.2 The implication of the two regulatory mechanisms in ESCRT-mediated processes.....	127
5.3 The implication of ALG-2/ALIX supported MVB sorting in cancer.....	128
5.4 The switch of ALIX between its ESCRT-dependent function and ESCRT-independent function.....	129
5.5 A potential new strategy to target activated receptor tyrosine kinases.....	130
5.6 Future directions.....	130
Chapter 6: Experimental procedures.....	133
References .....	151

Vita .....	166
------------	-----

## List of Figures

### Chapter 1

Figure 1: Endolysosomal trafficking of cell surface receptors.....	3
Figure 2: Illustration of ESCRT machinery in mammalian cells.....	10
Figure 3: Three classical ESCRT-mediated processes.....	11
Figure 4: Schematic diagram depicting the domain organization of ALIX and BRO1...	15
Figure 5: Model depicting ALIX transforming from closed conformation to open conformation.....	18

### Chapter 2

Figure 6: ALIX interacts with activated and ubiquitinated EGFR.....	24
Figure 7: ALIX V domain interacts with activated and ubiquitinated EGFR.....	26
Figure 8: EGF-induced EGFR activation promotes ALIX interaction with membrane- bound CHMP4.....	29
Figure 9: ALIX plays a pivotal role in MVB sorting of activated EGFR.....	34
Figure 10: ALIX plays an important role in terminating the downstream signaling of activated EGFR under EGF continuous stimulation condition.....	38
Figure 11: ALIX plays an important role in terminating the downstream signaling of activated EGFR under EGF pulse-chase condition.....	41

Figure 12: Depletion of the CHMP4-bound ALIX dimer retards EGF-induced degradation of activated EGFR under EGF continuous stimulation condition.....	44
--	----

Figure 13: Depletion of the CHMP4-bound ALIX dimer retards EGF-induced degradation of activated EGFR under EGF pulse-chase condition.....	47
---	----

### Chapter 3

Figure 14: Calcium-dependent ALG-2 interaction with ALIX transforms ALIX from closed conformation to open conformation.....	56
---	----

Figure 15: Calcium-dependent ALG-2 interaction with ALIX is essential for CHMP4-dependent ALIX membrane association.....	60
--	----

Figure 16: EGF-induced EGFR activation increases ALIX association with the membrane through promoting ALG-2 interaction with ALIX.....	64
--	----

Figure 17: Membrane-associated ALIX is in an open conformation.....	68
---	----

Figure 18: ALG-2-induced activation of ALIX plays an essential role in MVB sorting of activated EGFR.....	72
---	----

Figure 19: ALG-2/ALIX plays an essential role in MVB sorting of activated EGFR at early endosome.....	75
---	----

Figure 20: ALG-2-induced activation of ALIX plays an important role in EGF-induced EGFR degradation.....	78
--	----

Figure 21: ALG-2 is not required for supporting ALIX to function in cytokinetic abscission or retroviral budding.....	82
---	----

## Chapter 4

Figure 22: The intramolecular interaction of cytosolic ALIX is relieved in a phosphorylation-dependent manner during M phase entry.....	91
Figure 23: Phosphorylation of ALIX <sub>nPRD</sub> disrupts the interaction between ALIX <sub>Bro1</sub> and ALIX <sub>nPRD</sub> .....	94
Figure 24: Phosphorylation of both S718 and S721 residues disrupts the interaction between ALIX <sub>nPRD</sub> and ALIX <sub>Bro1</sub> .....	99
Figure 25: Phosphorylation of both S718 and S721 residues transforms ALIX from close conformation to open conformation in mitotic cells.....	104
Figure 26: The activating phosphorylation of ALIX is required for ALIX to recruit CHMP4 to the midbody.....	109
Figure 27: The activating phosphorylation of ALIX is required for ALIX to support cytokinetic abscission.....	112
Figure 28: The activating phosphorylation of ALIX is required for ALIX to support EIAV budding.....	115
Figure 29: The activating phosphorylation of ALIX is not important for ALIX to support MVB sorting of activated EGFR.....	119

## Chapter 5

Figure 30: Graphic abstract illustrating the mechanisms by which ESCRT function of ALIX is regulated in three ESCRT-mediated processes.....	126
---	-----

## **List of Tables**

Table 1: ESCRT proteins in yeast and mammalian cells.....	9
Table 2: Sequences of siRNAs used in this study.....	135
Table 3: Mammalian expression vectors used in this study.....	136
Table 4: PCR primers used in this study.....	139
Table 5: Antibodies used in this study.....	144



## **Chapter 1: Introduction**

### **1.1. Endolysosomal trafficking of cell surface receptors**

Ligand binding to cell surface receptors induces the activation of receptors, which then induces the internalization of these activated receptors in membrane-bounded vesicles through a plasma membrane invagination process, called endocytosis (Marsh and McMahon, 1999). These receptor-containing vesicles are then fused with early endosome.

From early endosome, there are three fates for these receptors. First, receptors can recycle back to cell surface. During the recycling process, these receptors still have signaling function, activating the downstream signaling pathways. Second, receptors can stay on the membrane of early endosome. This portion of receptors also keeps their signaling function. The third fate is to be sorted into the lumen of early endosome through an endosome membrane invagination and abscission process, called MVB (multivesicular body) sorting.

MVB sorting terminates the signaling function of the activated receptors and it is a very quick process, happening in ~30 min after ligand binding. Although the receptors both on the membrane and in the lumen of early endosome will be trafficked to late endosome and then lysosome for degradation, receptors staying on the endosome membrane will keep on sending signals to the downstream pathways during the trafficking process, which takes several hours. Thus, if activated receptors are not properly sorted into endosome through MVB sorting, the duration of the downstream signaling will be prolonged and it may lead to uncontrolled cell proliferation. Thus, MVB

sorting is an important process that functions as a negative regulator of activated receptors.

The whole process initiating from endocytosis of the activated receptors until to lysosome-dependent degradation of these receptors is called endolysosomal trafficking (Feyder et al., 2015; Goh and Sorkin, 2013; Mellman, 1996; Scott et al., 2014; Sorkin and Goh, 2009; Wegner et al., 2011) (Fig. 1).

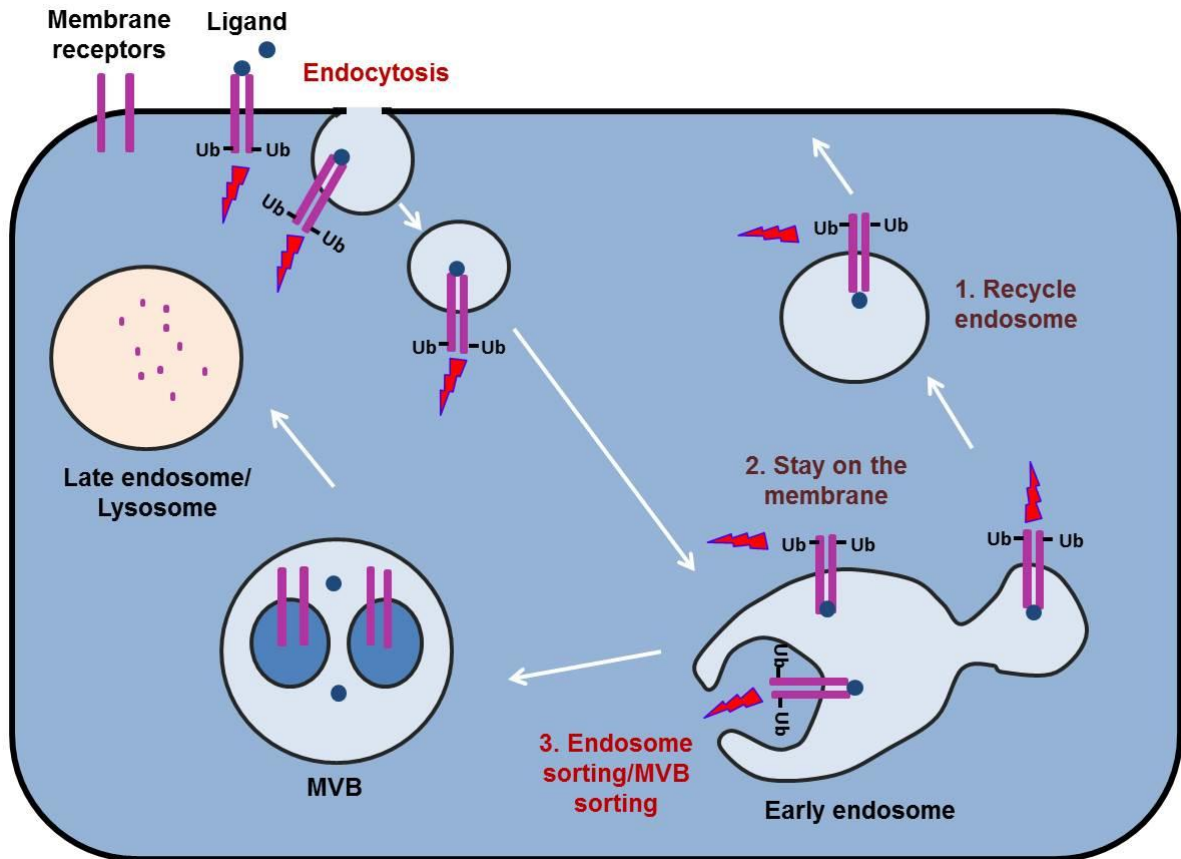


**Figure 1. Endolysosomal trafficking of cell surface receptors.** Endolysosomal trafficking initiates from the receptor activation-induced endocytosis. The endocytosed receptors either recycle back to cell surface (1), stay on the membrane of early endosome (2) or are sorted into the lumen of early endosome (MVB sorting) (3). Then, MVB will be fused with lysosome to deliver receptors for lysosome-dependent degradation.

## 1.2. Discovery of ESCRT and its MVB sorting function

MVB sorting is in the opposite topology of endocytosis. While endocytosis involves budding of vesicles into cytoplasm, MVB sorting involves budding of vesicles away from cytoplasm (Fig. 1). Thus, the mechanism underlining endocytosis does not apply to MVB sorting. Therefore, it is important to have a powerful model system to study the mechanism underlining MVB sorting. The researchers found that yeast *Saccharomyces cerevisiae* is the most powerful model system for studying MVB sorting for several reasons. First, MVB sorting pathway is conserved from yeast to human. In yeast cells, membrane proteins also go through MVB sorting to vacuole, the intracellular organelle sharing functional characteristics with mammalian lysosome (Banta et al., 1988; Henne et al., 2013). Second, it is convenient to perform genetic screen in yeast to search for the genes, whose products are involved in MVB sorting. Plasmids with no gene-specific sequences can be delivered into yeast cells and these sequences can integrate randomly throughout the genome and randomly disrupt the genes to generate various mutant yeast strains. Through observing the expected phenotypes, which are the abnormal morphology of endosome and the defective sorting of GFP-labelled vacuole enzyme, carboxypeptidase S (CPS), the researchers could identify the genes that are required for normal MVB sorting pathway (Banta et al., 1988; Forsburg, 2001). Third, the phenotypes induced by defective MVB sorting can be easily observed under microscope (Banta et al., 1988; Raymond et al., 1992; Robinson et al., 1988).

By using yeast as the model system, Emr and Stevens groups found that loss of several genes in yeast led to exaggerated endosome-like compartment (the class E compartment) and defective sorting of vacuole enzyme. They named this type of genes,

which is required for MVB sorting, as Class E *Vps* (vacuolar protein sorting) (Banta et al., 1988; Raymond et al., 1992; Robinson et al., 1988).

Further biochemical and cellular studies from Emr group found that products of Class E genes *Vps23*, *Vps28*, and *Vps37* form a protein complex, which binds the ubiquitinated sorting receptors in yeast. They named this protein complex as ESCRT-I (endosomal sorting complex required for transport-I) (Katzmann et al., 2001). Then, they found that products of Class E genes *Vps2*, *Vps20*, *Vps24*, and *Snf7* form a protein complex, which have direct effects on MVB sorting activity in yeast. They named this protein complex as ESCRT-III (Babst et al., 2002a). They also found that products of Class E genes *Vps22*, *Vps25*, and *Vps36* form a protein complex, which also binds ubiquitinated sorting proteins, associates with endosome membrane and interacts with ESCRT-III and promotes its assembly. They named this protein complex as ESCRT-II (Babst et al., 2002b).

Further studies in mammalian cells revealed that these Class E gene products are conserved from yeast to human. Mammalian cells contain the orthologs of all these yeast Class E gene products, which also constitute ESCRT-I, II, and III (Henne et al., 2013; Hurley, 2010) (Table 1 and Fig. 2). The studies in mammalian cells also identified a protein complex consisting of STAM (signal-transducing adaptor molecule) and Hrs (hepatocyte growth factor-regulated tyrosine kinase substrate). This protein complex, which was shown to bind ubiquitinated sorting receptors, associate with endosome membrane and is involved in MVB sorting, was named as ESCRT-0 (Table 1 and Fig. 2). Then, the genetic screen in yeast also identified two Class E *Vps* genes (*Hes1* and *Vps27*), whose products are orthologs of mammalian Hrs and STAM, respectively (Bilodeau et al., 2002; Katzmann et al., 2003) (Table 1).

The essence of MVB sorting is linking receptor recognition and endosome membrane abscission. ESCRT machinery is anchored on the endosome membrane through direct interaction between ESCRTs-0/-II components and endosome membrane-associated PtdIns(3)P lipid. ESCRT-0, -I, and -II function as a stable hetero-oligomers to recognize and concentrate ubiquitinated receptors through the ubiquitin-binding motifs in the components of these three ESCRTs (Fig. 2). ESCRT-II initiates the sequential activation and assembly of ESCRT-III, which, in default condition, exists as autoinhibited monomers in the cytoplasm. The formed oligomerized ESCRT-III filaments localize around the neck of the budding vesicle and perform the membrane abscission. AAA ATPase Vps4 interacts with ESCRT-III and provides energy to disassemble the ESCRT-III after MVB sorting (Babst et al., 1998; Boura et al., 2012; Caillat et al., 2015; Henne et al., 2012; McCullough et al., 2015; Teis et al., 2008; Yang et al., 2015) (Fig. 2). Thus, ESCRT is evolutionary conserved membrane remodeling machinery that execute MVB sorting pathway.

### **1.3. MVB sorting-related functions of ESCRT**

Besides MVB sorting, the second identified function of ESCRT is retroviral budding. ESCRTs were found to be hijacked by retroviruses for their budding away from the host cells. Retrovirus, such as HIV-1 and EIAV (equine infectious anemia virus), recruits ESCRT-III to the budding site through direct interaction between retroviral Gag protein and ESCRT-associated protein (Beata MierzwaVotteler and Sundquist, 2013; Martin-Serrano and Neil, 2011; Strack et al., 2003; von Schwedler et al., 2003). The studies by using siRNA knockdown and rescuing experiments indicated that among the ESCRT-III components, only CHMP4 (charged multivesicular body protein 4) and CHMP2 are critically involved in HIV-1 and EIAV budding. CHMP4

filaments are assembled in circular arrays that bend the plasma membrane away from the cytoplasm. Then, CHMP4 filaments are “capped” by recruiting CHMP2 subcomplex, which subsequently binds and recruits Vps4 (Sandrin and Sundquist, 2013).

The third identified function of ESCRT is cytokinetic abscission, the final step of cell division where daughter cells are physically separated (Carlton et al., 2008; Carlton and Martin-Serrano, 2007; Morita et al., 2007). The essential event in cytokinetic abscission is the recruitment of ESCRT-III to the midbody area and its assembly to oligomerized filaments, which perform the membrane abscission (Carlton et al., 2008; Carlton and Martin-Serrano, 2007; Morita et al., 2007). Three models have been proposed for how ESCRT-III filaments promote membrane abscission. One is “spiral-ingression” model, in which ESCRT-III forms filaments at the midbody and the spiral filaments wind from the midbody and the end of the narrowing spirals is the abscission zone. Another one is “sliding spiral” model, in which ESCRT-III forms filaments at the midbody and the spiral filaments slide along the intracellular bridge to form an abscission site  $\sim 1 \mu\text{m}$  from the midbody. The third one is “vesicle-mediated ingression” model, in which intracellular vesicles derived from recycling endosomes form the abscission zone by narrowing the intercellular bridge through fusion with the plasma membrane (Henne et al., 2013).

MVB sorting, cytokinetic abscission and retroviral budding are three best-characterized ESCRT-mediated processes with the same topology. Therefore, these three processes are called classical ESCRT-mediated processes (Fig. 3). Besides these three classical ESCRT-mediated processes, multiple novel functions of ESCRT have been reported recently, including exosome biogenesis (Baietti et al., 2012), plasma membrane wound repair (Jimenez et al., 2014; Scheffer et al., 2014),

autophagy (Murrow et al., 2015) and nuclear envelope reformation (Olmos et al., 2015; Vietri et al., 2015). These novel functions reveal remarkably widespread roles of ESCRTs in cellular processes.



**Table 1. ESCRT proteins in yeast and mammalian cells**

	Yeast	Human
ESCRT-0	Vps27	Hrs
	Hes1	STAM1/2
ESCRT-I	Vps23	TSG101
	Vps28	Vps28
	Vps37	Vps37
	Mvb12	hMvb12
ESCRT-II	Vps36	EAP45
	Vps22	EAP30
	Vps25	EAP20
ESCRT-III	Vps20	CHMP6
	Snf7	CHMP4
	Vps24	CHMP3
	Vps2	CHMP2

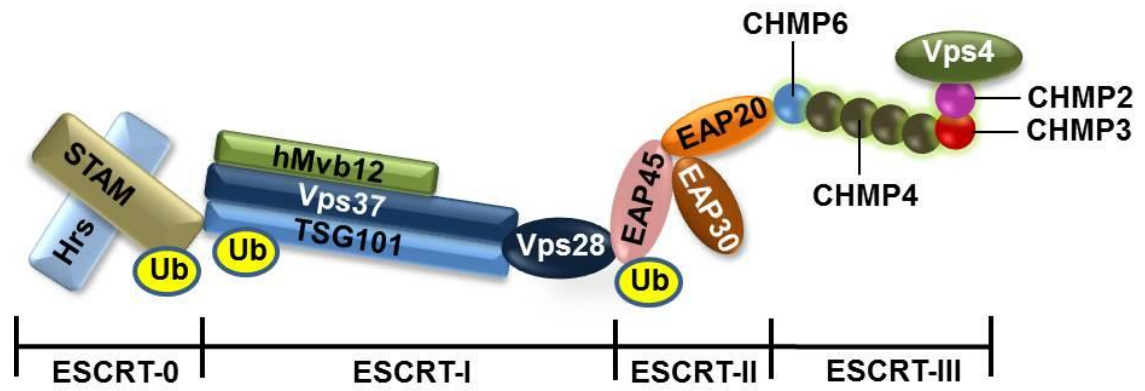


**Figure 2. Illustration of ESCRT machinery in mammalian cells.** The subunits of each ESCRT complex and Vps4 are shown. ESCRT-0 component STAM (signal-transducing adaptor molecule), ESCRT-I component TSG101 (tumor susceptibility gene 101) and ESCRT-II component EAP45 contain ubiquitin binding motifs that recognize ubiquitinated cargo proteins.

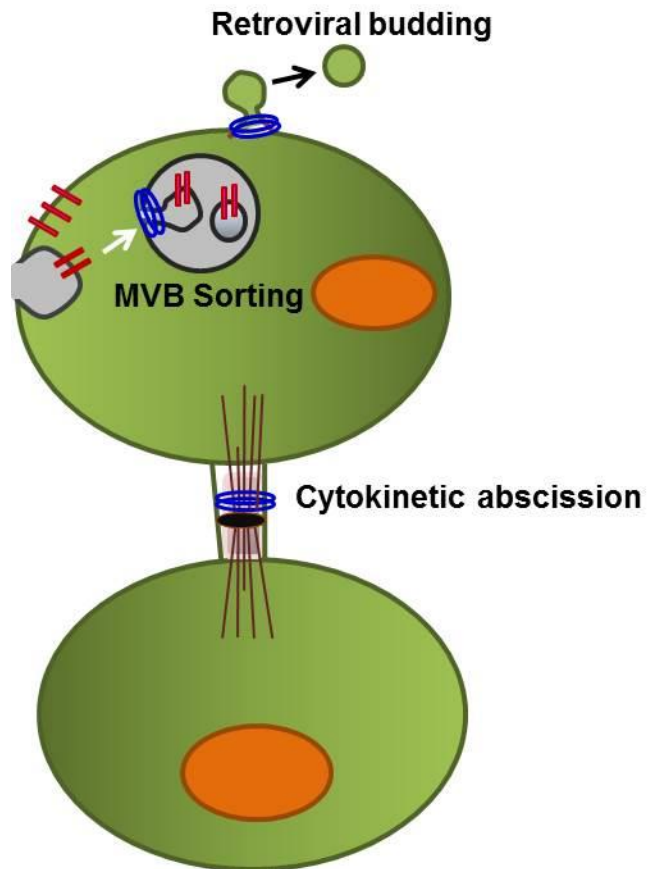


**Figure 3. Three classical ESCRT-mediated processes.** MVB sorting of internalized receptors, cytokinetic abscission and retroviral budding are three classical ESCRT-mediated processes, having the same topology (budding away from cytoplasm) and sharing the mechanism for membrane invagination and abscission (requiring ESCRTs).

#### 1.4. ESCRT-associated protein: ALIX

Through the genetic screen of the mutant class E *Vps* genes leading to defective MVB sorting of GFP-Labelled CPS in yeast, Emr and his colleagues identified that product of *BRO1* (BCK1-like Resistance to Osmotic shock) gene is required for normal MVB sorting pathway (Odorizzi et al., 2003). *BRO1* protein consists of three domains: an N-terminal Bro1 domain, a middle V letter-shape domain and a C-terminal proline-rich domain (PRD) (Odorizzi, 2006; Odorizzi et al., 2003). *BRO1* binds ubiquitinated receptors through its ubiquitin-binding motif in the V domain and this ubiquitin-binding activity is required for *BRO1* to support MVB sorting pathway (Pashkova et al., 2013). *BRO1* also interacts with ESCRT-III component Snf7 through its Bro1 domain and regulates the assembly and the membrane abscission capability of ESCRT-III filament (Odorizzi et al., 2003; Wemmer et al., 2011). Thus, *BRO1* functions to link the receptor recognition and ESCRT-III mediated membrane abscission.

ALIX (ALG-2 interacting protein X) (Missotten et al., 1999), also termed AIP1 (Vito et al., 1999) was initially identified and cloned by two independent studies searching for partner proteins of ALG-2 (apoptosis-linked gene 2 product) in mouse. Structural studies of ALIX revealed that ALIX and *BRO1* share structural organization. ALIX also consists of three domains: an N-terminal Bro1 domain, a middle V letter-shaped domain and a C-terminal PRD (Fisher et al., 2007). The Bro1 domain of ALIX contains a binding site (hydrophobic Patch 1) for ESCRT-III component CHMP4 and a docking site (hydrophobic Patch 2) for Src (Kim et al., 2005; McCullough et al., 2008). The V domain of ALIX contains the ubiquitin-binding motifs for preferably interacting with Lys-63 polyubiquitin chain (Dowlatsahi et al., 2012; Keren-Kaplan et al., 2013) and a hydrophobic three dimensional interaction site (F676 pocket) for proteins

containing YPX(n)L motif, such as retroviral Gag proteins (Lee et al., 2007; Zhai et al., 2008), syntenin (Baietti et al., 2012) and PAR1 (protease activated receptor 1) (Dores et al., 2012a; Dores et al., 2012b). The PRD of ALIX contains two linear docking sites (residues 717-720 and 852-855) for ESCRT-I component TSG101, an ALIX multimerization sequence and an ALG-2 binding site (residues 801-812) (Carlton et al., 2008) (Fig. 4).

As the ESCRT-associated protein, ALIX was first found to be involved in ESCRT-mediated retroviral budding, during which retroviral Gag proteins directly interact with the F676 pocket in the V domain of ALIX and through this interaction, retrovirus hijacks ESCRT-III of host cells to plasma membrane for membrane abscission (Strack et al., 2003; von Schwedler et al., 2003). Then, ALIX was demonstrated to be essential for ESCRT-mediated cytokinetic abscission, during which ALIX is recruited to the midbody through direct interaction with CEP55 (entrosomal protein of 55 kDa), which is recruited to midbody during cytokinesis. The midbody-localized ALIX recruits CHMP4 to the midbody area and promotes the assembly of ESCRT-III filaments, which perform the membrane abscission at the midbody area (Carlton et al., 2008; Carlton and Martin-Serrano, 2007; Morita et al., 2007).

As the mammalian ortholog of yeast BRO1, ALIX was predicted to be involved in MVB sorting of ubiquitinated receptors in mammalian cells, just as BRO1 does in yeast (Pashkova et al., 2013). However, by using EGFR as the model molecule, multiple previous studies generated negative results by showing that knockdown of ALIX produced no or only a minor inhibitory effect on degradation of activated EGFR in HeLa cells (Bowers et al., 2006; Cabezas et al., 2005; Doyotte et al., 2008; Schmidt et al., 2004). Since MVB sorting is generally thought to be required for lysosome-dependent

degradation of activated EGFR, these results led to a widely held notion that ALIX does not play a critical role in ESCRT-mediated MVB sorting of ubiquitinated membrane receptor in mammalian cells. However, two independent studies reported that inhibition of MVB sorting of activated EGFR by treating cells with PI3-kinase inhibitor wortmannin or by knocking down annexin 1 only generated a minor inhibitory effect on degradation of activated EGFR (Futter et al., 2001; White et al., 2006), indicating that MVB sorting may not be necessary for lysosome-dependent degradation of ubiquitinated receptors in mammalian cells. Thus, the lysosome-dependent degradation of activated EGFR may not be the reliable indication for MVB sorting of activated EGFR in mammalian cells. Moreover, both mammalian ALIX and yeast BRO1 contain ubiquitin binding motifs that interact with Lys63 poly-ubiquitin chain (Dowlathshahi et al., 2012; Pashkova et al., 2013), indicating that ALIX is probably able to recognize and interact with ubiquitinated receptors, such as activated EGFR, which requires Lys63 polyubiquitination for its lysosome-dependent degradation (Huang et al., 2013). Therefore, whether ALIX is critically involved in MVB sorting of activated EGFR has been controversial.

Since MVB sorting of activated receptor tyrosine kinases, such as EGFR, is involved in timely terminating the signaling function of these receptors (~30 min) before these receptors are delivered to lysosome for degradation (several hours), thus MVB sorting is an important regulatory mechanism that prevents uncontrolled cell proliferation induced by over-activation of receptor tyrosine kinases. Investigating the role of ALIX in MVB sorting of ubiquitinated receptors will provide great insights into the regulation of such an important process.

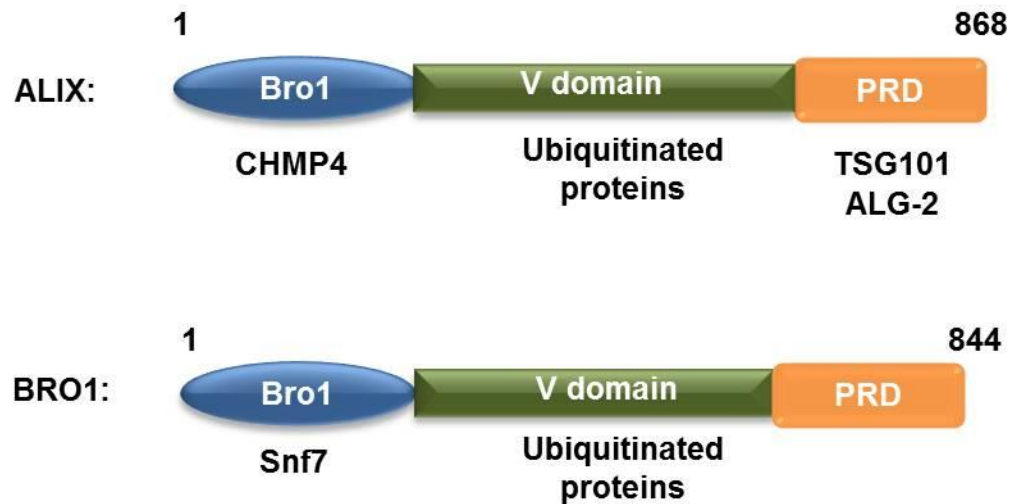


**Figure 4. Schematic diagram depicting the domain organization of ALIX and BRO1.** Mammalian ALIX contains 868 amino acids and yeast BRO1 contains 844 amino acids. In ALIX, Bro1 domain binds ESCRT-III component CHMP4, V domain binds Lys63 poly-ubiquitinated proteins and PRD binds ESCRT-I component TSG101 and ALG-2. In BRO1, Bro1 domain binds ESCRT-III component Snf7, which is yeast homolog of CHMP4 and V domain also binds Lys63 poly-ubiquitinated proteins.

## **1.5. Diverse cellular functions of ALIX**

Besides ESCRT-mediated processes, ALIX has also been reported to be involved in diverse cellular processes that do not need involvement of ESCRT. Studies from Böglér group found that ALIX interacts with focal adhesion kinase (FAK) and proline rich tyrosine kinase 2 (PYK-2) and through these interactions, ALIX regulates cell adhesion (Schmidt et al., 2003). Then, studies from our group found that ALIX directly interacts with F-actin and promotes actin cytoskeleton assembly. We also found that sub-population of ALIX can be secreted outside of the cells and the extracellular ALIX is involved in regulating integrin-mediated cell adhesion and extracellular matrix assembly (Pan et al., 2008; Pan et al., 2006). An important question is what decides ALIX to function in ESCRT-mediated cellular processes or in ESCRT-independent cellular processes.

## **1.6. The default intramolecular interaction of ALIX**

Native form of ALIX contains a default intramolecular interaction between Patch 2 in Bro 1 domain and one of the TSG101 docking site (TSD: residues 717-720) in PRD (Fig. 5). This intramolecular interaction renders ALIX a closed conformation, which prohibits ALIX interaction with ESCRT-III component CHMP4 (Zhou et al., 2009; Zhou et al., 2008; Zhou et al., 2010). Thus, native form of ALIX cannot perform its ESCRT function. Also, ALIX in the closed conformation exists as the monomer in the cytosol. ALIX in the open conformation can dimerize through its V domain in an anti-parallel manner and this dimerization was proposed to promote the assembly of CHMP4 filament and required for retroviral budding (Pires et al., 2009; Zhai et al., 2008). Since ALIX is an essential mediator for linking the upstream initiator and the downstream executor of ESCRT-mediated processes, investigating the regulatory



mechanisms that relieve the intramolecular interaction of ALIX will lead to a better understanding for ESCRT-mediated processes.

Based on the studies from previous graduate student in our group, three potential regulatory mechanisms that relieve the intramolecular interaction of ALIX were proposed. One is the partner protein interaction-induced conformational change. Another one is the competitive binding-induced disruption of intramolecular interaction. The third one is posttranslational modification-induced disruption of intramolecular interaction (Zhou et al., 2010).

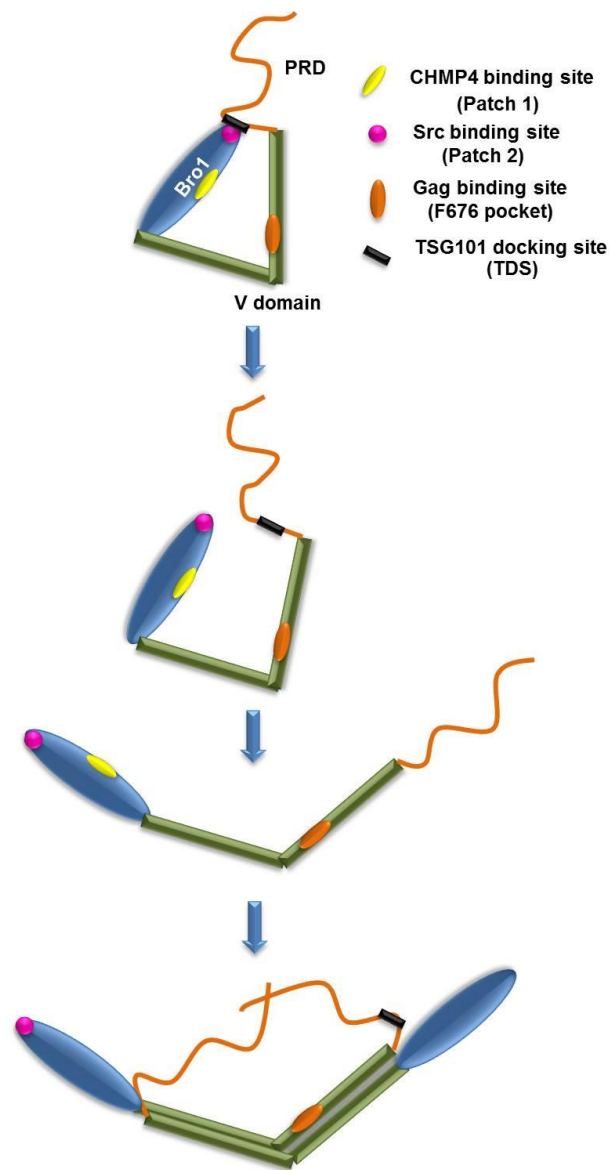


**Figure 5. Model depicting ALIX transforming from closed conformation to open conformation.** Native form of ALIX contains a default intramolecular interaction between Patch 2 in Bro1 domain and TDS in N-terminal portion of PRD, rendering a closed conformation of ALIX and blocking its ESCRT-functions. The activation of ALIX initiates from the dissociation of Bro1 domain and PRD. Then, the V domain of ALIX is open followed by V-domain-mediated anti-parallel dimerization.

## **1.7. The objective of the dissertation**

The default intramolecular interaction of ALIX has to be relieved to activate ESCRT functions of ALIX. Thus, the objective of my dissertation research is to identify the regulatory mechanisms that activate the ESCRT functions of ALIX in the three classical ESCRT-mediated processes. To accomplish this objective, I performed three parts of studies.

First, I comprehensively investigated the role of ALIX in binding, MVB sorting, silencing and degradation of activated EGFR in HEK293 and HeLa cells. My studies demonstrate that ALIX binds activated and ubiquitinated EGFR and plays an essential role in MVB sorting and timely silencing of activated EGFR. However, ALIX does not play an important role in trafficking of activated EGFR to lysosome for degradation. My studies thus identify ALIX as an important regulator for the signaling output of activated EGFR and possibly other receptor tyrosine kinases.

Then, I explored the mechanism that relieves the default intramolecular interaction of ALIX in MVB sorting process. My studies demonstrate that calcium-dependent ALG-2 interaction with ALIX induces a conformational change of ALIX that relieves its intramolecular interaction. ALG-2-supported activation of ALIX is required for ALIX to associate with membrane-bound CHMP4 and function in MVB sorting of activated EGFR. In contrast, ALG-2-supported activation of ALIX is not required for cytokinetic abscission or retroviral budding. My studies thus identify ALG-2 as a potential negative regulator of signaling transduction of activated EGFR and provide a new understanding for apoptotic induction effect of ALG-2. My studies also indicate that there should be other mechanisms that activate ESCRT function of ALIX in cytokinetic abscission and retroviral budding.

Further exploration demonstrate that ALIX is phosphorylated at the S718 and S721 residues, which locate at or near one of the intramolecular interaction sites, during mitotic entry and that this phosphorylation relieves the intramolecular interaction of ALIX in mitotic cells. This activating phosphorylation is required for inducing ALIX in open conformation that recruits CHMP4 to the midbody area and therefore essential for ALIX to support cytokinetic abscission. This activating phosphorylation also induces ALIX in open conformation that interacts with retroviral Gag proteins and therefore supports ALIX function in retroviral budding. In contrast, this phosphorylation is not important for MVB sorting function of ALIX. These findings provide a new understanding for the regulation of cytokinesis and retroviral budding and may provide new strategies for inhibiting cell division and retroviral budding.

## **Chapter 2: ALIX plays an essential role in MVB sorting of activated EGFR**

Contents of this chapter are based on Sun, S., Zhou, X., Zhang, W., Gallick, G.E., Kuang, J. Unravelling the pivotal role of Alix in MVB sorting and silencing of the activated EGFR. *Biochem J.* 2015;466(3):475-87. doi: 10.1042/BJ20141156.

Copyright permission is not required. Portland Press policy states “As long as the original article, or portion of the article, is properly cited, and a link to the article is included, Authors retain the following non-exclusive rights: To include their article in whole or in part in their own dissertation or thesis in print or electronic format provided that the full-text article is not then shared in an open repository unless it is published via the Gold Open Access route.”

### **Background**

EGFR is the model molecule for the study of ubiquitination-dependent endolysosomal trafficking of membrane receptors. EGF binding to plasma membrane EGFR induces the activation of EGFR, which is phosphorylated and ubiquitinated. The activated EGFR is internalized into cytoplasm through endocytosis and during this process, activated EGFR keeps on sending signals to its downstream pathways, such as ERK1/2. Then, the internalized EGFR is sorted into the ILVs of MVBs through MVB sorting. MVB sorting of activated EGFR is involved in timely terminating the signaling function of activated EGFR and delivering EGFR to lysosome for degradation (Gruenberg and Stenmark, 2004; Katzmann et al., 2002; Wegner et al., 2011).

MVB sorting of activated EGFR is performed by ESCRTs and their associated

proteins. The ubiquitinated receptors are recognized and clustered by ESCRTs -0, -I, and -II. ESCRT-0 binds ubiquitinated receptors through both subunits, Hrs (HGF-regulated tyrosine kinase substrate) and STAM1/2. ESCRT-I subunit TSG101 and ESCRT-II subunit hMvb12 are able to bind ubiquitinated receptors through their ubiquitin binding domain (UBD). The coordination of receptors recognition and membrane remodeling is achieved by the ability of ESCRT-II to both recognize the ubiquitinated receptors and initiate the assembly of highly oligomerized ESCRT-III complex. ESCRT-III subunit CHMP4 assembles into highly flexible filament that forms spirals at the surface of endosome membranes. CHMP4 spirals can deform under lateral compression and the relaxation of compressed CHMP4 spirals induces membrane deformation. Thus, ESCRT-III is the core machinery that performs the membrane scission at the budding site. ESCRT-III is timely disassembled by Vps4 (Henne et al., 2011; Henne et al., 2013; Hurley and Hanson, 2010; Lata et al., 2009).

Promoted by the previous reports that BRO1 plays a positive role in MVB sorting of ubiquitinated receptors in yeast (Pashkova et al., 2013) and that ALIX contains ubiquitin binding motifs, just as BRO1 does (Dowlatshahi et al., 2012; Pashkova et al., 2013), I hypothesized that ALIX may be critically involved in MVB sorting of activated EGFR in mammalian cells.

To test this hypothesis, I comprehensively study the role of ALIX in binding, MVB sorting, silencing and degradation of activated EGFR in mammalian cell lines. The results demonstrate that ALIX recognizes activated and ubiquitinated EGFR through its V domain and plays an essential role in MVB sorting and silencing of activated EGFR. However, ALIX does not have an essential role in lysosome-dependent degradation of activated EGFR. These findings identify ALIX as an important regulator of the signaling

output of activated EGFR and possibly other growth factor receptors.

## **Results**

### **2.1. ALIX interacts with activated and ubiquitinated EGFR through the V domain**

To determine whether ALIX recognizes ubiquitinated EGFR, I ectopically expressed GFP or GFP-ALIX in HEK293 cells, which were then mock-treated or stimulated with EGF, and examined the GFP-ALIX interaction with EGFR by using co-immunoprecipitation (co-IP). Cell lysates were prepared from mock-treated and EGF-stimulated cells with the membrane solubilizing lysis buffer containing 1% Triton X-100 in the presence or absence of the deubiquitinase inhibitor N-ethylmaleimide (NEM). Cell lysates were immunoprecipitated with negative control mouse IgG or anti-GFP antibody, and the immunocomplexes were immunoblotted to visualize EGFR, ubiquitinated EGFR, GFP-ALIX and CHMP4B. As shown in Fig. 6A-B, in the presence of NEM, EGF stimulation increased the association of GFP-ALIX with EGFR by ~4 fold, and the ubiquitination of EGFR was confirmed by immunoblotting with anti-ubiquitin antibodies. However, in the absence of NEM, there is only basal level of association of GFP-ALIX with non-ubiquitinated EGFR, even with EGF stimulation. In contrast, the association of GFP-ALIX with CHMP4B had no change under all conditions. In contrast to GFP-ALIX, ectopically expressed GFP did not interact with EGFR, demonstrating that the association of GFP-ALIX with EGFR is a specific event (Fig. 6C). These results identify two modes of interaction between ALIX and EGFR: a high level of EGF-induced and ubiquitination-dependent interaction and a low level of constitutive interaction.

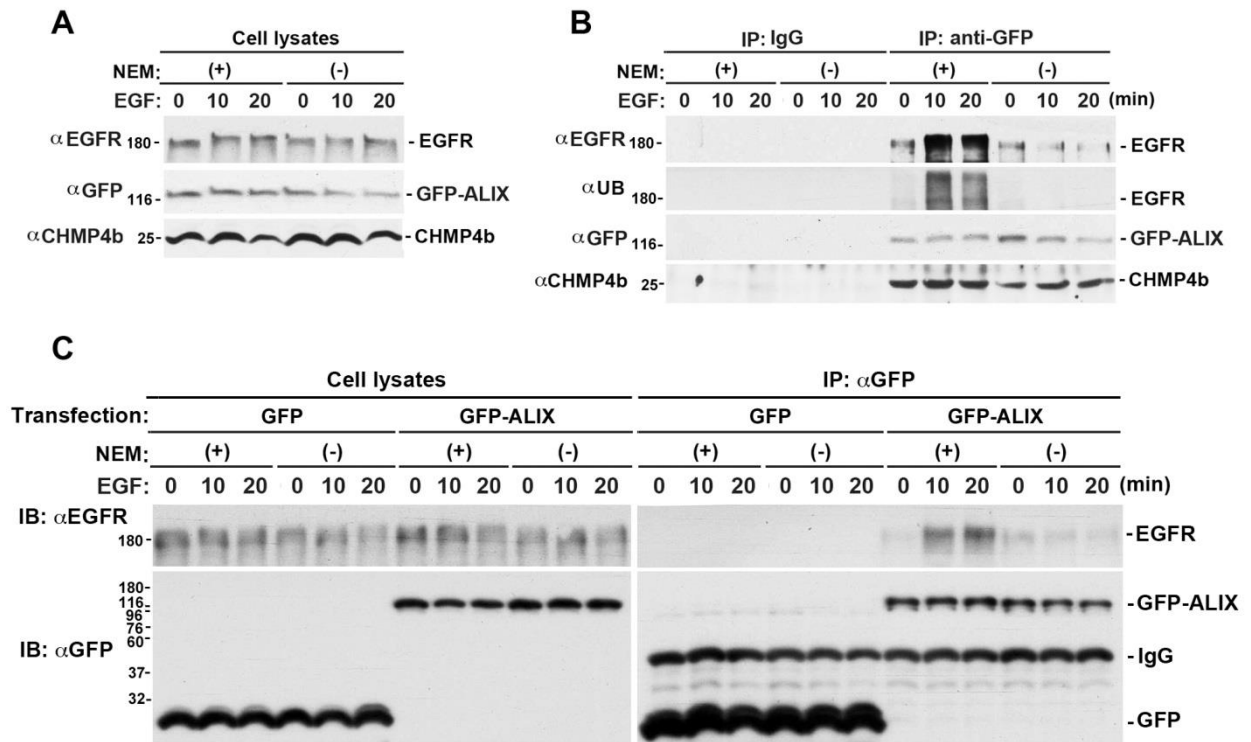


**Figure 6. ALIX interacts with activated and ubiquitinated EGFR.** (A&B) HEK293 cells were transfected with GFP-ALIX, serum starved for 12 h and stimulated with 100 ng/ml EGF for indicated minutes. Crude cell lysates were extracted in the presence or absence of NEM. (A) These cell lysates were directly immunoblotted to visualize EGFR, GFP-ALIX and CHMP4B. (B) These cell lysates were immunoprecipitated with anti-GFP antibody or mouse IgG followed by immunoblotting to visualize EGFR, ubiquitinated EGFR, GFP-ALIX and CHMP4b. Results represent two independent experiments. (C) HEK293 cells were transfected with GFP or GFP-ALIX, serum starved for 12 h and stimulated with 100 ng/ml EGF for indicated minutes. Crude cell lysates were prepared in the presence or absence of NEM and immunoprecipitated with anti-GFP antibody. Input cell lysates and immunocomplexes were immunoblotted with indicated antibodies to visualize GFP, GFP-ALIX, EGFR and ubiquitinated EGFR.



To identify which domain of ALIX is responsible for ALIX interaction with EGFR, HEK293 cells were transfected with FLAG-ALIX<sub>Br01</sub> or HA-ALIX<sub>V</sub>, and co-IP was performed to examine their interactions with EGFR. Cell lysates were prepared from mock-treated and EGF-stimulated cells with the membrane solubilizing lysis buffer in the presence of NEM. As shown in Fig. 7A, FLAG-ALIX<sub>Br01</sub> only had low level of constitutive interaction with EGFR irrespective of EGF stimulation. In contrast, HA-ALIX<sub>V</sub> had a high level of interaction with ubiquitinated EGFR in EGF-stimulated cells (Fig. 7B). These results indicate that ALIX<sub>Br01</sub> is responsible for constitutive ALIX interaction with EGFR and that ALIX<sub>V</sub> is responsible for EGF-induced and ubiquitination-dependent ALIX interaction with EGFR. The membrane proteins from mock-treated or EGF-stimulated HEK293 cells were then extracted in the presence of NEM and GST pull-down was performed by using GST-ALIX<sub>Br01</sub> or GST-ALIX<sub>V</sub> to examine their interactions with membrane-associated EGFR. As shown in Fig. 7C and Fig. 7D, although GST-ALIX<sub>Br01</sub> could not pull down detectable EGFR, GST-ALIX<sub>V</sub> preferentially pulled down EGFR from EGF-stimulated cells. These results further support the conclusion that ALIX<sub>V</sub> mediates ALIX interaction with ubiquitinated EGFR in EGF-stimulated cells.

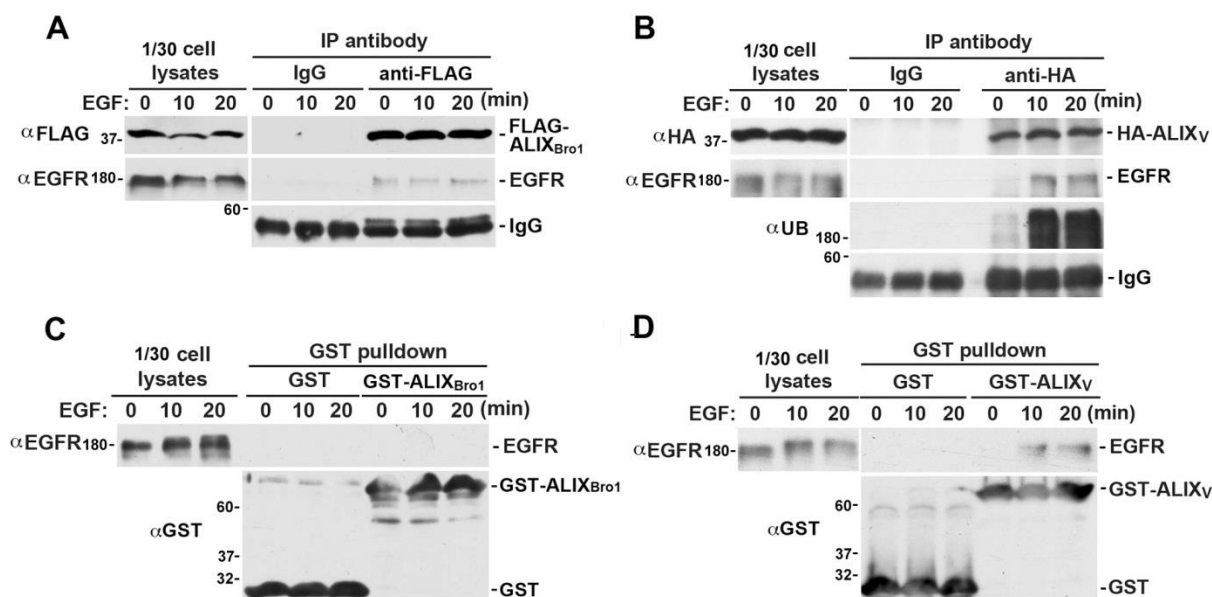


**Figure 7. ALIX V domain interacts with activated and ubiquitinated EGFR. (A&B)**

HEK293 cells were transfected with FLAG-ALIX<sub>Bro1</sub> (A) or HA-ALIX<sub>V</sub> (B) and stimulated with 100 ng/ml EGF for indicated minutes. Cell lysates were prepared in the presence of NEM and immunoprecipitated with anti-FLAG antibody and mouse IgG (A) or anti-HA antibody and mouse IgG (B). Cell lysates and immunocomplexes were immunoblotted to visualize EGFR and FLAG-ALIX<sub>Bro1</sub> in (A) or EGFR, ubiquitinated EGFR, and HA-ALIX<sub>V</sub> in (B). (C&D) Membrane proteins from HEK293 cells stimulated with 100 ng/ml EGF for indicated minutes were isolated and solubilized in the presence of NEM and incubated with immobilized GST and GST-ALIX<sub>Bro1</sub> in (C) or GST and GST-ALIX<sub>V</sub> in (D). Input and bound membrane proteins were immunoblotted to visualize EGFR, GST and GST-ALIX<sub>Bro1</sub> in (C) or EGFR, GST and GST-ALIX<sub>V</sub> in (D). Results represent two independent experiments.

## **2.2. EGF-induced EGFR activation promotes ALIX interaction with membrane-bound CHMP4**

ALIX involvement in all ESCRT-mediated processes requires ALIX interaction with membrane-bound CHMP4. Thus, to define the role of ALIX in MVB sorting of activated EGFR, I examined the interaction between ALIX and membrane-bound CHMP4. To this end, I fractionated post-nuclear supernatant (PNS) from mock-treated or EGF-stimulated HEK293 cells by using membrane flotation centrifugation. This established method utilized sucrose gradients (73%, 65% and 10%) to separate membrane vesicles (M) from soluble proteins (S) based on the density of membrane vesicles (Ono and Freed, 1999; Spearman et al., 1997). After ultracentrifugation, the membrane vesicles float at the interface between the layer of 65% sucrose and the layer of 10% sucrose, while the soluble proteins stay at the bottom. As shown in Fig. 8A, in mock-treated cells, ~13% of endogenous ALIX was membrane associated, and EGF stimulation increased the percentage of membrane associated ALIX to ~33%. Ectopically expressing wild type (WT) GFP-ALIX had the similar distribution as endogenous ALIX between M and S fraction in mock-treated and EGF-stimulated cells (Fig. 8B). However, only ~3% of CHMP4 interaction-defective mutant I212D GFP-ALIX associated with membrane in either mock-treated cells or EGF-stimulated cells (Fig. 8B). These results demonstrate that EGF-induced EGFR activation promotes ALIX interaction with membrane bound CHMP4.

ALIX can dimerize through the V domain in an antiparallel manner. This dimerization has been shown to promote assembly of CHMP4 filaments in vitro and be required for ALIX to support ESCRT-III-mediated retroviral budding (Pires et al., 2009). To determine whether membrane associated ALIX can dimerize through its V domain, I

first examined the dimerization of ALIX in whole cell lysates from HEK293 cells transfected with GFP-ALIX by using co-IP. The 1A3 anti-ALIX antibody, which recognizes both ALIX and HD-PTP (Zhou et al., 2009), was used for immunoblotting of input proteins and immunocomplexes. As shown in Fig. 8C, ectopically expressed GFP-ALIX interacted with endogenous ALIX, but not with detectable level of endogenous HD-PTP. I also performed co-IP of ectopically expressed GFP-ALIX and FLAG-ALIX to further examine the dimerization of ALIX (Fig. 8D-E). The results from this reciprocal co-IP further supported the conclusion. Together, these results demonstrate that membrane-associated ALIX can form a dimer through the interaction between the V domains.

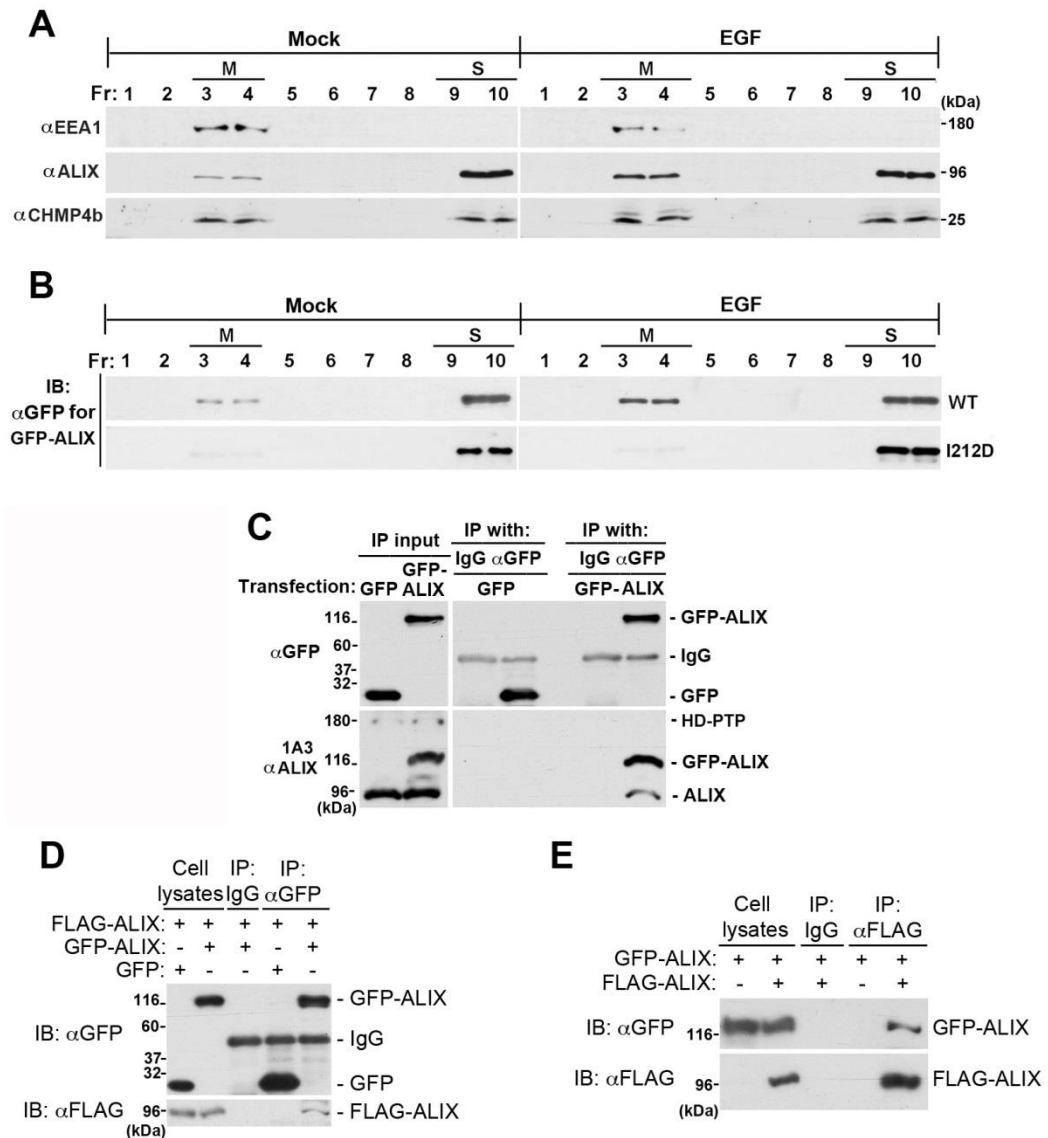


**Figure 8. EGF-induced EGFR activation promotes ALIX interaction with membrane-bound CHMP4.** (A) HEK293 cells were serum starved for 12 h and either mock-treated or stimulated with 100 ng/ml EGF for 1 h. The PNS was fractionated by membrane flotation centrifugation and 10 fractions were taken by pipette for each sample. The same volume of aliquot from each fraction was taken and immunoblotted with indicated antibodies to visualize EEA1, ALIX and CHMP4b. (B) HEK293 cells were transfected with WT or I212D GFP-ALIX and serum starved for 12 h before being processed as described for (A). (C) HEK293 cells were transfected with GFP or GFP-

ALIX. Lysates of the transfected cells were immunoprecipitated with IgG or anti-GFP antibody, and immunocomplexes were immunoblotted with indicated antibodies to visualize GFP and GFP-ALIX (top panel) and endogenous ALIX, GFP-ALIX and endogenous HD-PTP (lower panel). (D) HEK293 cells were transfected with FLAG-ALIX and either GFP or GFP-ALIX. The crude cell lysates were immunoprecipitated with anti-GFP antibody or IgG. Input cell lysates and immunocomplexes were then immunoblotted with indicated antibodies to visualize GFP, GFP-ALIX and FLAG-ALIX. (D) HEK293 were transfected with GFP-ALIX and either FLAG or FLAG-ALIX. The crude cell lysates were immunoprecipitated with anti-FLAG antibody or IgG. Input cell lysates were immunocomplexes were then immunoblotted with indicated antibodies to visualize GFP-ALIX and FLAG-ALIX.

### **2.3. ALIX plays a pivotal role in MVB sorting of activated EGFR**

The previous results showing that ALIX binds activated and ubiquitinated EGFR and that EGFR activation promotes ALIX association with membrane-bound CHMP4 generated a hypothesis that ALIX is positively involved in MVB sorting of activated EGFR. To test this hypothesis, I first examined MVB sorting of activated EGFR by using proteinase K protection assay, which involves isolation of intracellular membrane vesicles after the plasma membrane is specifically dissolved by digitonin treatment. The membrane vesicles were digested by proteinase K in the presence or absence of 0.1% Triton X-100. Since proteinase K cannot digest the EGFR that localizes within the lumen of the intact endosome, the percentage of proteinase K-insensitive EGFR in the absence of 0.1% Triton X-100 indicates the percentage of activated EGFR that is sorted into ILVs of MVB (Dores et al., 2012a; Malerod et al., 2007). As shown in Fig. 9A, after EGF stimulation for 30 min, the percentage of proteinase K-insensitive EGFR increased from ~5% to ~60%. EEA1, which is the peripheral endosome membrane protein, was used to demonstrate the efficient digestion by proteinase K.

To determine whether ALIX interaction with CHMP4 is required to support MVB sorting of activated EGFR under EGF continuous stimulation condition, I transfected HEK293 cells with FLAG-ALIX<sub>Bro1</sub> to compete with endogenous ALIX in binding CHMP4 and examined the effect on MVB sorting of activated EGFR. As shown in Fig. 9B, ectopically expressing WT FLAG-ALIX<sub>Bro1</sub>, but not I212D FLAG-ALIX<sub>Bro1</sub>, dramatically reduced the percentage of proteinase K-insensitive EGFR from ~60% to ~5%. The results demonstrate that ALIX interaction with CHMP4 plays an essential role in MVB sorting of activated EGFR.

To determine whether V domain-mediated ALIX dimerization is required to support MVB sorting of activated EGFR under EGF continuous stimulation condition, I transfected HEK293 cells with HA-ALIX<sub>V</sub> to compete with endogenous ALIX in dimerization and examined the effects on MVB sorting of activated EGFR. As shown in Fig. 9C, ectopically expressing WT HA-ALIX<sub>V</sub>, but not dimerization mutated (DM) HA-ALIX<sub>V</sub>, dramatically reduced the percentage of proteinase K-insensitive EGFR from ~60% to ~5%. Co-IP assay demonstrated that ectopically expressing WT HA-ALIX<sub>V</sub> interacts with ALIX, but not HD-PTP, excluding the possibility that the inhibitory effects of WT HA-ALIX<sub>V</sub> is due to the interaction with HD-PTP (Fig. 9D). The results demonstrate that V domain-mediated ALIX dimerization is required for ALIX to support MVB sorting of activated EGFR.

To further determine the role of ALIX in MVB sorting of activated EGFR under EGF continuous stimulation condition, I transfected HEK293 cells with ALIX targeting siRNA (si-ALIX) with or without co-expressing siRNA-insensitive GFP-ALIX (GFP-ALIX\*) and examined the effects on MVB sorting of activated EGFR. As shown in Fig. 9E, knockdown of ALIX decreased the percentage of proteinase K-insensitive EGFR from ~50% to ~15%. While ectopic expression of WT GFP-ALIX\* rescued the inhibitory effects of ALIX knockdown, ectopic expression of I212D GFP-ALIX\* or DM GFP-ALIX\* did not have this rescuing effect. These results further demonstrate that CHMP4-bound ALIX dimer plays an essential role in MVB sorting of activated EGFR.

Multiple previous studies used EGF pulse-chase condition to study the role of ALIX in degradation of activation of EGFR. Here, I examined the role of CHMP-4 bound ALIX dimer in MVB sorting of activated EGFR under EGF pulse-chase condition. Serum-starved cells were incubated with EGF at 4°C for 30 min (EGF pulse) and then



cultured at 37°C in the absence of EGF (chase) for indicated lengths of time. As shown in Fig. 9F, ectopic expression of WT HA-ALIX<sub>V</sub> or FLAG-ALIX<sub>Bro1</sub>, or knockdown of ALIX decreased percentage of protected EGFR from ~40% to <10% under EGF pulse-chase condition.

Together, these results demonstrate that CHMP4-bound ALIX dimer plays an essential role in MVB sorting of activated EGFR under both EGF continuous stimulation condition and EGF pulse-chase condition.

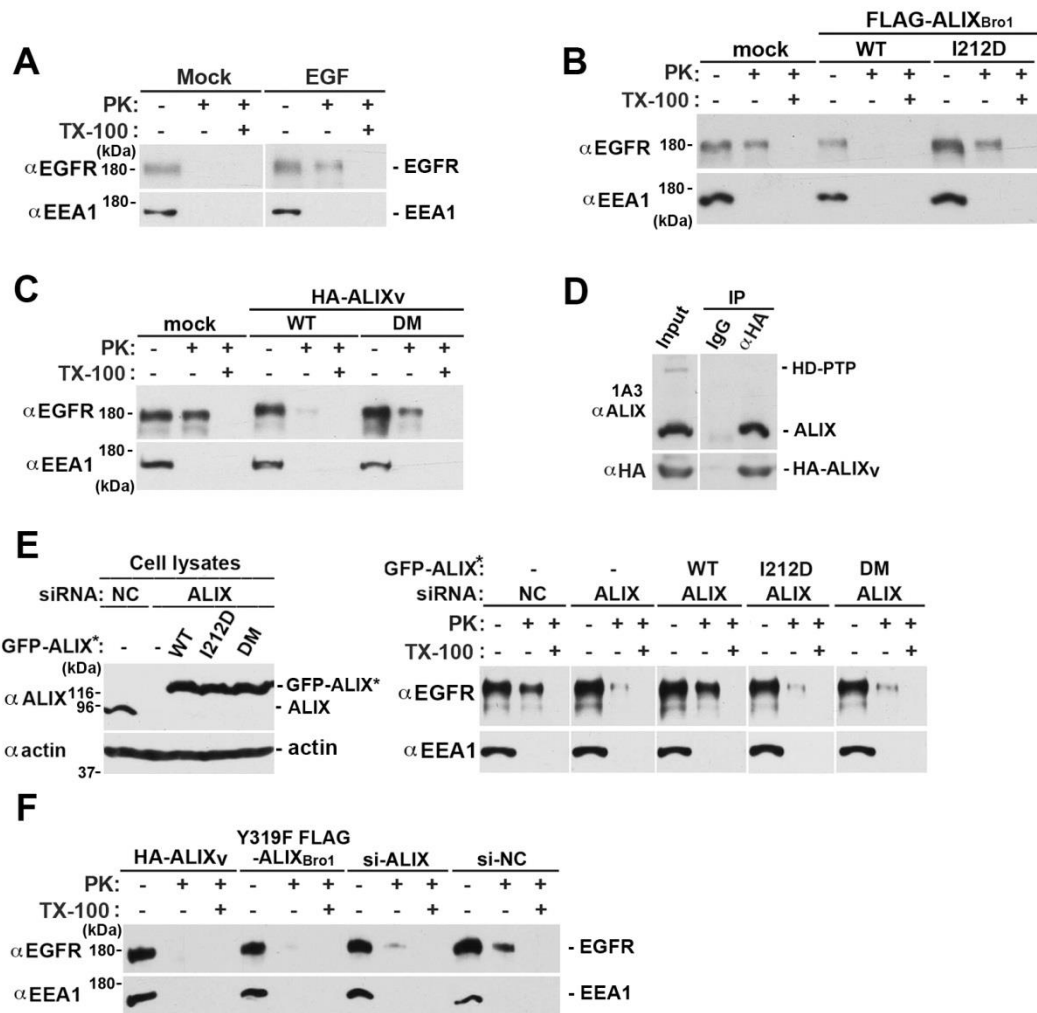


**Figure 9. ALIX plays a pivotal role in MVB sorting of activated EGFR.** (A) HEK 293 cells were mock-treated or EGF stimulated for 30 min. The proteinase K protection assay was performed to determine the percentage of proteinase K-insensitive EGFR. (B) HEK293 cells were transfected with FLAG, FLAG-ALIX<sub>Bro1</sub> or I212D FLAG-ALIX<sub>Bro1</sub>. The proteinase K protection assay was performed to determine the percentage of proteinase K-insensitive EGFR. (C) HEK293 cells were transfected with HA, WT HA-ALIX<sub>v</sub>, or DM HA-ALIX<sub>v</sub>. The proteinase K protection assay was performed to determine the percentage of proteinase K-insensitive EGFR. (D) HEK293 cells were transfected with HA-ALIX<sub>v</sub>, and the cell lysates were immunoprecipitated with anti-HA antibody or IgG. Input and immunocomplexes were immunoblotted with indicated

antibodies to visualize endogenous ALIX, endogenous HD-PTP and HA-ALIX<sub>v</sub>. (E) HEK293 cells were first transfected with si-NC or si-ALIX and cultured for 48 h. These cells were then transfected with constructs for indicated proteins and cultured for another 24 h. The proteinase K protection assay was performed to determine the percentage of proteinase K-insensitive EGFR. (F) HEK293 cells were transfected as indicated and stimulated with 100 ng/ml EGF under pulse-chase condition. The proteinase K protection assay was performed to determine the percentage of proteinase K-insensitive EGFR.

## **2.4. ALIX plays an important role in terminating the downstream signaling of activated EGFR**

ERK1/2 is the major downstream signaling of activated EGFR, and EGF-induced ERK1/2 activation is a highly transient event (Xu et al., 2012), due to the rapid silencing of activated EGFR by MVB sorting and the dephosphorylation by phosphatase.

To further support the conclusion that ALIX plays an essential role in MVB sorting of activated EGFR, I examined the roles of ALIX interaction with membrane-bound CHMP4 in terminating the downstream signaling of activated EGFR. For this purpose, HEK293 cells were transfected with Y319F FLAG-ALIX<sub>Bro1</sub> and the effects on the kinetics of EGF-induced ERK1/2 activation were examined under EGF continuous stimulation condition. The construct contains Y319F mutation to eliminate its interaction with Src (Schmidt et al., 2005). As shown in Fig. 10A, under EGF continuous stimulation condition, ERK1/2 activation was highly transient in mock-transfected cells, reaching to the peak level at 10 min and then decreasing dramatically to the basal level at 30 min. The ERK1/2 activation continued decreasing afterward to nearly undetectable level from 1 h to 3 h. In contrast, ectopic expression of Y319F FLAG-ALIX<sub>Bro1</sub> inhibited the decrease of ERK1/2 activation and prolonged the duration of ERK1/2 activation up to 3 h.

To determine whether V domain-mediated ALIX dimerization plays an important role in terminating the downstream signaling of activated EGFR, HEK293 cells were transfected with HA-ALIX<sub>V</sub> and the effects on the kinetics of EGF-induced ERK1/2 activation were examined under EGF continuous stimulation condition. Similar to the ectopic expression of Y319F FLAG-ALIX<sub>Bro1</sub>, ectopic expression of HA-ALIX<sub>V</sub> also prolonged the duration of ERK1/2 activation up to 3 h (Fig. 10B).

To further determine the role of ALIX in terminating the downstream signaling of activated EGFR, HEK293 cells were transfected with control siRNA or si-ALIX and the effects on the kinetics of EGF-induced ERK1/2 activation were examined under EGF continuous stimulation condition. Similarly, knockdown of ALIX prolonged the duration of ERK1/2 activation up to 3 h (Fig. 10C).

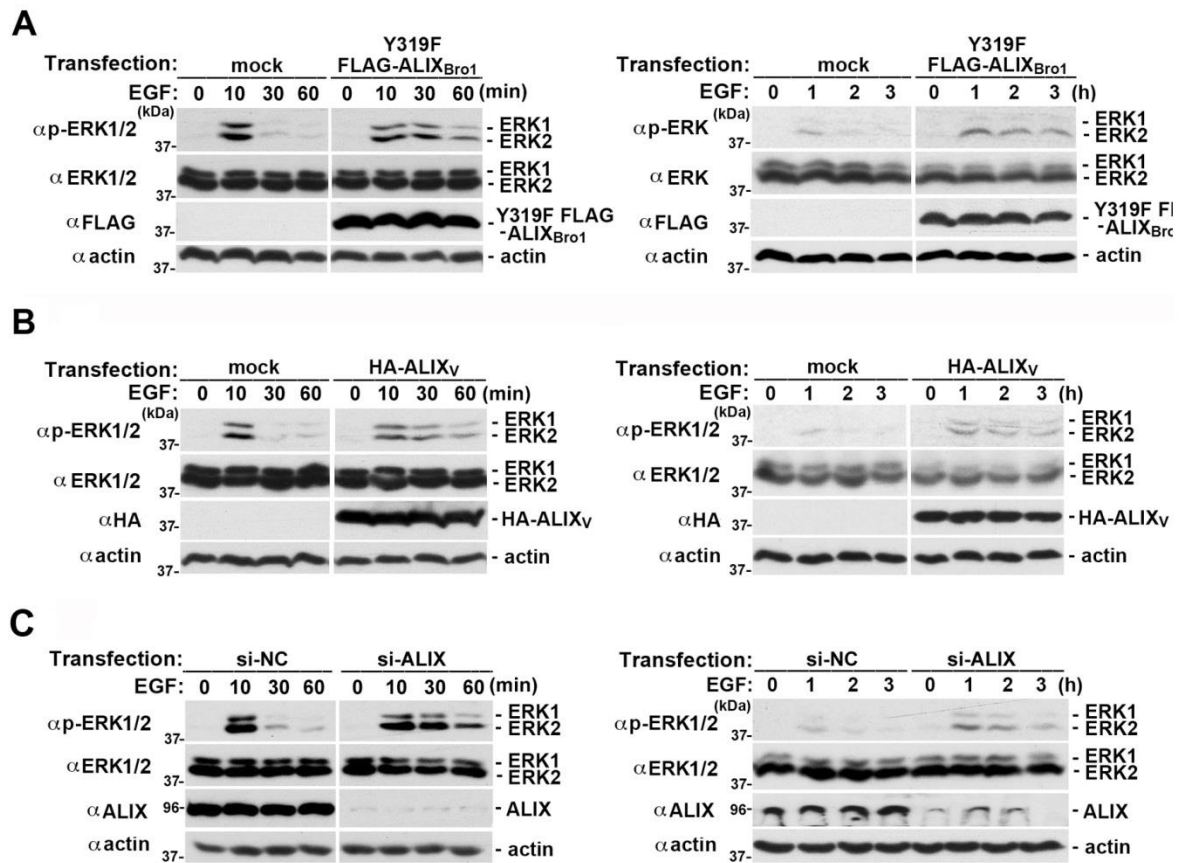


**Figure 10. ALIX plays an important role in terminating the downstream signaling of activated EGFR under EGF continuous stimulation condition.** (A) HEK293 cells were transfected with FLAG or Y319F FLAG-ALIX<sub>Bro1</sub> and were stimulated with 100 ng/ml EGF for indicated minutes (left panel) or hours (right panel). Cell lysates were immunoblotted with indicated antibodies to visualize phosphorylated ERK1/2 (p-ERK1/2), ERK1/2, FLAG-ALIX<sub>Bro1</sub> and actin. (B) HEK293 cells were transfected with HA or HA-ALIX<sub>V</sub> and were stimulated with 100 ng/ml EGF for indicated minutes (left panel) or hours (right panel). Cell lysates were immunoblotted with indicated antibodies to visualize p-ERK1/2, ERK1/2, HA-ALIX<sub>V</sub> and actin. (C) HEK293 cells were transfected with indicated siRNAs and stimulated with 100 ng/ml EGF for indicated minutes (left

panel) or hours (right panel). Cell lysates were immunoblotted with indicated antibodies to visualize p-ERK1/2, ERK1/2, ALIX and actin.

Then, I further determined whether ALIX plays an important role in terminating the downstream signaling of activated EGFR under EGF pulse-chase condition. Similar to the results obtained under EGF continuous stimulation condition, EGF-induced ERK1/2 activation decreased to nearly undetectable level from 1 h to 3 h. Ectopic expression of FLAG-ALIX<sub>Bro1</sub> or HA-ALIX<sub>V</sub>, or transfection of si-ALIX inhibited the decrease and prolonged the duration of ERK1/2 activation up to 3 h (Fig. 11A-C).

Together, these results demonstrate that CHMP4-bound ALIX dimer plays an important role in rapidly terminating the downstream signaling of activated EGFR under both EGF continuous stimulation and pulse-chase conditions and further support the essential role of CHMP4-bound ALIX dimer in MVB sorting of activated EGFR.



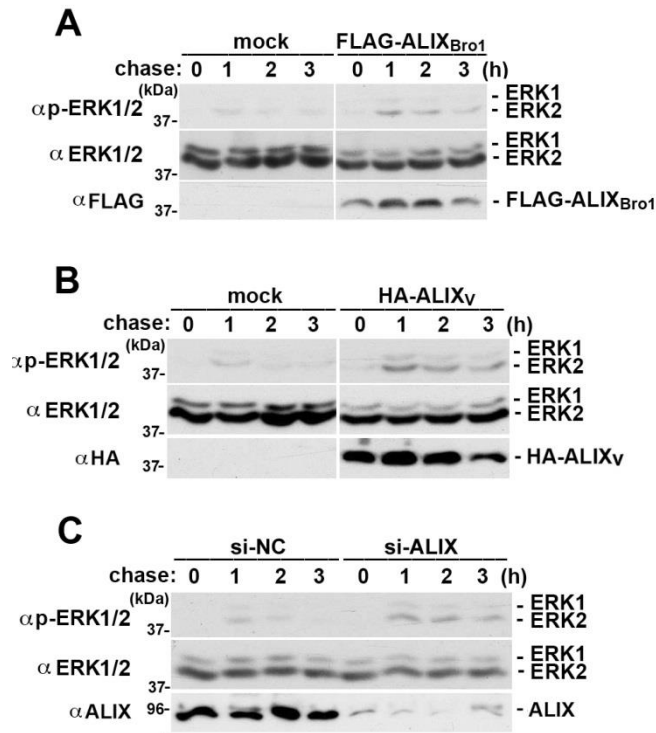


**Figure 11. ALIX plays an important role in terminating the downstream signaling of activated EGFR under EGF pulse-chase condition.** (A) HEK293 cells were transfected with FLAG or Y319F FLAG-ALIX<sub>Bro1</sub> and stimulated with 100 ng/ml EGF for 30 min (pulse) followed by incubation for indicated hours (chase). Cell lysates were immunoblotted with indicated antibodies to visualize p-ERK1/2, ERK1/2, FLAG-ALIX<sub>Bro1</sub> and actin. (B) HEK293 cells were transfected with HA or HA-ALIX<sub>v</sub> and stimulated with 100 ng/ml EGF for 30 min (pulse) followed by incubation for indicated hours (chase). Cell lysates were immunoblotted with indicated antibodies to visualize p-ERK1/2, ERK1/2, HA-ALIX<sub>v</sub> and actin. (C) HEK293 cells were transfected with indicated siRNAs and stimulated with 100 ng/ml EGF for 30 min (pulse) followed by incubation for indicated hours (chase). Cell lysates were immunoblotted with indicated antibodies to visualize p-ERK1/2, ERK1/2, ALIX and actin.

## **2.5. Depleting the CHMP4-bound ALIX dimer retards EGF-induced degradation of activated EGFR**

To determine whether ALIX-supported MVB sorting is required for EGF-induced degradation of activated EGFR, I examined the effects of depleting CHMP4-bound ALIX dimer on the kinetics of EGF-induced EGFR degradation under both EGF continuous stimulation and EGF pulse-chase conditions.

To determine whether ALIX interaction with membrane-bound CHMP4 plays a role in degradation of activated EGFR under EGF continuous stimulation condition, HEK293 cells were transfected with FLAG, Y319F FLAG-ALIX<sub>Bro1</sub> or Y319F-I212D FLAG-ALIX<sub>Bro1</sub> and stimulated with EGF for different time points. EGF stimulation induced progressive reduction in EGFR protein level in mock-transfected and Y319F-I212D FLAG-ALIX<sub>Bro1</sub> transfected cells. In contrast, ectopic expression of Y319F FLAG-ALIX<sub>Bro1</sub> inhibited EGFR degradation and increased the percentages of remaining EGFR at 1, 2, 3 and 4 h (Fig. 12A).

To determine whether V domain-mediated ALIX dimerization plays a role in the degradation of activated EGFR under EGF continuous stimulation condition, HEK293 cells were transfected with HA, WT HA-ALIX<sub>V</sub> or DM HA-ALIX<sub>V</sub> and stimulated with EGF for different time points. Similar to the results of ectopic expression of FLAG-ALIX<sub>Bro1</sub>, ectopic expression of WT HA-ALIX<sub>V</sub>, but not DM HA-ALIX<sub>V</sub>, increased the percentages of remaining EGFR at 30 min, 1, 2, 3 and 4 h (Fig. 12B).

To further determine the role of CHMP-4 bound ALIX dimer in the degradation of activated EGFR under EGF continuous stimulation condition, HEK293 cells were transfected with si-ALIX with or without co-transfection of indicated forms of GFP-ALIX\*

and the effects on degradation of activated EGFR were examined. As shown in Fig. 12C-E, EGF continuous stimulation induced a progressive reduction in EGFR protein level in mock-transfected cells. In contrast, knockdown of ALIX increased the percentages of remaining EGFR at 1, 2, 3 and 4 h. Although ectopic expression of WT GFP-ALIX\* could rescue the effects of ALIX knockdown, ectopic expression of I212D GFP-ALIX\* or DM GFP-ALIX\* did not have the rescuing effects.

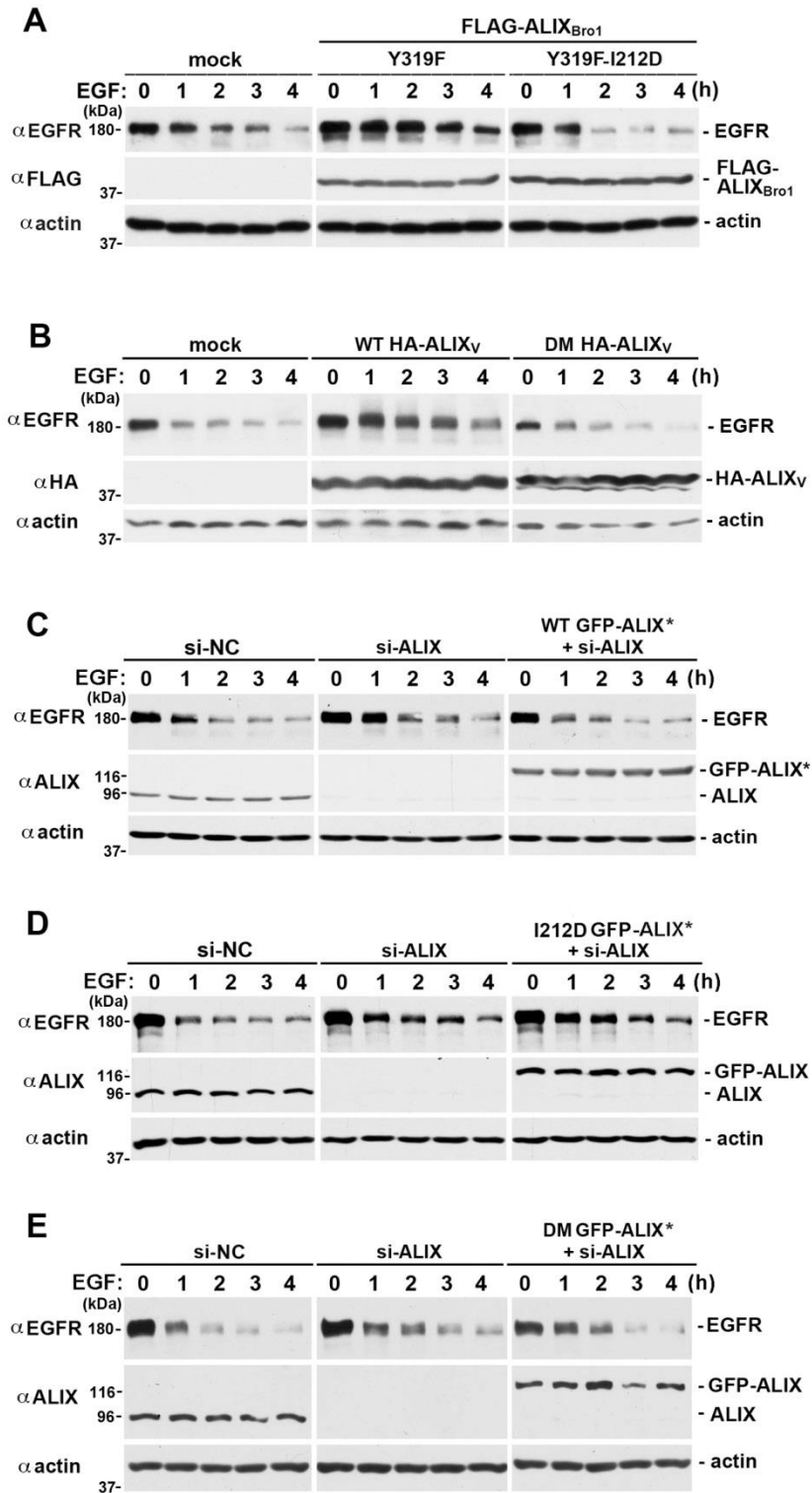


**Figure 12. Depletion of the CHMP4-bound ALIX dimer retards EGF-induced degradation of activated EGFR under EGF continuous stimulation condition. (A)** HEK293 cells were transfected with FLAG and indicated forms of FLAG-ALIX<sub>Bro1</sub> and

stimulated with 100 ng/ml EGF for indicated hours. Cell lysates were immunoblotted with indicated antibodies to visualize EGFR, FLAG-ALIX<sub>Bro1</sub> and actin. (B) HEK293 cells were transfected with HA and indicated forms of HA-ALIX<sub>V</sub> expressing cells and stimulated with 100 ng/ml EGF for indicated hours. Cell lysates were immunoblotted with indicated antibodies to visualize EGFR, HA-ALIX<sub>V</sub> and actin. (C-E) HEK293 cells transfected with indicated siRNA and indicated siRNA-insensitive constructs were stimulated with 100 ng/ml EGF for indicated hours. Cell lysates were immunoblotted with indicated antibodies to visualize EGFR, ALIX, GFP-ALIX and actin.

To determine the role of CHMP4-bound ALIX dimer in the degradation of activated EGFR under EGF pulse-chase condition, the effects of ectopic expression of Y319F FLAG-ALIX<sub>B01</sub> or HA-ALIX<sub>V</sub> or knockdown of ALIX on degradation of activated EGFR were examined. As shown in Fig. 13, EGF pulse-chase stimulation induced a progressive reduction in EGFR protein level in mock-transfected cells. Ectopic expression of Y319F FLAG-ALIX<sub>B01</sub> or HA-ALIX<sub>V</sub> increased the percentages of remaining EGFR at 1 and 2 h. Knockdown of ALIX only increased the percentage of remaining EGFR at 1 h.

All these results demonstrate that ALIX-supported MVB sorting of activated EGFR is not essential for trafficking of activated EGFR to lysosomes for degradation.

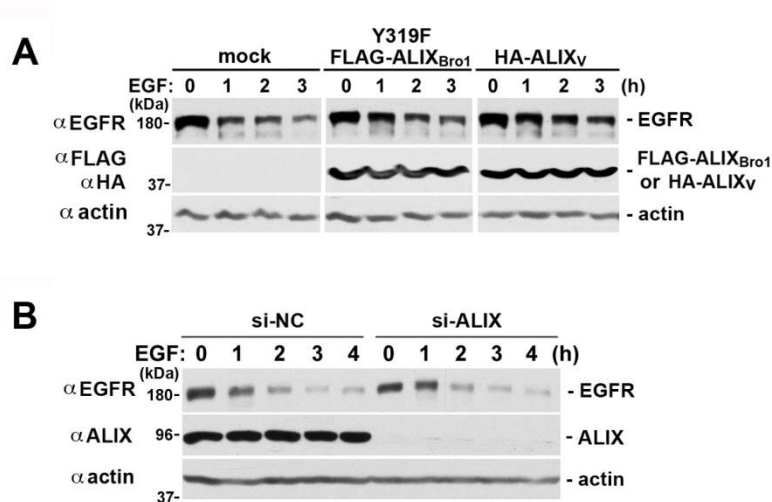


**Figure 13. Depletion of the CHMP4-bound ALIX dimer retards EGF-induced degradation of activated EGFR under EGF pulse-chase condition.** (A) HEK293 cells were mock-transfected or transfected with Y319F FLAG-ALIX<sub>Bro1</sub> or HA-ALIX<sub>V</sub> and stimulated with 100 ng/ml EGF for 30 min (pulse) followed by incubation for indicated hours (chase). Cell lysates were immunoblotted with indicated antibodies to visualize EGFR, FLAG-ALIX<sub>Bro1</sub> HA-ALIX<sub>V</sub> and actin. (B) HEK293 cells were transfected with indicated siRNAs and stimulated with 100 ng/ml EGF for 30 min (pulse) followed by incubation for indicated hours (chase). Cell lysates were immunoblotted with indicated antibodies to visualize EGFR, ALIX and actin.

## Discussion

Although my current study clearly demonstrate that the CHMP4-bound ALIX dimer plays an essential role in MVB sorting and silencing of activated EGFR under both EGF continuous stimulation and pulse-chase conditions, multiple previous studies led to a widely held notion that ALIX is not critically involved in ESCRT-mediated MVB sorting of ubiquitinated receptors due to the obtained negative results that ALIX knockdown had no or only a minor inhibitory effect on trafficking of activated EGFR to lysosomes for degradation under the EGF pulse-chase stimulation condition (Bowers et al., 2006; Cabezas et al., 2005; Doyotte et al., 2008; Schmidt et al., 2004). In this study, I demonstrate the validity of the previous observations that ALIX is not essential for lysosome-dependent degradation of activated EGFR. However, the previous studies did not directly examine the effects of ALIX knockdown on MVB sorting of activated EGFR; instead, they used lysosome-dependent degradation of activated EGFR as the indicator of MVB sorting because of a widely held notion that MVB sorting is required for trafficking activated EGFR to lysosome for degradation. However, multiple studies showed that even the MVB sorting process is inhibited, cell surface receptors can still be delivered to lysosome for degradation, although at a slower rate (Futter et al., 2001; White et al., 2006). These studies, together with my current studies, support a logical explanation that trafficking of activated EGFR to lysosomes for degradation in mammalian cells can be achieved through both MVB sorting-dependent and -independent mechanism and that ALIX is only involved in the MVB sorting-dependent mechanism.

Although MVB sorting is not required for trafficking of activated EGFR to lysosome for degradation in mammalian cells, it can work with a tyrosine phosphatase



to terminate the downstream signaling of activated EGFR much earlier than EGFR degradation. My results show that under both EGF continuous and pulse-chase stimulation conditions, inhibition of the ALIX-supported MVB sorting of activated EGFR prolong the duration of EGF-induced activation of ERK1/2 from <20 min to >2 h. These results indicate that ALIX-supported MVB sorting is one of the major players in rapidly silencing the signaling function of activated EGFR and predict that cells may regulate the signaling output of activated EGFR or possibly other receptor tyrosine kinases through regulating whether activated receptor is degraded through MVB sorting pathway or the alternative pathway.

### **Chapter 3: The mechanism that activates ESCRT function of ALIX in MVB sorting of activated EGFR**

Contents of this chapter are based on Sun, S., Zhou, X., Corvera, J., Gallick, G.E., Lin, S., Kuang, J. ALG-2 activates the MVB sorting function of ALIX through relieving its intramolecular interaction. *Cell Discovery* 2015; 1,15018. doi:10.1038/celldisc.2015.18

Copyright permission is not required. Nature Publishing Group policy states “You may reuse this material without obtaining permission from Nature Publishing Group, providing that the author and the original source of publication are fully acknowledged, as per the terms of the license.”

#### **Background**

The studies from the previous chapter demonstrate the essential role of ALIX in ESCRT-mediated MVB sorting of activated EGFR. ALIX involvement in ESCRT-mediated processes requires ALIX interaction with CHMP4. However, the native form of ALIX contains a default intramolecular interaction, which renders a closed conformation of ALIX and prohibits ALIX interaction with CHMP4 (Zhou et al., 2009; Zhou et al., 2010). This predicts that ALIX involvement in ESCRT-mediated processes requires an activation step that relieves the intramolecular interaction of ALIX.

ALG-2 was originally identified through a functional screen of genes critical for T-cell receptor (TCR)-induced programmed cell death in T cell hybridoma (Vito et al.,

1996). ALG-2 is a 22 kDa calcium-binding protein that interacts with ALIX in a calcium-dependent manner (Missotten et al., 1999; Vito et al., 1999). ALG-2 possesses two high-affinity calcium-binding sites (Lo et al., 1999) and mutation of the Glu<sup>47</sup> and Glu<sup>114</sup> residues to Ala (E47A/E114A) within both calcium-binding sites completely disrupts the calcium-binding capacity of ALG-2 (Lo et al., 1999). Calcium binding induces conformational change of ALG-2 and enables ALG-2 to bind four consecutive PxY motifs (PPYPTYPGYPGY at 802-813) near the C-terminus of ALIX (Missotten MTrioulier et al., 2004; Shibata et al., 2004). There is a spliced form of ALG-2, named as ALG-2.1, which lacks the amino acid residues Gly<sup>121</sup> and Phe<sup>122</sup>. Although ALG-2.1 is still able to bind to calcium, it cannot interact with ALIX (Marsh and McMahon, 1999).

The ALG-2 binding region in ALIX (802-813) is outside the region that forms intramolecular interaction (1-746). Thus, the intramolecular interaction of ALIX should not block ALIX interaction with ALG-2. Indeed, ALG-2 has been shown to be able to bind native form of recombinant ALIX in a calcium-dependent manner (Missotten et al., 1999; Vito et al., 1999). Moreover, inhibiting ALX interaction with ALG-2 by ectopic expression of a C-terminal fragment of ALIX or mutation of the ALG-2 binding site in ALIX attenuated the ability of ALIX in apoptotic induction (Mahul-Mellier et al., 2006; Mahul-Mellier et al., 2008), indicating that ALG-2 may be the regulator of the functions of ALIX. Due to its characteristics of calcium-binding, ALG-2 belongs to calmodulin superfamily, and the calmodulin has been demonstrated to regulate the conformational change of its partner proteins through relieving the intramolecular interaction of these partner proteins (Hoffman et al., 2011), indicating that ALG-2 may be able to regulate ALIX through similar mechanisms. Endocytosis of activated receptor tyrosine kinases, which precedes MVB sorting, induces a rapid increase of calcium concentration in the

vicinity of endosome (Gerasimenko et al., 1998; Gerasimenko and Tepikin, 2005), indicating that internalization of activated EGFR may be linked to ALG-2 conformational change and its interaction with ALIX. Moreover, the studies from the previous graduate student in our group, Xi Zhou, showed that knockdown of ALG-2 retarded degradation of ectopically expressed EGFR in HEK293 cells.

All these observations predict that calcium-dependent ALG-2 interaction with ALIX may be one of the mechanisms by which the intramolecular interaction of ALIX is relieved and the ESCRT functions of ALIX are activated. The preliminary data from the previous graduate student in our group also indicated that calcium-dependent ALG-2 interaction with ALIX may induce the open conformation of ALIX. To further test this prediction, a series of conformation-sensitive and -insensitive anti-ALIX monoclonal antibodies, which were produced in our previous studies (Zhou et al., 2009; Zhou et al., 2008), were used to examine the conformational change of ALIX. Conformation-sensitive anti-ALIX antibodies 1A3 and 2H12 recognize Patch 2/Src binding site and F676 pocket/Viral Gag binding site, respectively. In contrast, conformation-insensitive anti-ALIX antibodies 1A12 and 3A9 recognize the epitope in the V domain that is not blocked by intramolecular interaction. Thus, the 1A3 and 2H12 antibodies only immunoprecipitate ALIX in its open conformation; the 1A12 and 3A9 antibodies immunoprecipitate ALIX in both open and closed conformations.

My study demonstrates that calcium-dependent ALG-2 interaction with ALIX relieves the intramolecular interaction of ALIX and specifically activates the MVB sorting function of ALIX.

## **Results**

### **3.1. Calcium-dependent ALG-2 interaction with ALIX transforms ALIX from closed conformation to open conformation**

I first verified the calcium-dependent ALG-2 interaction with ALIX in our experimental system by using GST pull-down. In the presence of 10  $\mu\text{M}$   $\text{CaCl}_2$  but absence of EGTA, GST-ALG-2 pulled down ALIX from HEK293 cytosolic proteins prepared without detergent. In the presence of EGTA but absence of  $\text{CaCl}_2$ , GST-ALG-2 did not pull down detectable level of ALIX. In the absence of  $\text{CaCl}_2$  and EGTA, GST-ALG-2 still pulled down detectable level of ALIX, although the level is much less than that in the presence of  $\text{CaCl}_2$ , possibly due to the endogenous calcium in the cytosolic protein lysate (Fig. 14A). I also verified that WT GST-ALG-2, but not E47A/E114A (Mut) GST-ALG-2, pulled down ALIX from HEK293 cytosolic proteins in the presence of 10  $\mu\text{M}$   $\text{CaCl}_2$  (Fig. 14B).

To determine whether calcium-dependent ALG-2 interaction with ALIX relieves the intramolecular interaction of ALIX, I added GST or GST-ALG-2 to the cytosolic fraction of HEK293 cells and immunoprecipitated ALIX with the 2H12 or 1A12 antibodies in the absence of detergent. Due to the background level of calcium in the cytosolic fraction, which may activate a small portion of GST-ALG-2, the 2H12 antibody immunoprecipitated a low level of ALIX from cytosolic fraction incubated with GST-ALG-2. As a positive control, the 1A12 antibody immunoprecipitated similar level of ALIX from cytosolic fraction incubated with GST or GST-ALG-2 (Fig. 14C).

Since the intramolecular interaction of ALIX prohibits ALIX interaction with its partner proteins, such as CHMP4 and TSG101, I further determined the effects of calcium-dependent ALG-2 interaction with ALIX on the conformational change of ALIX by examining the co-IP of ALIX and its partner proteins. For this purpose, I added

noting,  $\text{CaCl}_2$ , or  $\text{CaCl}_2$  plus GST-ALG-2 to the cytosolic fraction of HEK293 cells ectopically expressing FLAG-CHMP4b or FLAG-TSG101 and immunoprecipitated FLAG-CHMP4b or FLAG-TSG101 with an anti-FLAG antibody in the absence of detergent. The results showed that cytosolic ALIX did not immunoprecipitate with FLAG-CHMP4b or FLAG-TSG101 in control cells. In the presence of  $\text{CaCl}_2$ , detectable level of ALIX was immunoprecipitated with FLAG-CHMP4b or FLAG-TSG101. In the presence of  $\text{CaCl}_2$  and GST-ALG-2, much higher level of ALIX was immunoprecipitated with FLAG-CHMP4b or FLAG-TSG101 (Fig. 14D-E). These results demonstrate that calcium-dependent ALG-2 interaction with cytosolic ALIX relieves the intramolecular interaction of ALIX and transforms ALIX from closed conformation to open conformation.

To determine whether ALG-2-induced open formation of ALIX is reversible, I first induced the open conformation ALIX by adding  $\text{CaCl}_2$  plus GST-ALG-2 to cytosolic fractions of HEK293 cells and then dissociated GST-ALG-2 by adding EGTA to cytosolic fractions of the cells. As shown in Fig. 14F-G, adding  $\text{CaCl}_2$  plus GST-ALG-2 relieved the intramolecular interaction of cytosolic ALIX, as demonstrated by immunoprecipitation with the 1A3 antibody. Adding EGTA reversed the conformational change of ALIX. However, if the cytosolic fractions contained ectopic expressing FLAG-TSG101, GST-p6 or GST-p9 before adding EGTA, then EGTA treatment only partially reversed the conformational change of ALIX. These results demonstrate that ALG-2-induced conformational change of ALIX is a reversible event and that occupation by partner proteins partially maintains the open conformation of ALIX.

Altogether, these results demonstrate that calcium-dependent ALG-2 interaction with ALIX relieves the intramolecular interaction of ALIX and induces an open

conformation of ALIX and that the open conformation of ALIX can be partially maintained by newly recruited partner proteins after ALG-2 dissociation.





with  $\text{CaCl}_2$  or  $\text{CaCl}_2$  plus GST-ALG-2. These cytosolic proteins were immunoprecipitated followed by immunoblotting with indicated antibodies. (F) GST-ALG-2 plus  $\text{CaCl}_2$  and GST or GST-p6 were added into cytosolic proteins extracted from HEK293 cells and incubated for 30 min. Then, the samples were treated with or without EGTA for 30 min before being immunoprecipitated with the 1A3 antibody. Input and immunocomplexes were immunoblotted with indicated antibodies to visualize ALIX, GST-ALG-2 and GST-p6. (G) The assay was performed as described for (F), except that GST-p6 was changed to GST-p9.

### **3.2. Calcium-dependent ALG-2 interaction with ALIX is essential for CHMP4-dependent ALIX membrane association**

I first determined whether ALIX association with the membrane is dependent on interaction with CHMP4 by using membrane flotation centrifugation. HEK293 cells were transfected with si-NC or a combination of two pairs of si-CHMP4B, and the distribution of ALIX in M fraction was examined. As shown in Fig. 15A, transfection of si-CHMP4B knocked down CHMP4B by ~70% and decreased the percentage of membrane associated ALIX from ~13% to ~5%. EEA1 and actin were used as internal control for membrane proteins and soluble proteins, respectively in order to eliminate the possibility of contamination. The results demonstrate that ALIX association with the membrane is dependent on CHMP4.

To determine the effects of calcium-dependent ALG-2 interaction with ALIX on ALIX membrane association, HEK293 cells were transfected with FLAG or FLAG-ALG-2 and the PNSs were fractionated by using membrane flotation centrifugation. If the cells were briefly treated with calcium ionophore A23187 before collection, ectopic expression of FLAG-ALG-2 increased the percentage of membrane associated ALIX from ~11% to ~53%. However, ectopic expression of FLAG-ALG-2 alone did not significantly increase the percentage of membrane associated ALIX (Fig. 15B-C). These results demonstrate that calcium-dependent ALG-2 interaction with ALIX promotes ALIX association with membrane.

To determine whether ALG-2-induced increase in ALIX membrane association is dependent on CHMP4, HEK293 cells were co-transfected with FLAG-ALG-2 and WT, I212D or ALG-2 binding site-deleted ( $\Delta$ PxY) GFP-ALIX and briefly treated with calcium ionophore A23187 before collection. The results of membrane flotation centrifugation

showed that ectopic expression of FLAG-ALG-2 in conjunction with a brief calcium ionophore A23187 treatment increased WT GFP-ALIX membrane association similarly as it did to the endogenous ALIX. However, I212D or  $\Delta$ PxY mutation abolished GFP-ALIX membrane association (Fig. 15D). These results demonstrate that ALG-2-induced ALIX association with membrane is dependent on ALIX interaction with CHMP4.

To further determine the role of ALG-2 in ALIX association with the membrane, HEK293 cells were transfected with si-NC or si-ALG-2 and the effects on ALIX association with the membrane was determined by membrane flotation centrifugation. The results showed that knockdown of ALG-2 decreased the percentage of membrane associated ALIX from ~13% to ~2-3%, suggesting that ALG-2 plays a physiological role in ALIX association with membrane (Fig. 15E-F).

Altogether, these results demonstrate that  $\text{Ca}^{2+}$ -dependent ALG-2 interaction with ALIX plays a rate-limiting role in CHMP-4 dependent ALIX association with membrane.

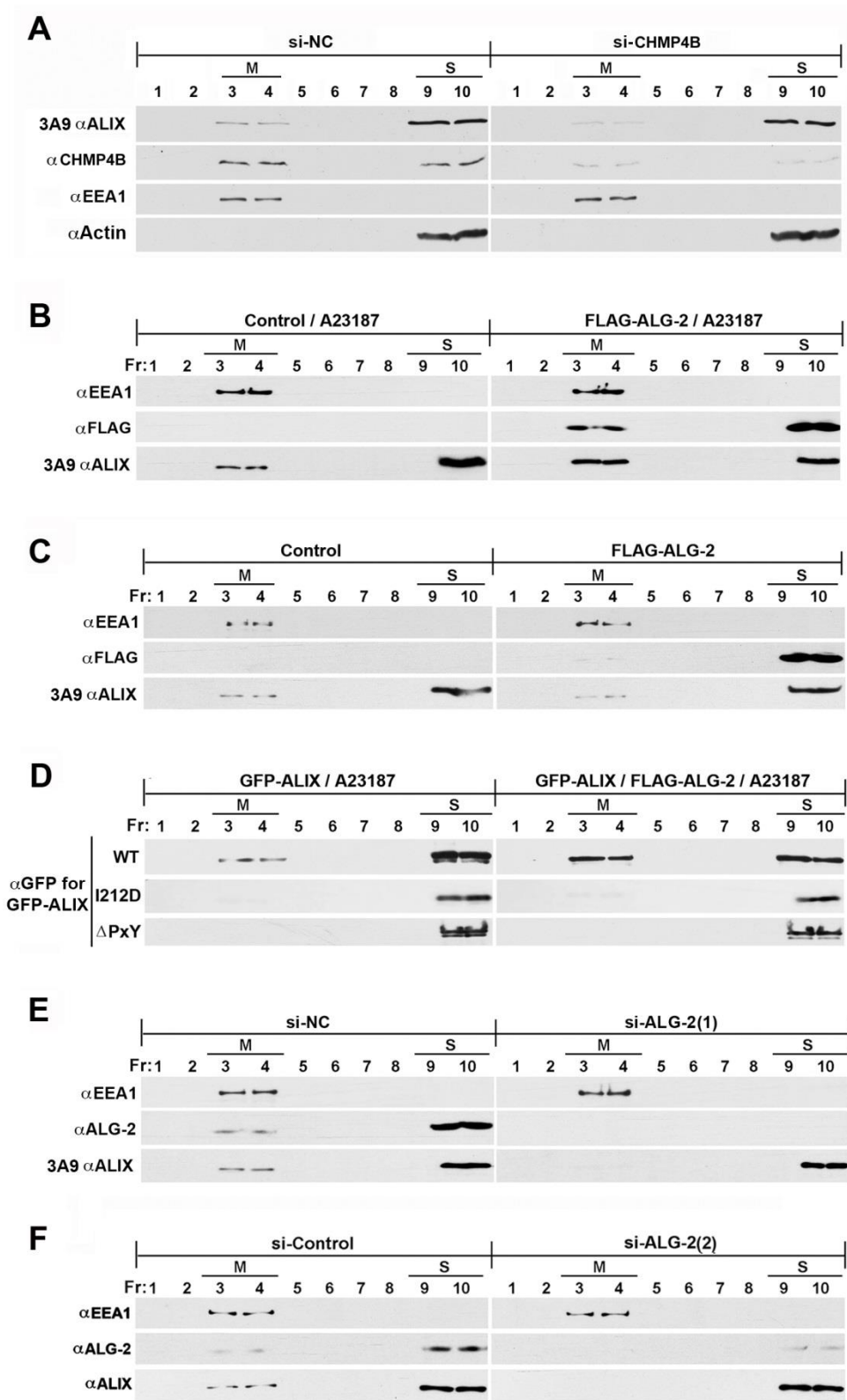


**Figure 15. Calcium-dependent ALG-2 interaction with ALIX is essential for CHMP4-dependent ALIX membrane association.** (A) HEK293 cells were transfected with si-NC or si-CHMP4B. PNSs from the transfected cells were fractionated by membrane flotation centrifugation. M and S protein fractions were immunoblotted to visualize ALIX, CHMP4B, EEA1 and actin. (B) HEK293 cells were transfected with FLAG or FLAG-ALG-2. PNSs were prepared from these transfected cells treated with calcium ionophore A23187 and processed as described in (A). (C) HEK293 cells were transfected with FLAG or FLAG-ALG-2. PNSs were prepared from these transfected cells and processed as described in (A). (D) HEK293 cells were co-transfected with FLAG or FLAG-ALG-2 and indicated forms of GFP-ALIX. PNSs were prepared from these transfected cells treated with calcium ionophore A23187 and processed as described in (A). (E-F) HEK293 cells were transfected with si-NC or si-ALG-2. PNSs were prepared from these transfected cells processed as described in (A).

### **3.3. EGF-induced EGFR activation increases ALIX association with the membrane through promoting ALG-2 interaction with ALIX**

To determine the effects of EGF-induced EGFR activation on ALIX and ALG-2 association with the membrane, HEK293 cells were stimulated with or without 100 ng/ml EGF for 1 h and PNSs were prepared for membrane flotation centrifugation. The results showed that EGF stimulation not only increased the percentage of membrane-associated ALIX from ~12% to ~35%, but also increased the percentage of membrane-associated ALG-2 from ~11% to ~44%. In contrast, the even distribution of CHMP4B between M fraction and S fraction was not changed (Fig. 16A).

To determine whether EGF stimulation promotes ALG-2 interaction with ALIX, HEK293 cells were stimulated with or without EGF and the cell lysates were prepared with 0.1% Triton X-100 to dissolve the membrane and 10  $\mu$ M  $\text{CaCl}_2$ . The results of co-IP showed that EGF stimulation increased ALG-2 interaction with ALIX by ~3.5 fold (Fig.16B).

Since ALG-2 interaction with ALIX is calcium-dependent and endocytosis of cell surface receptors induces a spike of calcium near endosomes, I then determined whether calcium is required for EGF-induced increase in ALIX association with the membrane. For this purpose, HEK293 cells were mock-treated or treated with cell permeable calcium chelator BAPTA-AM before EGF stimulation and the effects of BAPTA-AM treatment on ALIX association with the membrane was examined. As shown in Fig. 16C, BAPTA-AM treatment inhibited EGF-induced increase in ALIX association with the membrane. All these results suggest that calcium-dependent ALG-2 interaction with ALIX is required for EGF-induced increase of ALIX association with the membrane.

To further test this assumption, I knocked down endogenous ALG-2 or overexpressed FLAG-ALG-2 in HEK293 cells and examined the effects on EGF-induced ALIX association with the membrane. As shown in Fig. 16D, knockdown of ALG-2 decreased the percentages of membrane-associated ALIX to barely detectable level in both mock-treated and EGF-stimulated cells. In contrast, overexpression of WT FLAG-ALG-2, but not Mut FLAG-ALG-2, in EGF-stimulated cells increased the percentage of membrane-associated ALIX from ~35% to ~53% (Fig. 16E-F). HEK293 cells were then transfected with WT GFP-ALIX,  $\Delta$ PxY GFP-ALIX or I212D GFP-ALIX and then stimulated with or without EGF. The membrane association of GFP-ALIX was determined by using membrane flotation centrifugation. As shown in Fig. 16G, EGF stimulation increased the membrane association of WT GFP-ALIX. In contrast,  $\Delta$ PxY GFP-ALIX or I212D GFP-ALIX was barely detectable. These results support our assumption.

Altogether, these results demonstrate that EGF stimulation increases ALIX association with the membrane through promoting  $\text{Ca}^{2+}$ -dependent ALG-2 interaction with ALIX.

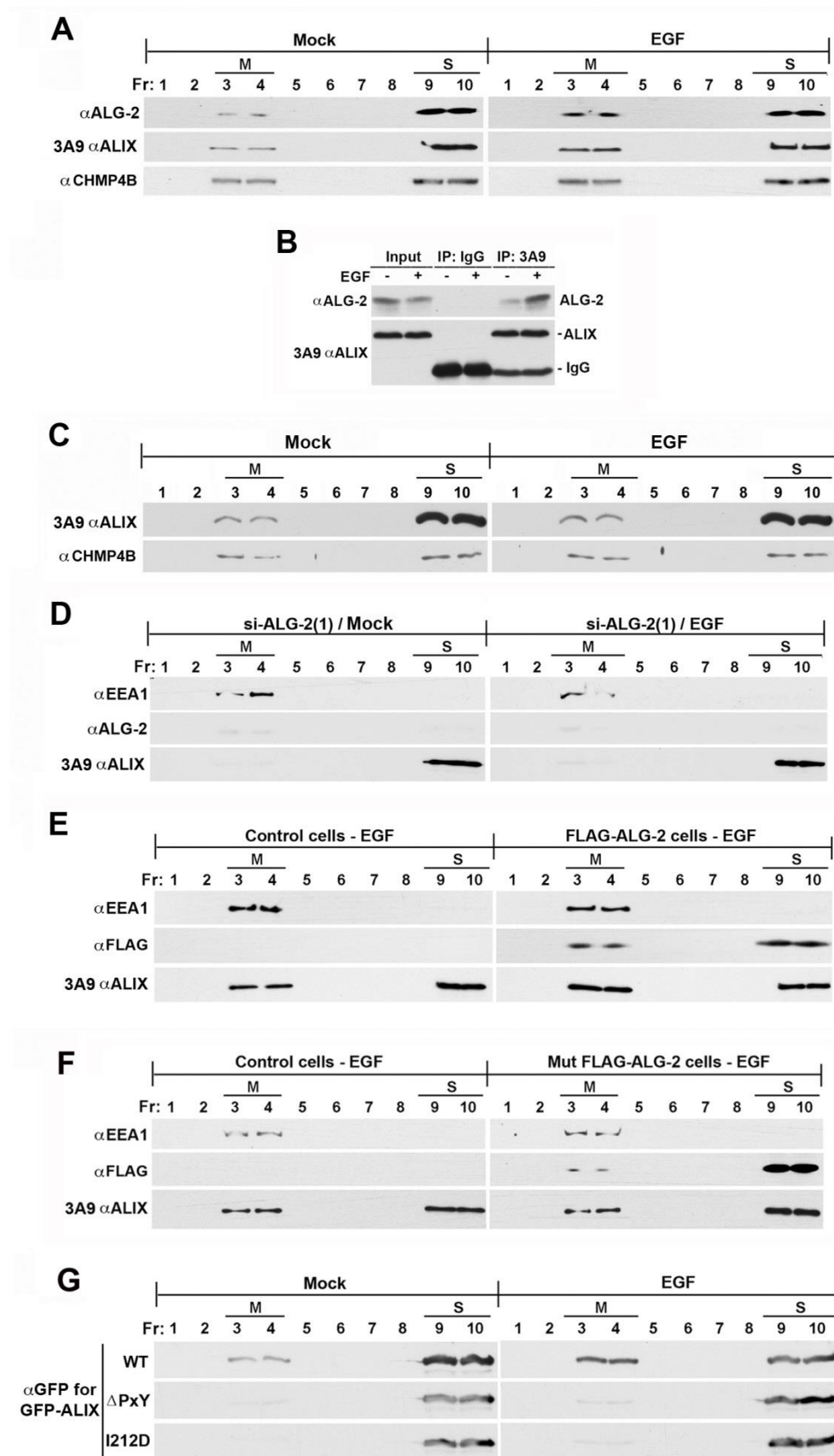




**Figure 16. EGF-induced EGFR activation increases ALIX association with the membrane through promoting ALG-2 interaction with ALIX.** (A) Serum starved HEK293 cells were stimulated with or without EGF for 1 h. PNSs were prepared for membrane flotation centrifugation. (B) Serum starved HEK293 cells were stimulated with or without EGF for 1 h. Cell lysates were prepared in the presence of 0.1% Triton X-100 and 10  $\mu$ M  $\text{CaCl}_2$  and immunoprecipitated with the 3A9 antibody. Input proteins and immunocomplexes were immunoblotted to visualize ALIX and ALG-2. (C) Serum starved HEK293 cells were treated with BAPTA-AM starting 1 h before EGF stimulation. PNSs were prepared for membrane flotation centrifugation. (D) HEK293 cells were transfected with si-ALG-2(1) and serum starved for 12 h before mock-treated or stimulated with EGF for 1 h. PNSs were prepared for membrane flotation centrifugation. (E&F) HEK293 cells were transfected with FLAG or WT FLAG-ALG-2 (E) or Mut FLAG-ALG-2 (F) and serum starved for 12 h before stimulated with EGF for 1 h. PNSs were prepared for membrane flotation centrifugation. (G) HEK293 cells were transfected with indicated forms of GFP-ALIX and serum starved for 12 h. These cells were stimulated with or without EGF for 1 h. PNSs were prepared for membrane flotation centrifugation.

### **3.4. Membrane-associated ALIX is in an open conformation**

To determine whether membrane-associated ALIX is in an open conformation, M fraction and S fraction were fractionated by membrane flotation centrifugation and the pooled M fraction proteins and pooled S fraction proteins were extracted with 0.1% Triton X-100, which dissolves the membrane vesicles and preserves the intramolecular interaction of ALIX, and then immunoprecipitated with anti-ALIX antibodies. 5×M fraction proteins were used to make the total protein level is comparable to that of 1×S fraction proteins. Although conformation-sensitive 1A3 antibody immunoprecipitated ALIX from 5×M fraction, it did not immunoprecipitate ALIX from 1×S fraction. In contrast, conformation-insensitive 3A9 antibody immunoprecipitated comparable levels of ALIX from 5×M fraction and 1×S fraction (Fig. 17A).

To determine whether ALG-2-induced membrane-associated ALIX is in an open conformation, PNSs of HEK293 cells ectopically expressing FLAG-ALG-2 and being treated with calcium ionophore A23187 were fractionated by membrane flotation centrifugation. Pooled M fraction and pooled S fraction proteins were extracted with 0.1% Triton X-100 for co-IP with the 3A9 antibody. Although FLAG-ALG-2, TSG101 and CHMP4B were co-immunoprecipitated with ALIX in M fraction, no detectable levels of any of these three proteins were co-immunoprecipitated with ALIX in S fraction, indicating that ALIX in M fraction of FLAG-ALG-2 expressing cells is in an open conformation (Fig. 17B).

To determine whether EGF-induced membrane-associated ALIX is in an open conformation, PNSs of HEK293 cells stimulated with EGF were fractionated by membrane flotation centrifugation. 5×pooled M fraction and 1×pooled S fraction proteins were extracted with 0.1% Triton X-100 for co-IP with the 3A9 antibody. The

results showed that ALIX in M fraction, but not S fraction, was co-immunoprecipitated with endogenous ALG-2 and CHMP4B (Fig. 17C).

Altogether, these results demonstrate that EGF-induced and ALG-2-dependent membrane-associated ALIX is in an open conformation and interacts with partner proteins.

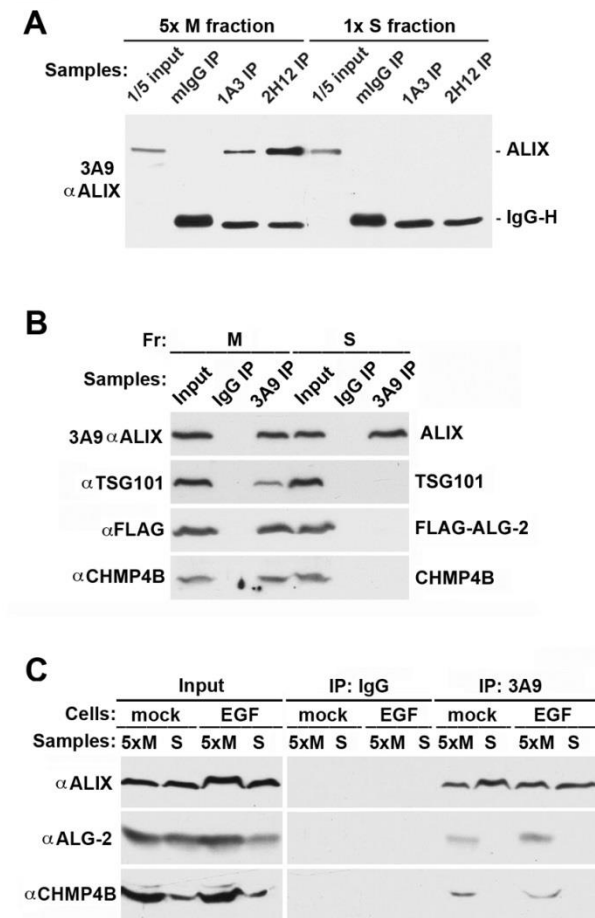


**Figure 17. Membrane-associated ALIX is in an open conformation.** (A) PNSs extracted from HEK293 cells were fractionated by membrane flotation centrifugation. 5xvolumes of M fractions were pooled and 1xvolume of S fraction was pooled. These pooled M and S fractions were immunoprecipitated with indicated antibodies. Input and immunocomplexes were immunoblotted to visualize ALIX and IgG. (B) HEK293 cells were transfected with FLAG-ALG-2. The transfected cells were treated with calcium ionophore A23187 for 15 min before collection. PNSs were fractionated by membrane flotation centrifugation. Pooled M fraction and S fractions were immunoprecipitated with the 3A9 antibody. Input and immunocomplexes were immunoblotted to visualize ALIX, FLAG-ALG-2, TSG101, and CHMP4B. (C) HEK293 cells were serum starved for 12 h and then stimulated with or without EGF for 1 h. 5xvolumes of M fractions were pooled

and 1×volume of S fraction was pooled. These pooled M and S fractions were immunoprecipitated with the 3A9 antibody. Input and immunocomplexes were immunoblotted to visualize ALIX, ALG-2, and CHMP4B.

### **3.5. ALG-2-induced activation of ALIX plays an essential role in MVB sorting of activated EGFR at early endosomes**

The data demonstrating that calcium-dependent ALG-2 interaction with ALIX is essential for EGF-induced ALIX association with membrane suggests that ALG-2 may play an essential role in MVB sorting of activated EGFR. To test this hypothesis, I first examined whether knockdown of ALG-2 affects MVB sorting of activated EGFR by using proteinase K protection assay. HEK293 cells were first transfected with si-NC or si-ALG-2 and then transfected with WT or Mut FLAG-ALG-2\* and the effects on MVB sorting of activated EGFR were examined. The results showed that knockdown of ALG-2 decreased the percentage of the proteinase K-insensitive EGFR from ~60% to ~17%. Ectopically expressing WT FLAG-ALG-2\* rescued the percentage of the proteinase K-insensitive EGFR to near control level. In contrast, ectopically expressing Mut FLAG-ALG-2\* only slightly rescued the defect in MVB sorting of activated EGFR (Fig. 18A). These results demonstrate that ALG-2 interaction with ALIX plays an essential role in MVB sorting of activated EGFR.

To further test this hypothesis, HEK293 cells were first transfected with si-ALIX and then transfected with WT or PxY GFP-ALIX\* and the effects on MVB sorting of activated EGFR were examined. Knockdown of ALIX decreased the percentage of the proteinase K-insensitive EGFR from ~60% to ~14%. Ectopically expressing WT GFP-ALIX\*, but not PxY GFP-ALIX\*, rescued the defect in MVB sorting of activated EGFR (Fig. 18B). These results support our conclusion.

I already demonstrated that ALIX-supported MVB sorting of activated EGFR is essential for rapidly terminating the downstream signaling of activated EGFR. Thus, I further examined the effects of ALG-2 on the kinetics of EGF-induced ERK1/2

activation under EGF continuous stimulation condition. As shown in Fig. 18C, EGF stimulation for 10 min induced the peak level of ERK1/2 activation and the activation of ERK1/2 dramatically decreased to basal level after 30 min of EGF stimulation. The level of ERK1/2 activation continued decreasing to nearly undetectable level from 1 h to 3 h of EGF stimulation. Knockdown of ALG-2 prevented the decrease of ERK1/2 activation in 1 h of EGF stimulation and promoted the sustained ERK1/2 activation from 1 h to 3 h of EGF stimulation. These results demonstrate that ALG-2 plays an important role in regulating the downstream signaling of activated EGFR and also further support our conclusion that ALG-2 is required for ALIX-supported MVB sorting of activated EGFR.

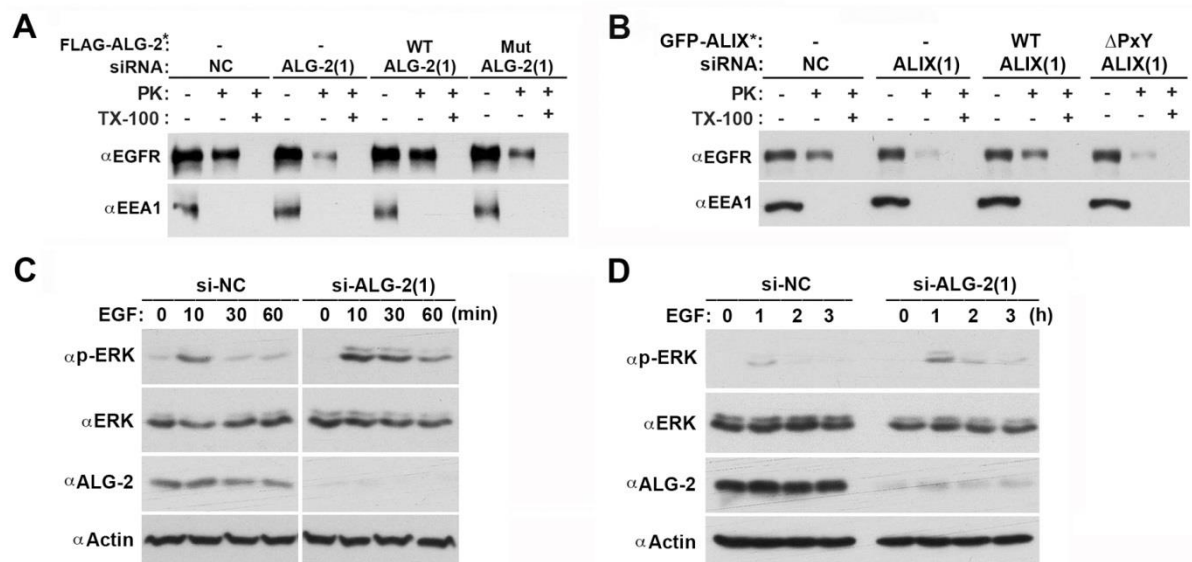


**Figure 18. ALG-2-induced activation of ALIX plays an essential role in MVB sorting of activated EGFR.** (A) HEK293 cells were first transfected with si-NC or si-ALG-2 and then mock-transfected or transfected with indicated forms of FLAG-ALG-2\*. These cells were serum starved for 12 h and stimulated with EGF for 30 min before being measured by the proteinase K protection assay. (B) HEK293 cells were first transfected with si-NC or si-ALIX and then mock-transfected or transfected with indicated forms of GFP-ALIX\*. These cells were serum starved for 12 h and stimulated with EGF for 30 min before being measured by the proteinase K protection assay. (C&D) HEK293 cells were transfected with si-NC or si-ALG-2 and serum starved for 12 h before being stimulated with EGF for indicated minutes (C) or hours (D). Cell lysates were immunoblotted to visualize p-ERK1/2, ERK1/2 and actin.



Since endocytosis of activated EGFR is prerequisite for MVB sorting of activated EGFR, thus it is possible that the inhibitory effects of ALG-2 or ALIX knockdown on MVB sorting of activated EGFR is from the inhibitory effects on endocytosis. To test this possibility, I knocked down ALIX or ALG-2 in HEK293 cells and stimulated the serum-starved cells with EGF for indicated time points. Then, the levels of cell surface EGFR were examined by biotinylation of cell surface proteins followed by pull-down of these biotinylated proteins by streptavidin beads. Immunoblotting with anti-EGFR antibody showed that knockdown of ALIX only slightly decreased the percentage of cell surface EGFR at the time point of 10 min (Fig. 19A). Knockdown of ALG-2 did not affect the levels of cell surface EGFR before and after EGF stimulation (Fig. 19B). These results eliminate the possibility that endocytosis of activated EGFR plays any roles in ALG-2-ALIX-dependent MVB sorting of activated EGFR.

To determine whether ALG-2/ALIX regulates MVB sorting of activated EGFR at early endosome or late endosome, I transfected HeLa cells with GFP-Rab5 (Q79L), which generates enlarged early endosome that can be observed by fluorescent microscope (Brankatschk et al., 2012; Raiborg et al., 2002), stimulated the serum-starved cells with EGF for 30 min and examined the localization of EGFR by using immunostaining with an anti-EGFR antibody. In control knockdown cells, ~60% of EGFR localized within the GFP-labelled early endosomes. Knockdown of ALIX or ALG-2 decreased the percentage of intraluminal EGFR to ~20% (Fig. 19C). These results support the role of ALG-2/ALIX in promoting MVB sorting of activated EGFR at early endosomes.

To further test this conclusion, I treated HEK293 cells with microtubule poison nocodazole to block early to late endosome trafficking (Abrami et al., 2004) and

examined whether the inhibitory effects of ALG-2 knockdown on MVB sorting of activated EGFR was affected. The results of proteinase K protection assay showed that treatment with nocodazole did not affect the inhibitory effects of ALG-2 knockdown on MVB sorting of activated EGFR (Fig. 19D), further supporting our conclusion.

Taken together, these results demonstrate that ALG-2 induced activation of ALIX promotes MVB sorting of activated EGFR at early endosome.

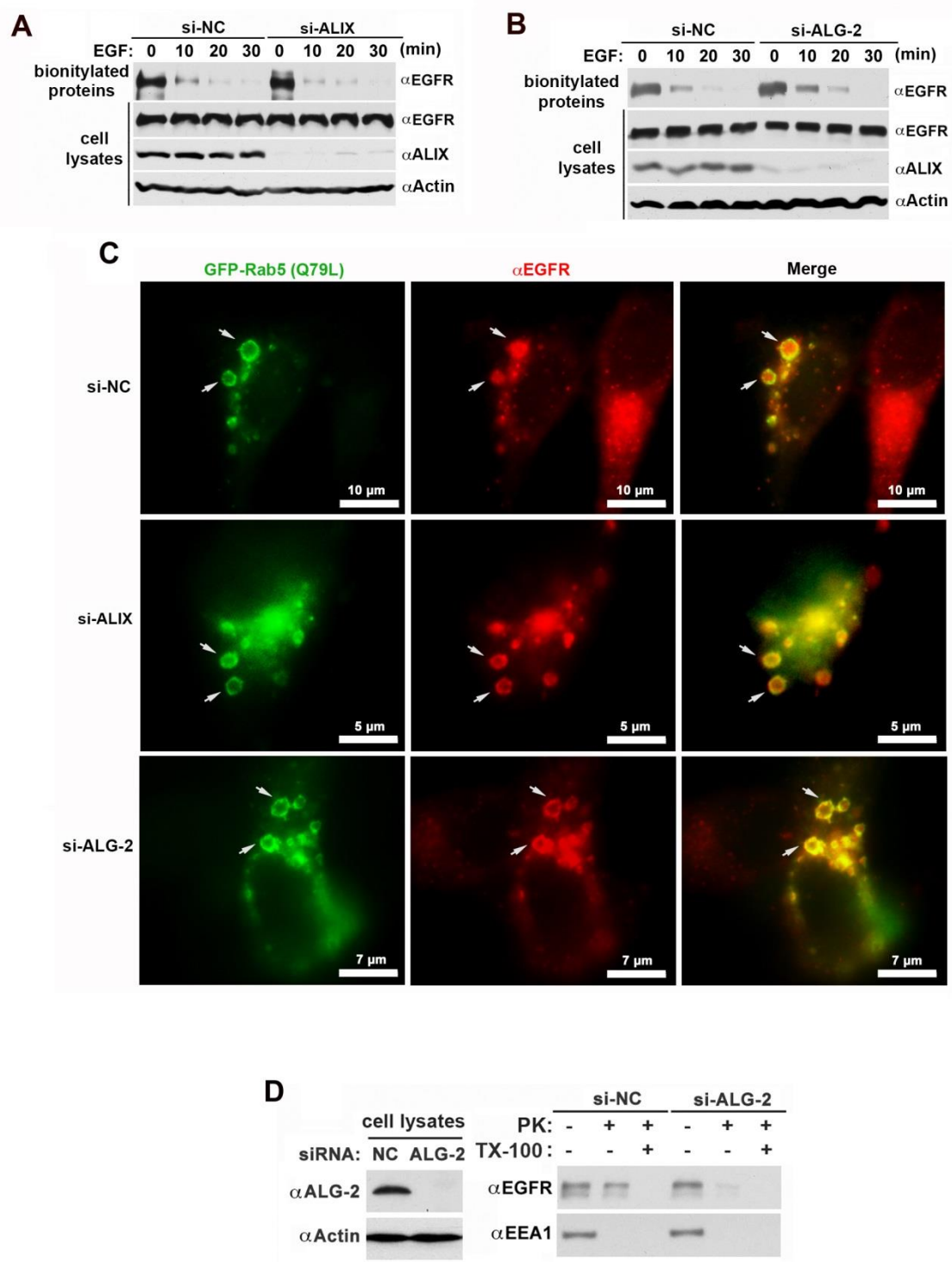


**Figure 19. ALG-2/ALIX plays an essential role in MVB sorting of activated EGFR at early endosome.** (A&B) HEK293 cells were transfected with si-NC or si-ALIX (A) or si-ALG-2 (B) and serum starved for 12 h before being stimulated with EGF for indicated

minutes. These cells were biotinylated and cell lysates extracted from these cells were incubated with streptavidin beads for pull-down of biotinylated cell surface proteins. Input and bound proteins were immunoblotted to visualize EGFR, ALIX and actin. (C) HeLa cells were first transfected with si-NC, si-ALIX or si-ALG-2 and then transfected with GFP-Rab5 (Q79L) before serum starvation for 12 h. These cells were stimulated with EGF for 30 min, fixed and stained with an anti-EGFR antibody (red). Total and intra-luminal EGFR were scored for 10 GFP-labeled endosomes for each condition, and the percentages of intra-luminal EGFR were determined. (D) HEK293 cells were transfected with si-NC or si-ALG-2 and serum starved for 12 h. These cells were treated with 10  $\mu$ M nocodazole for 2 h before and during EGF stimulation before being measured by proteinase K protection assay.

### **3.6. ALG-2-induced activation of ALIX plays an important role in EGF-induced EGFR degradation**

The results in the previous chapter showed that knockdown of ALIX inhibited MVB sorting of activated EGFR and retarded the degradation of activated EGFR under EGF continuous stimulation condition. Since ALG-2 is required for ALIX to support MVB sorting of activated EGFR, I hypothesized that ALG-2-induced activation of ALIX plays an important role in EGF-induced EGFR degradation under EGF continuous stimulation condition. To test this hypothesis, I first knocked down ALG-2 and examined the effects on the kinetics of EGF-induced EGFR degradation under EGF continuous stimulation condition. As shown in Fig. 20A-B, knockdown of ALG-2 increased the percentage of remaining EGFR at 1, 2, 3 and 4 h, resulting in retardation of the 50% EGFR degradation from 1 h to 2-2.5 h. Ectopically expressing WT FLAG-ALG-2\*, but not Mut FLAG-ALG-2\*, rescued the defect in EGFR degradation induced by knockdown of ALG-2. Then, WT or Mut FLAG-ALG-2 was overexpressed in HEK293 cells and the effect on EGF-induced EGFR degradation was examined. As shown in Fig. 20C, overexpression of WT FLAG-ALG-2, but not Mut FLAG-ALG-2 decreased the percentage of remaining EGFR at 1, 2 and 3 h, accelerating the 50% EGFR degradation from 1 h to 0.5 h. To further test the hypothesis, I examined the rescuing effects of WT or  $\Delta$ PxY GFP-ALIX\* on EGF-induced EGFR degradation in ALIX knockdown cells. As shown in Fig. 12C and 20D, WT, but not  $\Delta$ PxY GFP-ALIX\*, rescued the defect in EGFR degradation in ALIX knockdown cells.

Taken together, these results demonstrate that ALG-2 induced activation of ALIX plays an important role in EGF-induced EGFR degradation under EGF continuous stimulation condition.

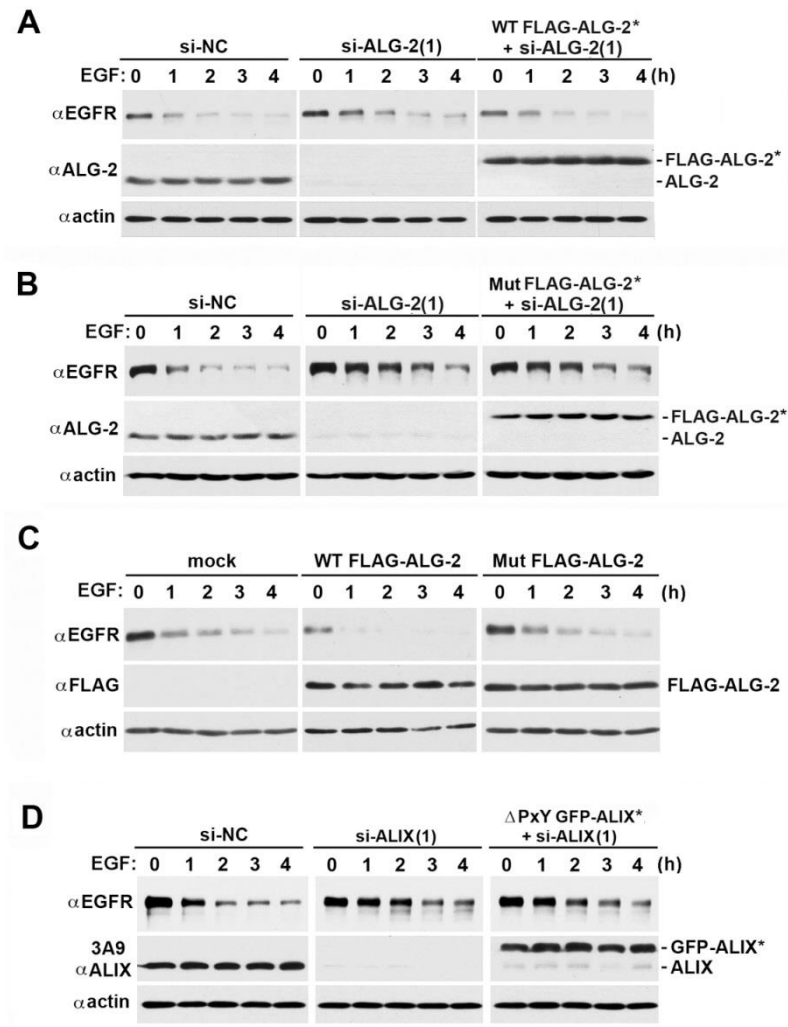


**Figure 20. ALG-2-induced activation of ALIX plays an important role in EGF-induced EGFR degradation.** (A&B) HEK293 cells were first transfected with si-NC or si-ALG-2(1) and then transfected with WT FLAG-ALG-2\* (A) or Mut FLAG-ALG-2\* (B) before being serum starved for 12 h. These cells were then stimulated with EGF for indicated hours, and cell lysates were immunoblotted to visualize EGFR, ALG-2, FLAG-ALG-2 and actin. (C) HEK293 cells were transfected with WT FLAG-ALG-2 or Mut FLAG-ALG-2 before being serum starved for 12 h. These cells were then stimulated with EGF for indicated hours, and cell lysates were immunoblotted to visualize EGFR, FLAG-ALG-2 and actin. (D) HEK293 cells were transfected with si-NC or si-ALIX(1) and then transfected with  $\Delta$ PxY GFP-ALIX\* before being serum starved for 12 h. These

cells were then stimulated with EGF for indicated hours, and cell lysates were immunoblotted to visualize EGFR, ALIX, GFP-ALIX and actin.

### **3.7. ALG-2 is not required for supporting ALIX to function in cytokinetic abscission or retroviral budding**

Besides MVB sorting function, ALIX has been demonstrated to be critically involved in cytokinetic abscission and retroviral budding. Since all these ESCRT-mediated processes require relieving the intramolecular interaction of ALIX, I examined whether ALG-2 is also required for supporting ALIX to function in cytokinetic abscission and retroviral budding. First, I examined whether ALG-2 is required to support cytokinetic abscission. The failure in cytokinetic abscission induces multinucleated cells and midbody-stage cells. As a positive control, knockdown of ALIX in HeLa cells increased the percentages of multinucleated and midbody-stage cells from ~5% to ~35% (Fig. 21A), consistent with the previous studies (Carlton and Martin-Serrano, 2007; Morita et al., 2007). In contrast, knockdown of ALG-2 did not significantly increase the percentages of multinucleated and midbody-stage cells (Fig. 21A), suggesting that ALG-2 is not important for cytokinetic abscission.

Then, I examined whether ALG-2 is required to support retroviral budding. For this purpose, I first knocked down ALG-2 in HEK293 cells by using siRNA and then transfected the cells with pEV53B-EIAV<sup>GAG</sup>. Virus-like particles (VLPs) were collected from culture medium by ultracentrifugation. The levels of VLPs were examined by immunoblotting of VLP lysates using anti-capsid (CA) antibodies. As a positive control, knockdown of ALIX significantly inhibited EIAV budding from infected HEK293 cells (Fig. 21B), consistent with the previous reports (Strack et al., 2003; von Schwedler et al., 2003). In contrast, knockdown of ALG-2 did not inhibit EIAV budding (Fig. 21B), suggesting that ALG-2 is not important for EIAV budding.



Taken together, these results suggest that ALG-2 specifically generates functional ALIX in MVB sorting of activated EGFR and that there should be other mechanisms by which ALIX is activated to function in cytokinetic abscission and retroviral budding.

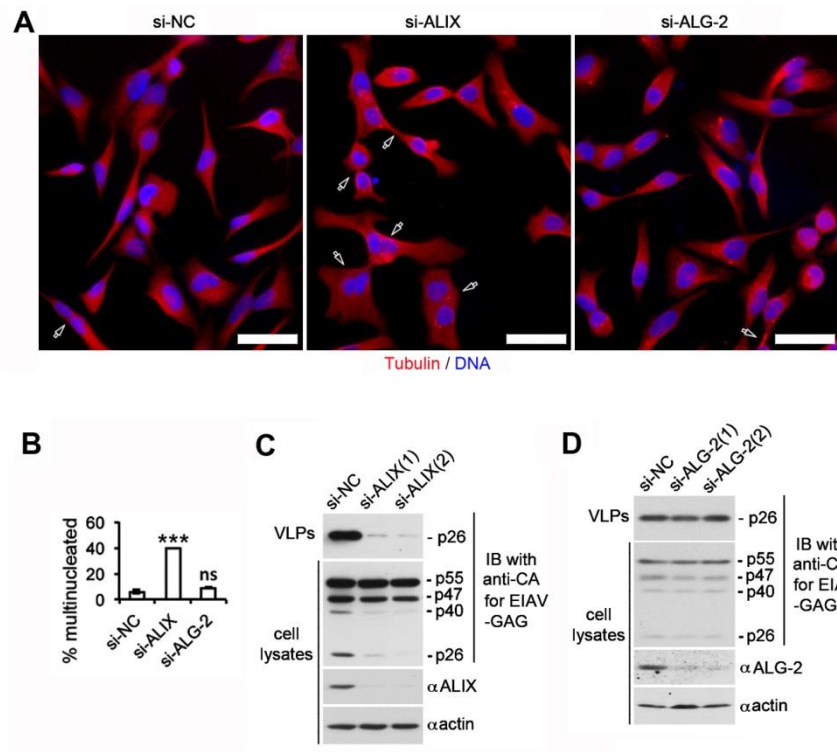


**Figure 21. ALG-2 is not required for supporting ALIX to function in cytokinetic abscission or retroviral budding.** (A&B) HeLa cells were transfected with si-NC, si-ALIX or si-ALG-2, fixed and stained with anti-tubulin antibodies (red) and counterstained with DAPI (blue). (A) Hollow arrows indicate multinucleated or midbody-stage cells. Scale bar: 50  $\mu$ m. (B) Average percentages of multinucleated and midbody-stage cells and SDs for each condition were determined from three independent experiments and plotted (lower panel). (C&D) HEK293 cells were first transfected with si-NC, si-ALIX(1) or si-ALIX(2) (C) or with si-NC, si-ALG-2(1) or si-ALG-2(2) (D) and then transfected with EIAV pEV53B. Released VLPs were collected by using ultracentrifugation. Cell lysates and VLPs were immunoblotted with anti-CA antibodies.

## Discussion

Results from the previous chapter demonstrate the essential role of CHMP4-bound ALIX dimer in MVB sorting and silencing of activated EGFR. However, the default intramolecular interaction of ALIX inhibits MVB sorting function of ALIX through prohibiting ALIX interaction with CHMP4. Here, my studies demonstrate that calcium-dependent ALG-2 interaction with ALIX completely relieves the intramolecular interaction of ALIX and promotes ALIX association with membrane-bound CHMP4. Although this mechanism is essential for activating ESCRT function of ALIX in MVB sorting of activated EGFR, it is not involved in activating ESCRT function of ALIX in cytokinetic abscission and retroviral budding.

In default condition, only ~10%-15% of ALIX is membrane associated and this membrane association is dependent on ALG-2, indicating that calcium is one of the rate-limiting factors in this regulatory mechanism. However, treating cells with calcium ionophore A23187 alone only slightly increased the level of ALIX in open conformation. Combination of overexpressing ALG-2 and adding calcium ionophore A23187 significantly increased the level of ALIX in open conformation, indicating that ALG-2 availability is also the rate-limiting factor in this regulatory mechanism.

Activation of EGFR induces a calcium spike near endosomes (Gerasimenko et al., 1998; Gerasimenko and Tepikin, 2005). Consistent with this, our results showed that EGF stimulation promoted ALG-2 interaction with ALIX. However, there is possible that EGFR activation also increases the availability of ALG-2. Although the underlining mechanism is still unknown, I predict that EGFR activation may induce the phosphorylation of ALG-2, which increases the availability of ALG-2. This prediction needs to be examined in the future studies.

ALG-2 was originally identified as apoptotic induction protein (Vito et al., 1996). The studies exploring the mechanisms of the pro-apoptotic function of ALG-2 identified ALIX as the ALG-2 interacting proteins and this interaction is essential for apoptotic induction. The studies in this chapter lead us to hypothesize that ALG-2 may induce apoptosis through terminating the downstream signaling of activated receptor tyrosine kinases.

## **Chapter 4: The mechanism that activates ALIX function in cytokinetic abscission and retroviral budding**

The contents of this chapter are based on Sun, S., Sun, L., Zhou, X., Wu, C., Wang, R., Lin, S.H., Kuang, J. Phosphorylation-Dependent Activation of the ESCRT Function of ALIX in Cytokinetic Abscission and Retroviral Budding. *Dev Cell*. 2016;36(3):331-43. doi: 10.1016/j.devcel.2016.01.001.

Copyright permission is required and obtained from Cell Press (License No.: 3830440570477).

### **Background**

The results from chapter 3 showing that ALG-2 is not important for ALIX-mediated cytokinetic abscission or retroviral budding suggest that there should be other mechanisms that activate ESCRT functions of ALIX in these two processes.

Cytokinesis initiates during early anaphase with a primary ingression of the cleavage furrow mediated by contraction of the actomyosin ring. As furrowing progresses, the spindle midzone, which is the structure formed during anaphase between the separating chromosomes by overlapping spindle microtubules, transforms into the intercellular bridge. Two daughter cells are connected by the intercellular bridge, at the middle of which is a dense structure termed the midbody. The midbody contains antiparallel arrays of microtubules that cross the Flemming body, which is the electron-dense structure that forms at the center of the midbody when the spindle

midzone's microtubules are compacted after furrow ingression. The midbody provides the anchorage to the ingressed cleavage furrow and the platform for the recruitment and assembly of ESCRTs. Before abscission occurs, a secondary ingression forms and decreases the thickness of the intercellular bridge from 1.5-2  $\mu\text{m}$  to 100-200 nm (Agromayor and Martin-Serrano, 2013; Mierzwa and Gerlich, 2014). During late telophase, FIP3 endosomes deliver p50RhoGAP and SCAMP2/3 to the intercellular bridge, where SCAMP2/3 and p50RhoGAP are involved in depolymerization of the cortical actin. The depolymerization of the cortical actin is required for successful completion of abscission. Knockdown of SCAMP2/3 or p50RhoGAP was shown to significantly decrease the percentage of cells with secondary ingression. FIP3, SCAMP2/3 or p50RhoGAP was also shown to be required for ESCRT machinery to be recruited to the abscission site to perform the final cut (Schiel et al., 2012).

Before cytokinetic abscission, Cep55 is recruited to the midbody through the direct interaction between Cep55 and midbody component MKLP1 (mitotic kinesin-like protein 1) (Bastos and Barr, 2010). Cep55 recruits ESCRT-associated protein ALIX to the midbody through the direct interaction. ALIX in turn recruits ESCRT-III component CHMP4 to the midbody area and promotes the assembly of 17-nm ESCRT-III filament. Membrane abscission occurs  $\sim 1 \mu\text{m}$  away from the midbody where the microtubules are removed by microtubule-severing protein, spastin, enabling full constriction at the abscission site. ESCRT-III filaments assemble at both the midbody and membrane abscission site but appear to be discontinuous (Carlton et al., 2008; Guizetti et al., 2011; Morita et al., 2007).

The budding of enveloped viruses away from the infected cells is the process in which the membrane is distorted away from the cytoplasm and ultimately wrapped

around the assembling viral particles followed by severing membrane connected the viral particles and cells to release the viral particles (Martin-Serrano and Neil, 2011; Votteler and Sundquist, 2013). Retroviral assembly and budding is driven primarily by Gag, a polyprotein that contains all the necessary domains. Retroviruses hijack ESCRTs in host cells through direct interaction between YPXL motif in L domain of Gag protein and the F676 pocket in ALIX (Martin-Serrano and Neil, 2011; Strack et al., 2003; von Schwedler et al., 2003; Votteler and Sundquist, 2013).

Previous studies of the *Xenopus* ortholog of ALIX, Xp95, during meiotic maturation of *Xenopus* oocytes showed that Xp95 is phosphorylated both at the conserved tyrosine residue (Y318) within the Patch 2 of the Bro1 domain (Dejournett et al., 2007), and at multiple sites within N-terminal portion of PRD (nPRD) in M phase-arrested mature oocytes (Dejournett et al., 2007). Alignment of the sequence of Xp95 and ALIX showed that most of the phosphorylation sites within the Bro1 domain and nPRD are conserved. Since protein phosphorylation may disrupt the intramolecular interaction of a protein, we hypothesized that phosphorylation of one or both of the intramolecular interaction sites in ALIX relieves the intramolecular interaction of ALIX and transforms ALIX from closed to open conformation during M phase induction. The preliminary data from a previous graduate student in our group, Xi Zhou, showed that ALIX transformed from closed conformation to open conformation in mitotic arrested HEK293 cells, suggesting that mitotic cells may be a good platform to study the possible role of phosphorylation in conformational change of ALIX.

To test our hypothesis, I designed and performed this part of study. My study demonstrates that ALIX phosphorylation at the intramolecular interaction site within the nPRD relieves the default intramolecular interaction of cytosolic ALIX in mitotic cells

and that this activating phosphorylation of ALIX is required for ALIX to support cytokinetic abscission and EIAV budding but does not affect the function of ALIX in MVB sorting of activated EGFR.

## **Results**

### **4.1. The intramolecular interaction of cytosolic ALIX is relieved in a phosphorylation-dependent manner during M phase entry**

To determine whether the intramolecular interaction of ALIX is relieved during M phase entry, conformation-sensitive anti-ALIX antibodies were used to immunoprecipitate cytosolic ALIX from asynchronously growing (>95% interphase cells) or mitotically arrested (>80% mitotic cells) HEK293 cells, which were extracted with the cell extraction buffer without detergent. The extraction buffer for mitotically arrested cells contains ATP and the PP1/PP2A inhibitor microcystin to stabilize the M phase status of the extracts. Immunoprecipitation of asynchronously growing cell lysates (IE) or mitotically arrested cell lysates (ME) showed that conformation-sensitive anti-ALIX antibodies, 1A3 and 2H12, specifically immunoprecipitated cytosolic ALIX from ME, indicating that cytosolic ALIX in ME is in an open conformation. In contrast, conformation-insensitive anti-ALIX antibodies, 1A12 and 3A9, immunoprecipitated comparable levels of cytosolic ALIX from both IE and ME (Fig. 22A). Immunoblotting of IE and ME with the mitotic phosphoprotein monoclonal antibody 2 (MPM-2) (Wu et al., 2010) showed robust increase of the level of protein phosphorylation in mitotic cells, demonstrating the mitotic state of ME. Since the extraction buffer for mitotically arrested cells contains ATP and microcystin, there is a possibility that the added ATP



and microcystin induce the open conformation of ALIX. To test this possibility, I used the extraction buffer containing ATP and microcystin to prepare both IE and ME, and performed immunoprecipitation with the 2H12 and 3A9 antibodies. As shown in Fig. 22B, although the 2H12 antibody immunoprecipitated detectable level of ALIX from IE, it immunoprecipitated much higher level of ALIX from ME as did the 3A9 antibody, indicating that the conformational change of ALIX in mitotic cells is not due to the buffer condition. These results demonstrate that the intramolecular interaction of ALIX is relieved to transform ALIX from closed conformation to open conformation during M phase induction.

To further test the conclusion, I examined the interactions between cytosolic ALIX and some of its partner proteins, such as CHMP4, TSG101, and Src in IE and ME. These interactions are inhibited by the intramolecular interaction of ALIX. Ectopically expressing FLAG-CHMP4B or endogenous TSG101 was not co-immunoprecipitated with cytosolic ALIX in IE. In contrast, both of them were co-immunoprecipitated with cytosolic ALIX in ME (Fig. 22C-D). These results further support the conclusion.

To determine whether the conformational change of ALIX during M phase entry is induced by mitotic phosphorylation, I treated ME with calf intestinal alkaline phosphatase (CIP) and examined the effect on ALIX conformational change. As shown in Fig. 22E, the 1A3 antibody specifically immunoprecipitated cytosolic ALIX from ME, indicating the open conformation of ALIX in ME. Treatment of ME with CIP eliminated the 1A3 immunoprecipitability of ALIX in ME, indicating that mitotic phosphorylation is required for conformational change of ALIX. To determine whether the phosphorylation-induced open conformation of ALIX is reversible event, purified protein GST-CHMP4B or in-vitro translated myc-TSG101 was added into ME before CIP treatment, it partially

rescued the 1A3 immunoprecipitability of ALIX (Fig. 21F-G), suggesting that partner protein interaction partially keeps the open conformation of ALIX. Immunoblotting of IE, ME and ME plus CIP with MPM2 demonstrated the mitotic state of ME and the efficacy of CIP treatment.

These results demonstrate that mitotic phosphorylation induces an open conformation of ALIX during M phase entry.

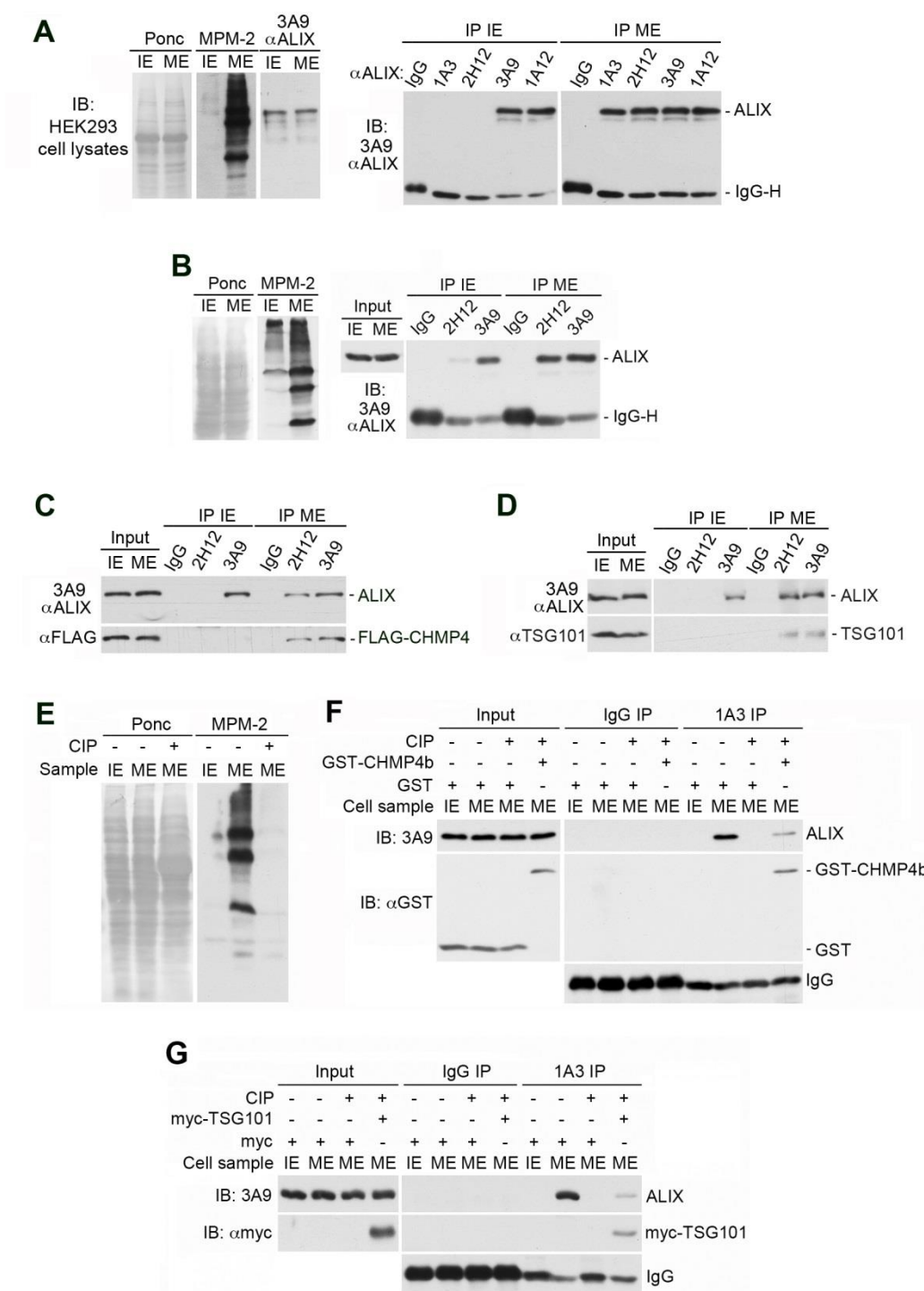


**Figure 22. The intramolecular interaction of cytosolic ALIX is relieved in a phosphorylation-dependent manner during M phase entry.** (A) IE and ME from HEK293 cells were prepared and immunoblotted with MPM-2 and the 3A9 antibody (left panel). IE and ME were immunoprecipitated with indicated conformation-sensitive

or conformation-insensitive anti-ALIX antibodies followed by immunoblotting. (B) IE and ME from HEK293 cells were prepared with the same extraction buffer containing ATP and microcystin and immunoblotted with MPM-2 and the 3A9 antibody (left panel). IE and ME were immunoprecipitated with indicated conformation-sensitive or conformation-insensitive anti-ALIX antibodies followed by immunoblotting. (C&D) IE and ME were immunoprecipitated with indicated antibodies, and immunocomplexes were immunoblotted to visualize ALIX and FLAG-CHMP4B (C) or ALIX and TSG101 (D). (E) IE, ME and CIP-treated ME were immunoblotted with MPM-2. (F&G) ME was first incubated with GST or GST-CHMP4B (F) or myc or myc-TSG101 (G) at 4°C for 2 h, and then treated with CIP. All the samples were immunoprecipitated with IgG or the 1A3 antibody followed by immunoblotting.

#### 4.2. Phosphorylation of ALIX<sub>nPRD</sub> disrupts the interaction between ALIX<sub>Bro1</sub> and ALIX<sub>nPRD</sub>

Since the intramolecular interaction of ALIX is achieved between Bro1 domain and nPRD (Fig. 23A), the next step is to determine phosphorylation of which domain is responsible for relieving the intramolecular interaction. For this purpose, I first treated in-vitro translated myc-ALIX<sub>nPRD</sub> with interphase-arrested *Xenopus* oocyte extracts (IOE), M phase-arrested *Xenopus* egg extracts (MEE) or MEE plus CIP and then incubated the treated myc-ALIX<sub>nPRD</sub> with immobilized GST-ALIX<sub>Bro1</sub>. Immunoblotting of input proteins showed that MEE treatment induced a phosphorylation-dependent gel mobility shift. The results of GST pull-down showed that although IOE or MEE plus CIP treated myc-ALIX<sub>nPRD</sub> was pulled down by GST-ALIX<sub>Bro1</sub>, MEE treated myc-ALIX<sub>nPRD</sub> could not be pulled down by GST-ALIX<sub>Bro1</sub> (Fig. 23B), suggesting that phosphorylation of ALIX<sub>nPRD</sub> by MEE disrupts the interaction between ALIX<sub>nPRD</sub> and ALIX<sub>Bro1</sub>. Then, I treated GST-ALIX<sub>Bro1</sub> with IOE, MEE, or MEE plus CIP and immobilized treated GST-ALIX<sub>Bro1</sub> onto GSH beads. Immunoblotting of washed GST-ALIX<sub>Bro1</sub> with anti-p-Tyr antibody demonstrated that ALIX<sub>Bro1</sub> was phosphorylated by MEE (Fig. 23C). The ability of washed GST-ALIX<sub>Bro1</sub> to interact with myc-ALIX<sub>nPRD</sub> was examined by GST pull-down. MEE-treated GST-ALIX<sub>Bro1</sub> still pulled down myc-ALIX<sub>nPRD</sub>, although its ability decreased by ~30% compared to IOE or MEE plus CIP treated GST-ALIX<sub>Bro1</sub> (Fig. 23D). The results suggest that phosphorylation of ALIX<sub>Bro1</sub> by MEE only weakens the interaction between ALIX<sub>nPRD</sub> and ALIX<sub>Bro1</sub>.

Taken together, these results indicate that phosphorylation of ALIX<sub>nPRD</sub> plays a major role in relieving the intramolecular interaction of ALIX.

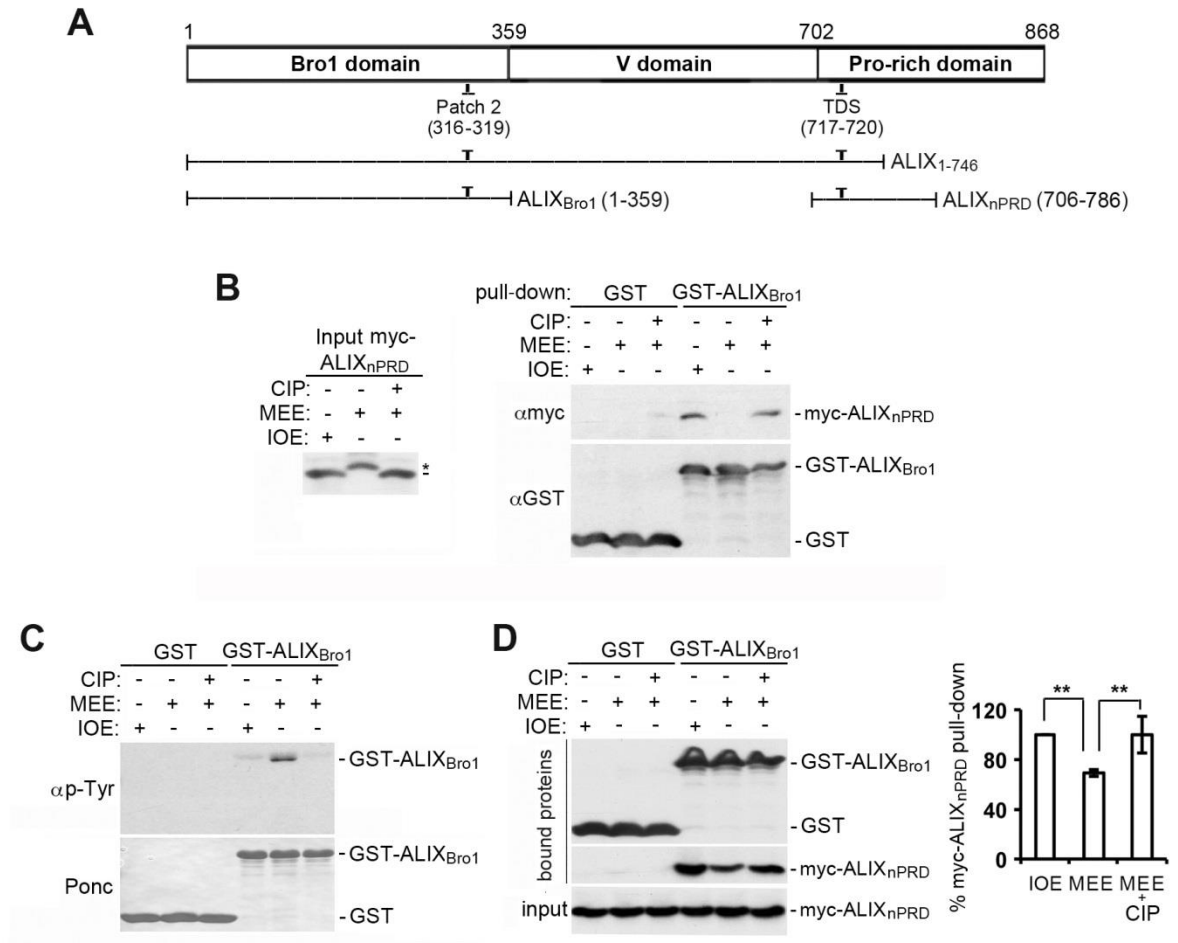


**Figure 23. Phosphorylation of ALIX<sub>nPRD</sub> disrupts the interaction between ALIX<sub>Bro1</sub> and ALIX<sub>nPRD</sub>.** (A) Schematic illustration of ALIX and ALIX fragments used in this study. (B) The in vitro translated myc-ALIX<sub>nPRD</sub> was incubated with IOE, MEE, or MEE plus CIP. GST pull-down was used to examine the interaction between treated myc-ALIX<sub>nPRD</sub> and immobilized GST-ALIX<sub>Bro1</sub>. Input of the treated myc-ALIX<sub>nPRD</sub> was immunoblotted; the gel mobility shift of treated myc-ALIX<sub>nPRD</sub> was indicated (left panel); bound proteins from GST pull-down were immunoblotted (right panel). (C) GST or GST-ALIX<sub>Bro1</sub> was first incubated with IOE, MEE, or MEE plus CIP, and immobilized onto GSH beads. The beads were washed and immunoblotted with an anti-phosphotyrosine (p-Tyr) antibody. (D) GST or GST-ALIX<sub>Bro1</sub> was first incubated with

IOE, MEE, or MEE plus CIP, and then immunoblized onto GSH beads. The beads were washed and then incubated with in-vitro translated myc-ALIX<sub>nPRD</sub>. GST pull-down was used to examine the interaction between treated myc-ALIX<sub>nPRD</sub> and myc-ALIX<sub>nPRD</sub> (left panel). The level of myc-ALIX<sub>nPRD</sub> pulled down by treated GST-ALIX<sub>Br01</sub> was quantified and plotted (right panel).

### **4.3. Phosphorylation of both S718 and S721 residues disrupts the interaction between ALIX<sub>nPRD</sub> and ALIX<sub>Bro1</sub>**

Since the studies above demonstrate that phosphorylation of ALIX<sub>nPRD</sub> makes major contribution to disrupting the intramolecular interaction, I focused on ALIX<sub>nPRD</sub> in the following studies. Sequence alignment of ALIX<sub>nPRD</sub> and Xp95<sub>nPRD</sub> showed that two conserved residues, Ser718 (S718) and Ser721 (S721) in ALIX<sub>nPRD</sub>, locate at one of the intramolecular interaction site (residues 717-720: PSAP) (Fig. 24A). Since phosphorylation may disrupt the protein interaction, I hypothesized that phosphorylation at the S718 and S721 residues may be responsible for disrupting the interaction between ALIX<sub>Bro1</sub> and ALIX<sub>nPRD</sub>. To test this hypothesis, I first examined whether these two residues in ALIX<sub>nPRD</sub> are phosphorylated in our in-vitro experimental system.

For this purpose, phospho-specific antibodies that recognize the phosphorylated S718 and S721 residues were needed. First, we found that the Phospho-(Ser/Thr) PKD Substrate Antibody from Cell Signaling Technology (Catalog number: #4381) detects peptides and proteins containing a phospho-S/T residue with arginine at the -3 position and leucine at the -5 position, preferring proline at the -1 position. Since the S718 context fits these criteria, the #4381 antibody was used to determine whether the S718 residue in ALIX<sub>nPRD</sub> is phosphorylated by MEE treatment. We also produced rabbit polyclonal antibodies against a synthetic ALIX peptide that is phosphorylated at both S718 and S721 residues. The antibody, which was named as anti-pS2 antibody, was also used in the following studies.

As shown in Fig. 24B, the #4381 antibody recognized MEE-treated WT GST-ALIX<sub>nPRD</sub>, but not mock-treated WT GST-ALIX<sub>nPRD</sub> or MEE-treated phosphodeficient S718A-S721A (S2A) mutant form GST-ALIX<sub>nPRD</sub>. Immunoprecipitation with the #4381



antibody showed that the #4381 antibody specifically immunoprecipitated MEE-treated WT myc-ALIX<sub>nPRD</sub>, but not mock-treated WT myc-ALIX<sub>nPRD</sub> or MEE-treated S2A myc-ALIX<sub>nPRD</sub>. These results suggest that the S718 residue in ALIX<sub>nPRD</sub> is phosphorylated by MEE treatment. As shown in Fig. 24C, the anti-pS2 antibody specifically recognized MEE-treated GST-ALIX<sub>nPRD</sub>, and also specifically immunoprecipitated MEE-treated myc-ALIX<sub>nPRD</sub>. These results further demonstrate that the S718 and S721 residues in ALIX<sub>nPRD</sub> are phosphorylated by MEE treatment.

To determine whether phosphorylation at the S718 and S721 residues by MEE disrupts the interaction between ALIX<sub>nPRD</sub> and ALIX<sub>Bro1</sub>, I further made constructs of myc-ALIX<sub>nPRD</sub> containing phosphomimetic mutations at the S718 and S721 residues (S718D-S721D, S2D) or phosphodeficient mutations at the adjacent residues S712 and S729 (S712A-S729A, S2A-). The S2A, S2D or S2A- myc-ALIX<sub>nPRD</sub> was treated with IOE, MEE or MEE plus CIP and pulled down by GST-ALIX<sub>Bro1</sub>. As shown in Fig. 24D, GST-ALIX<sub>Bro1</sub> pulled down S2A myc-ALIX<sub>nPRD</sub> under all three conditions, pulled down S2A- myc-ALIX<sub>nPRD</sub> only upon treatment with IOE or MEE plus CIP but did not pull down S2D myc-ALIX<sub>nPRD</sub> under any of the conditions. These results suggest that phosphorylation at the S718 and S721 residues are required to disrupt the interaction between ALIX<sub>Bro1</sub> and ALIX<sub>nPRD</sub>.

To further determine whether the disruption of the interaction between ALIX<sub>Bro1</sub> and ALIX<sub>nPRD</sub> is a direct effect from phosphorylation or an indirect effect from phosphorylation-dependent recruitment of cofactors, I examined this interaction by using GST pull-down in the absence of any treatment. As shown in Fig. 24E, GST-ALIX<sub>Bro1</sub> pulled down comparable levels of WT, S2A or S2A- myc-ALIX<sub>nPRD</sub>, but an undetectable level of S2D myc-ALIX<sub>nPRD</sub>. The results indicate that phosphorylation at

S718 and S721 residues directly disrupts the interaction between ALIX<sub>Bro1</sub> and ALIX<sub>nPRD</sub>.

The S718 residue localizes in a context that fits the phosphorylation consensus sequences for PLK1 and PKD. To determine whether PLK1 and PKD, both of which are active in mitosis (Golsteyn et al., 1995; Kienzle et al., 2013), are responsible for phosphorylating the S718 and S721 residues, I pre-treated MEE with DMSO, PKD inhibitor CID755673, PLK1 inhibitor BI-2536, combination of both inhibitors, and pan-kinase inhibitor staurosporine. Then, the treated MEE was used to phosphorylate GST-ALIX<sub>nPRD</sub> in the presence of these inhibitors. Immunoblotting with the anti-pS2 antibody showed that the pan kinase inhibitor significantly inhibited the phosphorylation of GST-ALIX<sub>nPRD</sub>. However, the PKD and PLK1 inhibitors only reduced the phosphorylation of GST-ALIX<sub>nPRD</sub> by ~17% and ~35%, respectively, and together reduced the phosphorylation by ~41% (Fig. 24F). These results suggest that PLK1 and PKD are among the multiple kinases in MEE that phosphorylate the S718 and S721 residues in ALIX<sub>nPRD</sub>.

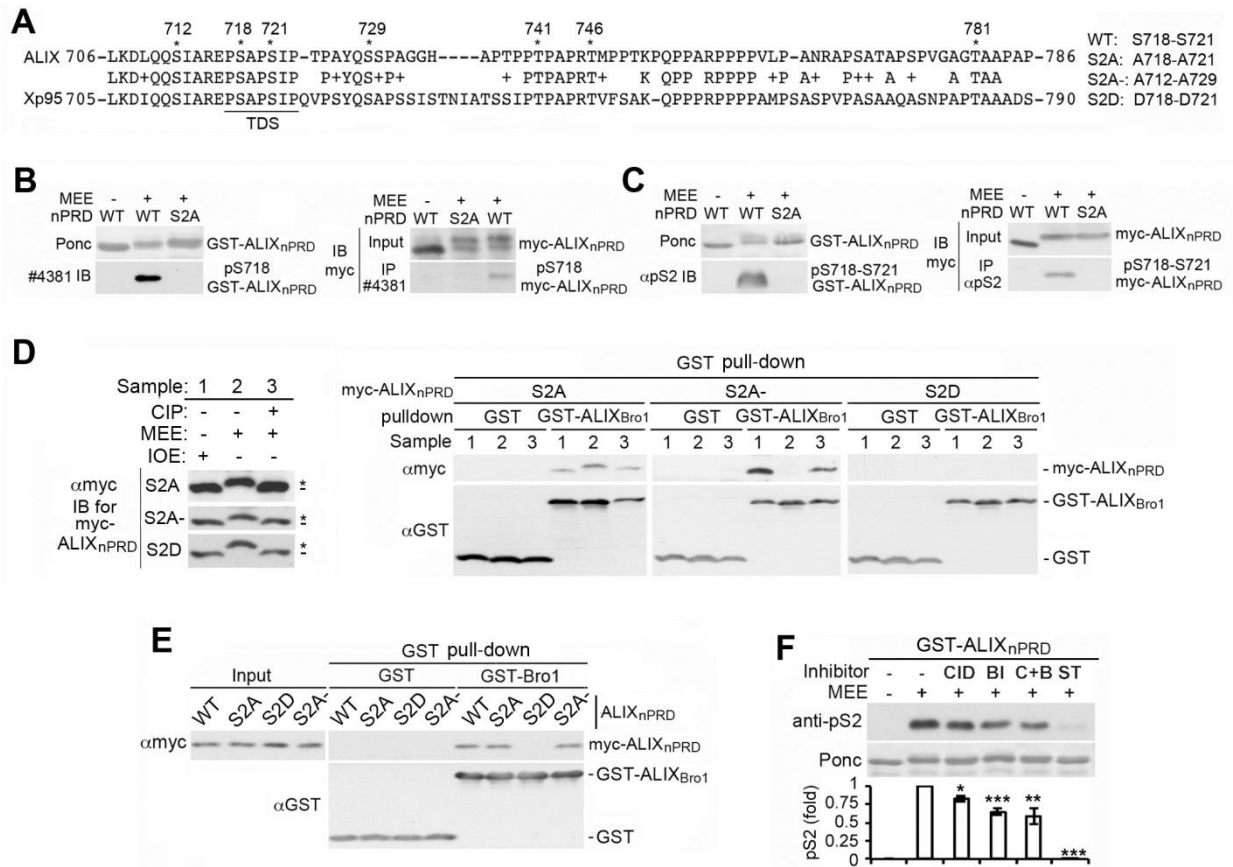


**Figure 24. Phosphorylation of both S718 and S721 residues disrupts the interaction between ALIX<sub>nPRD</sub> and ALIX<sub>Bro1</sub>.** (A) Sequence alignment of ALIX<sub>nPRD</sub> and Xp95<sub>nPRD</sub>; conserved S/T residues are highlighted. (B) WT and S2A GST-ALIX<sub>nPRD</sub> were mock treated or incubated with MEE and immobilized onto GSH beads. The beads were washed and immunoblotted with the #4381 antibody (left panel). In-vitro translated myc-ALIX<sub>nPRD</sub> was mock-treated or incubated with MEE. The treated myc-ALIX<sub>nPRD</sub> was immunoprecipitated under denaturing condition (dIP) with the #4381 antibody followed by immunoblotting (right panel). (C) WT and S2A GST-ALIX<sub>nPRD</sub> were mock treated or incubated with MEE and immobilized onto GSH beads. The beads were washed and immunoblotted with the anti-pS2 antibody (left panle). In-vitro translated myc-ALIX<sub>nPRD</sub> was mock-treated or incubated with MEE. The treated myc-ALIX<sub>nPRD</sub> was immunoprecipitated under denaturing condition (dIP) with the anti-pS2

antibody followed by immunoblotting (right panel). (D) In vitro translated products of indicated forms of myc-ALIX<sub>nPRD</sub> were incubated with IOE, MEE, or MEE plus CIP, and immunoblotted with anti-myc antibodies (left panel). The interaction between treated myc-ALIX<sub>nPRD</sub> and GST-ALIX<sub>Br01</sub> was examined by GST pull-down (right panel). (E) In vitro translated products of indicated forms of myc-ALIX<sub>nPRD</sub> were incubated with immobilized GST or GST-ALIX<sub>Br01</sub>. Input and pull-down proteins were immunoblotted. (F) GST-ALIX<sub>nPRD</sub> was mock treated or incubated with MEE in the presence or absence of PKD inhibitor CID755673 (CID), PLK1 inhibitor BI-2536 (BI), both inhibitors (C+B) or pan-kinase inhibitor staurosporine (ST). Then, the treated GST-ALIX<sub>nPRD</sub> was immobilized onto GSH beads, which was washed after binding, and immunoblotted with the anti-pS2 antibody (left panel). Relative levels of phosphorylated GST-ALIX<sub>nPRD</sub> were determined and normalized against the level of total GST-ALIX<sub>nPRD</sub> (right panel).

#### **4.4. Phosphorylation of both S718 and S721 residues transforms ALIX from close conformation to open conformation in mitotic cells**

To determine whether the S718 and S721 residues are also phosphorylated in mitotic cells, I first performed denaturing immunoprecipitation (dIP) of IE and ME by using the #4381 antibody. The results showed that the #4381 antibody specifically immunoprecipitated ALIX from ME, indicating that the S718 residue is phosphorylated in mitotic cells. Then, I performed dIP of IE and ME by using the 3A9 antibody followed by immunoblotting of immunocomplex with the anti-pS2 antibody. The results showed that the anti-pS2 antibody specifically recognized ALIX in ME, indicating that both S718 and S721 residues are phosphorylated in mitotic cells (Fig. 25A).

To determine whether the recognition by two phospho-specific antibodies is due to the phosphorylation at the S718 and S721 residues, I transfected HEK293 cells with WT or S2A GFP-ALIX and performed dIP of IE and ME by using the #4381 antibody. The results showed that the #4381 antibody specifically immunoprecipitated WT GFP-ALIX from ME, but not IE. The #4381 antibody did not immunoprecipitate S2A GFP-ALIX from either IE or ME. The dIP of IE and ME was also performed by using anti-GFP antibody followed by immunoblotting of immunocomplex with the anti-pS2 antibody. The results showed that the anti-pS2 antibody specifically recognized WT GFP-ALIX from ME, but not IE. Similar to the #4381 antibody, the anti-pS2 antibody also did not recognize S2A GFP-ALIX from either IE or ME (Fig. 25B-C). The results further demonstrate that the S718 and S721 residues are phosphorylated in mitotic cells.

To determine whether phosphorylation at the S718 and S721 residues are responsible for relieving the intramolecular interaction of ALIX in mitotic cells, I

transfected HEK293 cells with WT, S2A, S2D or S2A- GFP-ALIX and performed immunoprecipitation of IE and ME with the 2H12 and 3A9 antibodies. As shown in Fig. 25D, the 2H12 antibody only immunoprecipitated S2D GFP-ALIX from IE, indicating that only S2D GFP-ALIX is in the open conformation in IE. The 2H12 antibody immunoprecipitated WT, S2D and S2A- GFP-ALIX from ME. In contrast, the 2H12 antibody did not immunoprecipitate S2A GFP-ALIX from either IE or ME, indicating that S2A GFP-ALIX could not transform to the open conformation in mitotic cells. The 2H12-immunoprecipitable GFP-ALIX was also co-immunoprecipitated with CHMP4B and TSG101. These results demonstrate that phosphorylation at the S718 and S721 residues are responsible for relieving the intramolecular interaction of ALIX and inducing the open conformation of ALIX in mitotic cells.

To determine whether phosphorylation at both residues are required for relieving the intramolecular interaction of ALIX, I transfected HEK293 cells with WT, S718A, S721A or S2A GFP-ALIX and performed immunoprecipitation of ME with the 2H12 and 3A9 antibodies. As shown in Fig. 25E, the levels of S718A GFP-ALIX and S721A GFP-ALIX immunoprecipitated by the 2H12 antibody are ~40% and ~70% of the level of WT GFP-ALIX immunoprecipitated by the 2H12 antibody. These results suggest that complete relieve of the intramolecular interaction of ALIX requires phosphorylation at both S718 and S721 residues. Co-IP results showed that mutations at S718 and S721 residues did not affect ALIX interaction with TSG101 (Fig. 25F).

To determine whether PLK1 or/and PKD are also responsible for phosphorylating the S718 and S721 residues in mitotic cells, HEK293 cells were synchronized in mitosis in the presence or absence of the PLK1 inhibitor and/or the PKD inhibitor, or the pan kinase inhibitor, and determined the phosphorylation of ALIX

with the anti-pS2 antibody. As shown in Fig. 25G-H, the immunoblotting of the whole cell lysates with MPM-2 showed that only the pan kinase inhibitor inhibited mitotic entry. The PKD inhibitor inhibited the phosphorylation of the S718 and S721 residues in ALIX by ~15%, the PLK1 inhibitor inhibited the phosphorylation by ~25% and the combination of two inhibitors inhibited the phosphorylation by ~39%. As anticipated, the pan kinase inhibitor completely inhibited the phosphorylation. These results suggest that PKD and PLK1 are among the multiple protein kinases that phosphorylate the S718 and S721 residues in ALIX in mitotic cells.

Taken together, these results demonstrate that the phosphorylation at the 718 and S721 residues in mitotic cells completely relieves the intramolecular interaction of ALIX.

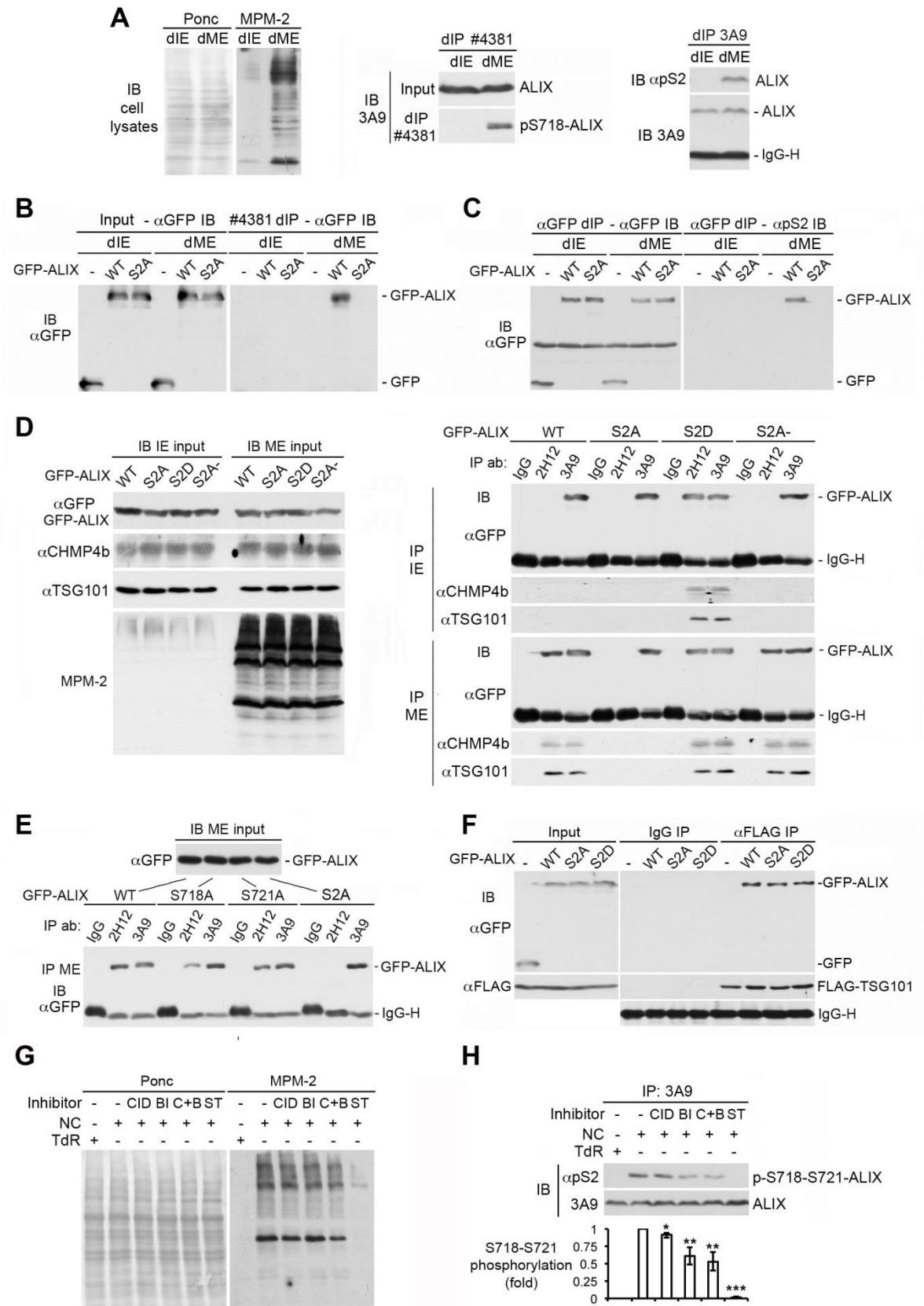


**Figure 25. Phosphorylation of both S718 and S721 residues transforms ALIX**



**from close conformation to open conformation in mitotic cells.** (A) IE and ME from HEK293 cells were immunoblotted with MPM2 (left panel). IE and ME were immunoprecipitated under denaturing condition (dIP) with the #4381 antibody followed by immunoblotting (middle panel). IE and ME were immunoprecipitated under denaturing condition (dIP) with the 3A9 antibody followed by immunoblotting with the 3A9 antibody and anti-pS2 antibody (right panel). (B&C) HEK 293 cells were transfected with WT or S2A GFP-ALIX. IE and ME from these transfected cells were immunoprecipitated under denaturing condition (dIP) with the #4381 antibody followed by immunoblotting with an anti-GFP antibody (B), or with an anti-GFP antibody followed by immunoblotting with an anti-GFP antibody and the anti-pS2 antibody (C). (D) HEK293 cells were transfected with WT or indicated mutant forms of GFP-ALIX. IE and ME these transfected cells were immunoblotted with indicated antibodies or immunoprecipitated with indicated anti-ALIX antibodies followed by immunoblotting. (E) HEK293 cells were transfected with WT or indicated mutant forms of GFP-ALIX. IE and ME from these transfected cells were immunoprecipitated with indicated anti-ALIX antibodies. Input proteins and immunocomplexes were immunoblotted with an anti-GFP antibody. (F) HEK293 cells were co-transfected FLAG-TSG101 and GFP, WT, S2A, or S2D GFP-ALIX. IE from these transfected cells were immunoprecipitated with anti-FLAG antibodies in the presence of 1% Triton X-100. Input proteins and immunocomplexes were immunoblotted. (G&H) HEK293 cells were cultured in the presence of 2.5 mM TdR for 16 h. The cells were either cultured in the continued presence of TdR or in the presence of 100 ng/ml nocodazole (NC). At 5-6 h after NC block, when most of cells had not entered mitosis, DMSO, CID (3  $\mu$ M), BI (100 nM), both inhibitors (CID+BI: 3  $\mu$ M+100 nM) or ST (50 nM) were added to the culture

medium, and cells were further cultured for 2-3 h to be accumulated in mitosis. IE and ME from collected cells were immunoblotted with MPM2 (G) or immunoprecipitated under denaturing condition with the 3A9 antibody followed by immunoblotting with the 3A9 antibody and anti-pS2 antibody. Relative levels of the phosphorylated ALIX were determined and normalized against the levels of total ALIX (H).

#### **4.5. The activating phosphorylation of ALIX is required for ALIX to recruit CHMP4 to the midbody**

ALIX has been demonstrated to be critically involved in ESCRT-mediated cytokinetic abscission. During cytokinetic abscission, ALIX and TSG101 were recruited to the midbody through direct interaction with Cep55. ALIX and TSG101 promoted ESCRT-III assembly at the midbody through recruiting CHMP4 (Carlton et al., 2008). Since the intramolecular interaction of ALIX prohibits ALIX interaction with CHMP4, I hypothesized that phosphorylation at the S718 and S721 residues that relieves the intramolecular interaction of ALIX is required for ALIX to support cytokinetic abscission.

To test this hypothesis, I first determined whether ALIX is required for CHMP4 or TSG101 recruitment to the midbody. For this purpose, the ALIX knockdown HeLa cells were transfected with mCherry-CHMP4B or mCherry-TSG101, fixed and stained with anti-tubulin antibody. As shown in Fig. 26A, knockdown of ALIX inhibited the midbody localization of mCherry-CHMP4B in ~70% of the midbody-stage cells examined. In contrast, knockdown of ALIX did not affect the midbody localization of mCherry-TSG101 (Fig. 26B). These results suggest that ALIX is important for the midbody localization of CHMP4.

To further determine the role of the activating phosphorylation of ALIX in recruiting CHMP4 to the midbody, I ectopically expressed WT, S2A, or S2A- GFP-ALIX\* in the ALIX knockdown HeLa cells and examined the effects on the midbody localization of mCherry-CHMP4B. As shown in Fig. 26C, although WT or S2A- GFP-ALIX\* rescued the midbody localization of mCherry-CHMP4B to the near control level, S2A GFP-ALIX\* did not have the rescuing effects. These results suggest that the

phosphorylation at the S718 and S721 residues are required for ALIX to recruit CHMP4 to the midbody.

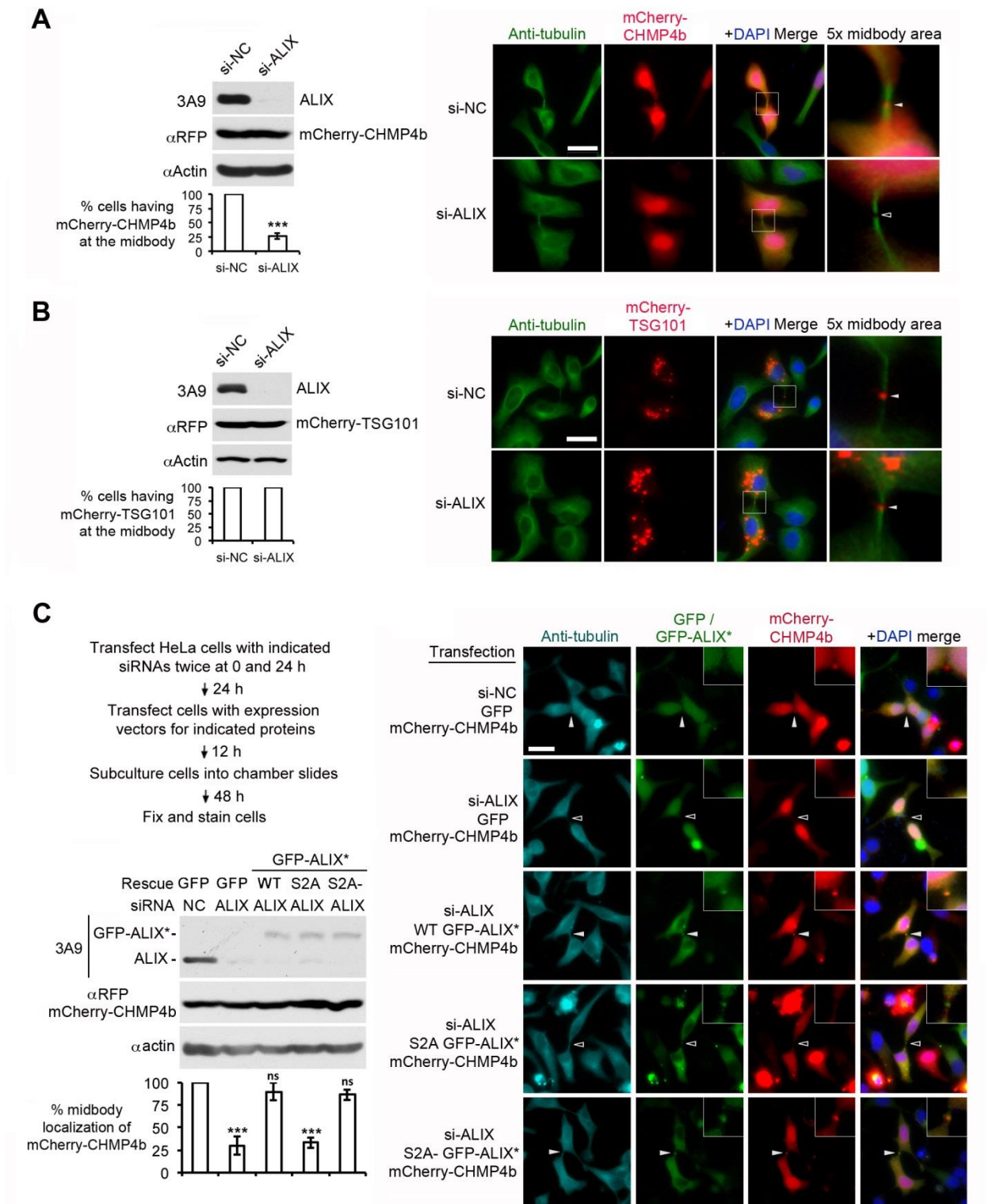


**Figure 26. The activating phosphorylation of ALIX is required for ALIX to recruit CHMP4 to the midbody.** (A&B) HeLa cells were transfected with mCherry-CHMP4B (A) or mCherry-TSG101 (B), fixed and stained with anti-tubulin antibody (green). Cell

lysates were immunoblotted to visualize ALIX, mCherry-CHMP4b (A), mCherry-TSG101 (B) and actin (left panel). The average percentages of mCherry positive cells with midbody localization of mCherry-CHMP4b and SDs (A) or mCherry-TSG101 (B) were determined from three independent experiments and plotted (left panel). Representative images are shown with the squares showing the 5x enlarged midbody areas. Solid and hollow arrowheads indicate the presence and absence of mCherry-CHMP4b (A) or mCherry-TSG101 (B) at the midbody, respectively. Scale bar: 50  $\mu$ m.

(C) HeLa cells were transfected with indicated siRNAs for 72 h, and cell lysates were immunoblotted with indicated antibodies to visualize ALIX and actin. Fixed cells were immunostained with an anti-tubulin antibody (red), and counterstained with DAPI (blue). The average percentages of midbody-stage cells or multinucleated cells and SDs were determined from three independent experiments and plotted. Representative images are shown with solid and hollow arrows indicating mononucleated and multinucleated cells, respectively, and hollow arrowheads indicating midbodies between daughter cells. Scale bar: 50  $\mu$ m.

#### **4.6. The activating phosphorylation of ALIX is required for ALIX to support cytokinetic abscission**

The midbody localization of CHMP4 is essential for cytokinetic abscission. Thus, I then determined whether the activating phosphorylation of ALIX is required for cytokinetic abscission. As shown in Fig. 27, knockdown of ALIX in HeLa cells increased the percentages of midbody-stage and multinucleated cells from <2% to ~14% and ~17%, respectively. Ectopic expressing WT, S2A or S2A- GFP-ALIX\* localized at the midbody in the ALIX knockdown cells. Although WT or S2A- GFP-ALIX\* rescued the percentages of midbody-stage and multinucleated cells to the near control levels, S2A GFP-ALIX\* did not have the rescuing effects. These results demonstrate that the phosphorylation at the S718 and S721 residues are important for ALIX to support cytokinetic abscission.

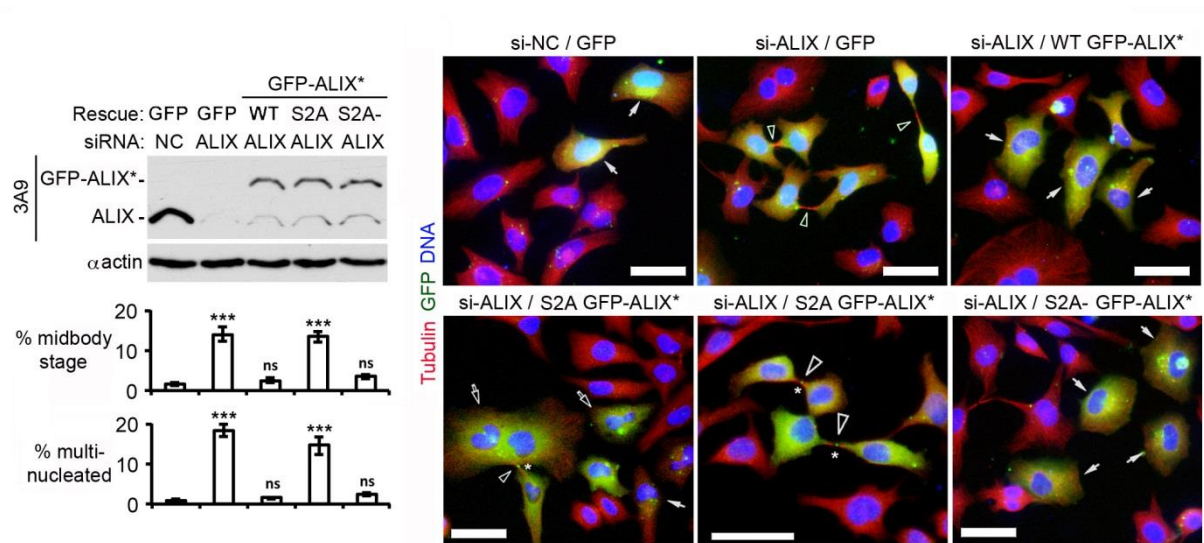


**Figure 27. The activating phosphorylation of ALIX is required for ALIX to support cytokinetic abscission.** HeLa cells were transfected with indicated siRNAs for 48 h and then transfected with indicated constructs for 24 h before fixation. The fixed cells were stained with an anti-tubulin antibody (red). Cell lysates were immunoblotted to visualize GFP-ALIX, ALIX and actin (left panel). The percentages of GFP-positive midbody-stage cells and multinucleated cells were scored and plotted (left panel). Representative images are shown with solid and hollow arrows indicating GFP-positive mononucleated and multinucleated/midbody-stage cells, respectively. Scale bar: 50  $\mu$ M.



#### **4.7. The activating phosphorylation of ALIX is required for ALIX to support EIAV budding**

ALIX has been demonstrated to be critically involved in ESCRT-mediated EIAV budding, which is a model system for studying of retroviral budding. ALIX involvement in EIAV budding requires ALIX interaction with p9<sup>GAG</sup> and CHMP4 (Strack et al., 2003). Thus, I hypothesized that the activating phosphorylation of ALIX is important for it to support EIAV budding.

To test this hypothesis, I first confirmed the previous reports that ALIX interaction with p9<sup>GAG</sup> needs opened ALIX by showing that GST-p9<sup>GAG</sup> specifically pulled down ALIX from ME, but not IE (Fig. 28A). Moreover, p9<sup>GAG</sup> interaction with opened ALIX could partially keep the open conformation of ALIX even after dephosphorylation of ALIX (Fig. 28B).

To determine whether there is a conformational change of ALIX during EIAV budding, HEK293 cells were co-transfected with an infection-defective EIAV Gag (pEV53B-Gag<sup>EIAV</sup>) and WT, S2A or S2A- GFP-ALIX, and the conformation of GFP-ALIX was examined by immunoprecipitation with the 1A3 antibody. As shown in Fig. 28C, expression of Gag<sup>EIAV</sup> induced 1A3-immunoprecipitable WT or S2A- GFP-ALIX, suggesting that the activating phosphorylation is required for generating opened ALIX during EIAV budding.

To determine whether the activating phosphorylation of ALIX is required for it to support EIAV budding, the ALIX knockdown HEK293 cells were co-transfected with pEV53B-Gag<sup>EIAV</sup> and WT, S2A, or S2A- GFP-ALIX\*, and the levels of VLPs were examined by collecting the VLPs through ultracentrifugation of culture medium followed

by immunoblotting with anti-CA antibody. As shown in Fig. 28D, knockdown of ALIX significantly inhibited the budding VLPs, consistent with the previous studies (Strack et al., 2003; von Schwedler et al., 2003). Ectopic expression of WT or S2A- GFP-ALIX\*, but not S2A GFP-ALIX, rescued the defect in EIAV budding, suggesting that the phosphorylation at S718 and S721 residues are important for ALIX to support EIAV budding. Further studies showed that arresting cells in mitosis blocked EIAV budding and that arresting cells in interphase did not affect EIAV budding (Fig. 28E), suggesting that EIAV budding only happens in interphase.

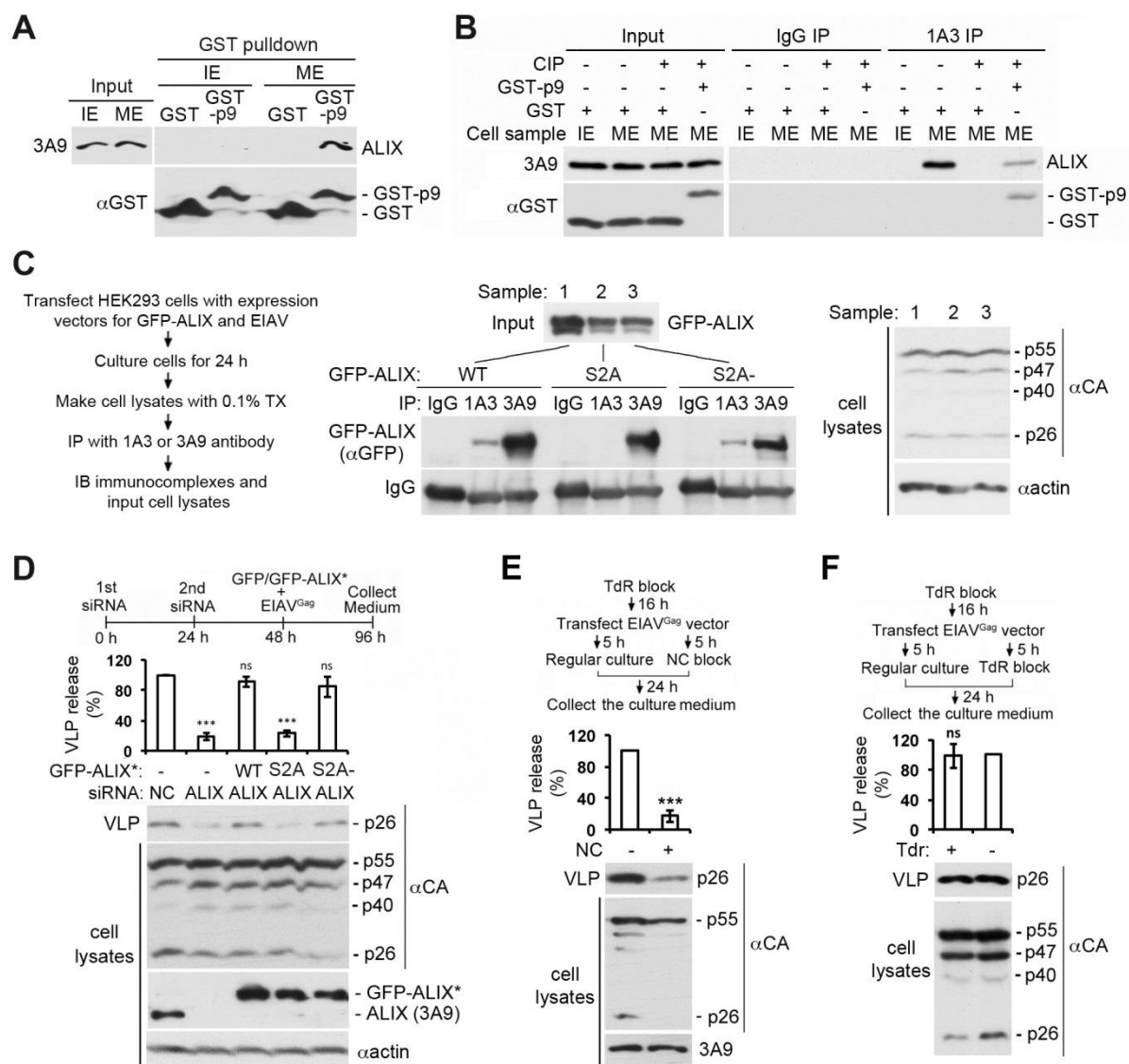


**Figure 28. The activating phosphorylation of ALIX is required for ALIX to support EIAV budding.** (A) GST or GST-p9 was incubated with IE or ME from HEK293 cells. Input and bound proteins were immunoblotted to visualize ALIX, GST and GST-p9. (B) ME from HEK293 cells was incubated with GST or GST-p9 at 4°C for 2 h, and then treated with CIP. The samples were immunoprecipitated with IgG or the 1A3 antibody, followed by immunoblotting to visualize ALIX, GST and GST-p9. (C) HEK293 cells were co-transfected with pEV53B EIAV<sup>Gag</sup> and indicated forms of GFP-ALIX. IE from the transfected cells were immunoprecipitated with indicated anti-ALIX antibodies. Input

and immunocomplexes were immunoblotted to visualize GFP-ALIX, Gag and actin. (D-F) HEK293 cells were processed as diagrammed. VLPs and cell lysates were immunoblotted with indicated antibodies. Relative levels of VLPs production and SDs were determined from three independent experiments and plotted.

#### **4.8. The activating phosphorylation of ALIX is not important for ALIX to support MVB sorting of activated EGFR**

ALIX has been demonstrated to be critically involved in ESCRT-III mediated MVB sorting of activated EGFR. Calcium-dependent ALG-2 interaction with ALIX activates the MVB sorting function of ALIX through relieving its intramolecular interaction. To determine whether the activating phosphorylation collaborates with ALG-2 interaction to promote MVB sorting of activated EGFR, I first examined whether the activating phosphorylation is required for EGF-stimulated increase of ALIX association with the membrane by using membrane flotation centrifugation. As shown in Fig. 29A, EGF stimulation increased the percentage of membrane associated WT or S2A GFP-ALIX from ~10% to ~30%. In contrast, the membrane association of  $\Delta$ PxY GFP-ALIX is dramatically decreased irrespective of EGF stimulation. These results suggest that the activating phosphorylation is not important for EGF-stimulated ALIX association with the membrane.

I then determined whether the activating phosphorylation is required for ALIX to promote MVB sorting of activated EGFR by using proteinase K protection assay. As shown in Fig. 29B, after 30 min of EGF stimulation, the percentage of protected EGFR is ~60%, indicating that ~60% of EGFR was sorted into the lumen of MVB. Knockdown of ALIX decreased the percentage of protected EGFR from ~60% to ~15%. WT, S2A or S2A- GFP-ALIX similarly rescued the protected percentage of EGFR to the near control level, suggesting that the activating phosphorylation is not important for ALIX to support MVB sorting of activated EGFR. Further, I determined the effects of the activating phosphorylation on the downstream signaling of activated EGFR by examining the levels of EGF-stimulated p-ERK1/2. As shown in Fig. 29C-D, knockdown of ALIX

prolonged the duration of p-ERK1/2 from 10 min to 60 min. WT or S2A GFP-ALIX\* rescued the effect of ALIX knockdown, reducing the duration of p-ERK1/2 to 10 min. These results support our conclusion.

Finally, I determined the effects of the activating phosphorylation on EGF-induced EGFR degradation under EGF continuous stimulation condition. As shown in Fig. 29E-F, knockdown of ALIX retarded the 50% EGFR degradation from 1 h to 2 h. Although  $\Delta$ PxY GFP-ALIX\* did not rescue the retardation effect of ALIX knockdown on EGFR degradation, WT or S2A GFP-ALIX\* could rescue the retardation effect, indicating that the activation phosphorylation of ALIX is not important for ALIX to function in the degradation of activated EGFR.

Taken together, these results demonstrate that the phosphorylation at S718 and S721 residues is not important for ALIX to support MVB sorting of activated EGFR.

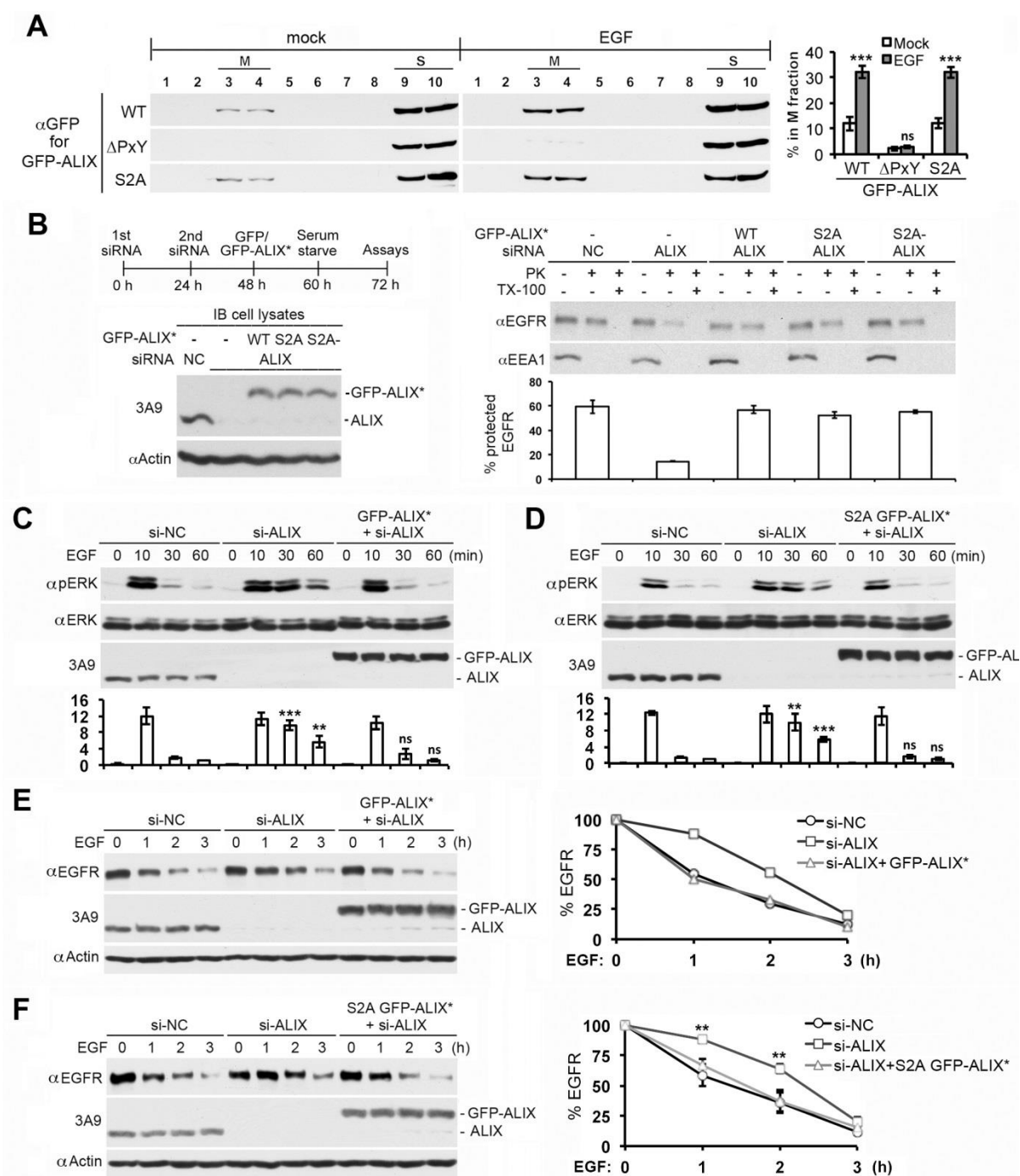


**Figure 29. The activating phosphorylation of ALIX is not important for ALIX to support MVB sorting of activated EGFR.** (A) HEK293 cells were transfected with indicated forms of GFP-ALIX and stimulated with or without EGF for 1 h. PNSs were fractionated by membrane flotation centrifugation. M and S fractions were determined by immunoblotting with an anti-GFP antibody. The average percentage of each GFP-ALIX

in the M fraction and SDs was determined and plotted. (B-F) HEK293 cells were transfected and serum-starved as diagrammed. (B) These cells were stimulated with EGF for 30 min before being assayed by the proteinase K protection assay. The average percentages of proteinase K-insensitive EGFR were determined and plotted. Error bars indicate the range of the data. (C&D) Cells were stimulated with EGF for indicated minutes, and cell lysates were immunoblotted to visualize p-ERK, ERK, GFP-ALIX and ALIX. The relative levels of p-ERK at different time points were determined and normalized against the level of si-NC cells at 60 min. (E&F) Cells were stimulated with EGF for indicated hours, and cell lysates were immunoblotted to visualize EGFR, GFP-ALIX, ALIX and actin. The percentages of remaining EGFR at different time points were determined and plotted.



## Discussion

My results show that ALG-2 is not important for ALIX-mediated cytokinetic abscission or retroviral budding, suggesting that different mechanisms are required to activate ALIX in these two processes. Using mitotic cells as the platform, I discovered that phosphorylation of the S718 and S721 residues at or near the intramolecular interaction site within the nPRD of ALIX in mitotic cells relieves the intramolecular interaction of ALIX and that multiple protein kinases, including PLK1 and PKD, are responsible for this activating phosphorylation. The functional studies demonstrate that this activating phosphorylation is required for ALIX to support cytokinetic abscission and retroviral budding, but is not important for MVB sorting of activated EGFR.

Cytokinetic abscission happens in early interphase when most of the mitotic kinases have been inactivated. How the mitotic phosphorylation-induced open conformation of ALIX can be maintained in interphase to support cytokinetic abscission? There are two possible explanations. One is that multiple mitotic kinase and phosphoproteins remain active at the midbody after mitotic exist. For example, the midbody was specifically recognized by the mitotic phosphoprotein monoclonal antibody MPM-2 (Sun et al., 2016; Vandre et al., 1986), by antibodies that recognize activated MEK, ERK and RSK (Sun et al., 2016; Willard and Crouch, 2001), by antibodies that recognize aurora B (Crosio et al., 2002; Sun et al., 2016), and by antibodies that recognize citron kinase and its activator RhoA (Madaule et al., 1998; Sun et al., 2016). Thus, it is possible that some of the kinases that catalyze the activating phosphorylation of ALIX in mitotic cells localize and remain active at the midbody and continue to catalyze the activating phosphorylation of ALIX. My results indicate that PLK1 and PKD are among the multiple mitotic kinases that catalyze the

activating phosphorylation of ALIX. Phosphorylation of Cep55 by PLK1 inhibits recruitment of Cep55 to the midbody (Bastos and Barr, 2010), making PLK1 less likely to be the candidate. However, immunostaining with anti-PKD substrate antibodies showed that the staining is barely detectable in interphase, very high and widespread in metaphase, decreased and concentrated in the spindle pole and midzone in anaphase and early telophase, and specifically lingered in the midbody area in late telophase and the midbody stage after most of the staining disappeared. There also may be unidentified kinases that remain active in the midbody area. The other explanation is that opened ALIX recruits CHMP4 and interacts with TSG101 and that the occupation of these partner proteins keeps the open conformation of ALIX even if ALIX is dephosphorylated at the midbody. My results indicate that increased occupation by partner proteins partially maintain the open conformation of ALIX. These two mechanisms may function together to keep a pool of opened ALIX in the midbody area to support cytokinetic abscission. The failure of cytokinetic abscission induces multinucleated cell. Proliferating multinucleated cells are genetically unstable and can promote tumorigenesis.

Retroviral budding does not expect to happen in mitosis; actually, if the cells are arrested in mitosis, the retroviral budding is significantly inhibited. Then, how phosphorylation at the S718 and S721 residues affects retroviral budding? There are two possible explanations. One possibility is that the infection of retrovirus induces the activity of certain kinases that catalyze the phosphorylation of ALIX. However, I could not detect the signal of phosphorylation by using the #4381 antibody or anti-pS2 antibody, suggesting that either the infection does not induce kinase activity or the level of phosphorylation is too low to be detected by our antibodies. The other possibility is

that the high level of p9<sup>GAG</sup> in EIAV expressing cells may occupy the opened ALIX and keep its open conformation. My results demonstrate that GST-p9<sup>GAG</sup> interacts with opened ALIX and partially keeps the open conformation of ALIX even after dephosphorylation of ALIX. Thus, these two mechanisms may function together to generate ALIX in open conformation to support retroviral budding.

## **Chapter 5: Discussion, perspective and future directions**

### **5.1. The regulation of ALIX in ESCRT-mediated processes**

ALIX is involved in numerous ESCRT-mediated membrane remodeling processes, including MVB sorting, cytokinetic abscission, retroviral budding, plasma membrane wound repair, exosome biogenesis, autophagy and nuclear envelope reformation, and all these processes are fundamental cellular processes that are critically involved in cell growth and survival (Bissig and Gruenberg, 2014; Hurley, 2015). Although much advancement has been made in discovery of key factors in these multi-step processes, the regulatory mechanism that links the initiator and the executor of this cascade is still poorly understood. ALIX is an essential mediator for linking the upstream initiator and the downstream executor of ESCRT-mediated processes by direct interaction with cargo proteins and CHMP4. Since CHMP4 interaction is inhibited by the default intramolecular interaction of ALIX, the regulation of ALIX in ESCRT-mediated processes is a very important question that should be explored for better understanding of these essential cellular processes. For investigating the regulation of ALIX in ESCRT-mediated processes, I chose the three classical ESCRT-mediated processes as the model systems because these three classical ESCRT-mediated processes are the most fundamental ones and the mechanisms underlining these processes are well studied.

Three potential mechanisms that relieve the intramolecular interaction have been proposed in previous studies from our group (Zhou et al., 2010). One is partner protein interaction-induced conformational change; another one is competitive binding-induced disruption of intramolecular interaction; the third one is posttranslational modification-induced disruption of intramolecular interaction.

My studies demonstrate that calcium-dependent ALG-2 interaction with ALIX specifically activates MVB sorting function of ALIX and that phosphorylation at the S718 and S721 residues in the nPRD specifically activates the function of ALIX to support cytokinetic abscission and retroviral budding (Fig. 30).

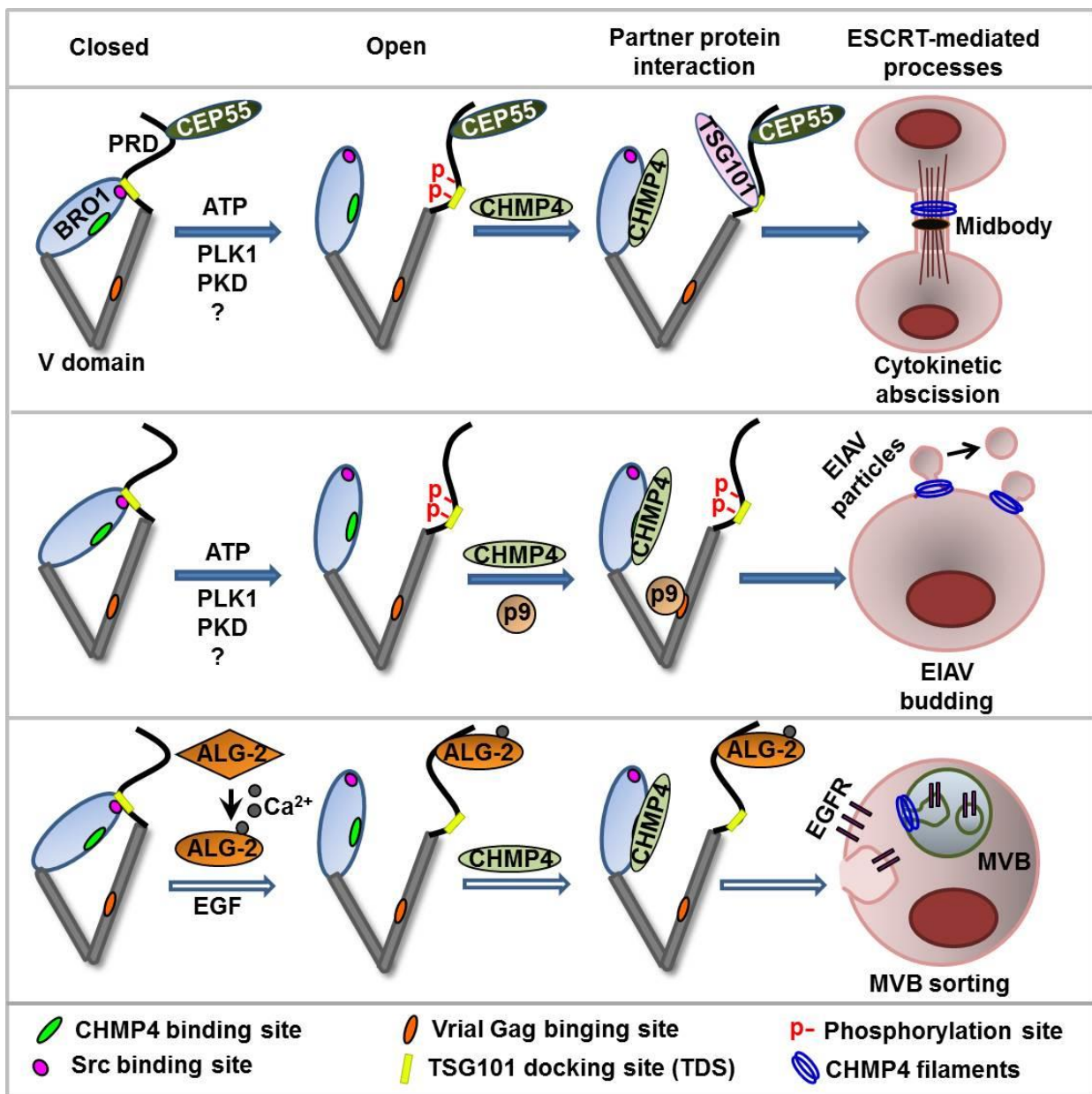


**Figure 30. Graphic abstract illustrating the mechanisms that activate ESCRT functions of ALIX in three classical ESCRT-mediated processes (Sun et al., 2016).**

(Permission obtained from Cell Press, License No.: 3830440570477)

## **5.2. The implication of the two regulatory mechanisms in ESCRT-mediated processes**

Since ALG-2 interaction with ALIX is calcium dependent (Missotten MTrioulier et al., 2004; Shibata et al., 2004), it is possible that the ESCRT-mediated processes that induce calcium spike will activate ALIX through this mechanism. In my current study, endocytosis-induced calcium spike promotes ALG-2-mediated activation of ALIX in MVB sorting of activated EGFR. Plasma membrane damage also induces calcium spike near the damaged site. ALG-2 is important for recruiting ALIX and ESCRT-III to the damaged site for repair (Jimenez et al., 2014; Scheffer et al., 2014). Exosome biogenesis and autophagosome formation share the similar mechanism for MVB sorting, involving sorting cargo proteins into endosome. Thus, calcium-dependent ALG-2 interaction with ALIX may be also involved in activating ALIX in these processes.

Phosphorylation-dependent activation of ALIX happens when the kinases responsible for catalyzing this phosphorylation are active. Thus, it is possible that ESCRT-mediated processes that induce the activities of those responsible kinases will activate ALIX through this mechanism. In my current studies, in mitotic cells, which have numerous mitotic kinases activated, S718 and S721 residues can be phosphorylated by some of these kinases. Partner protein occupation maintains the open conformation of ALIX during cytokinetic abscission, which actually happens in interphase. Retroviral infection may induce a very low level of phosphorylation at S718 and S721 residues, even falling below our antibody detection range, through either inducing a very low level of kinase activity or utilizing the basal level of kinase activity. Low level of phosphorylation may cooperate with partner protein (p6/p9) occupation to generate a pool of ALIX in open conformation to support retroviral budding. Proper and

timely nuclear envelope reformation prevents DNA damage and protects genomic stability (Olmos et al., 2015; Vietri et al., 2015). Recent studies showing that Aurora B and ULK3 (Unc-51-like kinase 3)-mediated phosphorylation of CHMP4 delayed cytokinetic abscission through inducing defective ESCRT-III polymerization (Caballe et al., 2015; Carlton et al., 2012) suggest that phosphorylation-dependent regulation may be involved in protecting genomic stability and preventing DNA damage. Thus, in the process of ESCRT-mediated nuclear envelope reformation, which may induce activities of many kinases, ALIX may be activated in a phosphorylation-dependent manner.

Thus, my studies of regulation of ALIX in the three classical ESCRT-mediated processes provide perspective into the regulation of all ESCRT-mediated membrane remodeling processes.

### **5.3. The implication of ALG-2/ALIX supported MVB sorting in cancer**

Based on my studies demonstrating the essential role of ALG-2/ALIX-supported MVB sorting in silencing of activated EGFR, an interesting question would be: whether ALG-2/ALIX-supported MVB sorting also regulate other receptor tyrosine kinases or other types of membrane receptors? Recent studies demonstrated the essential role of ALIX in MVB sorting of PAR1, a GPCR family member (Dores et al., 2012a). Although involvement of ALG-2 was not examined in that study, it is reasonable to expect that ALG-2 is involved in activating ALIX in this process.

In the absence of normal ESCRT function, the signaling of EGFR and other receptor tyrosine kinases, including Insulin receptor, platelet-derived growth factor receptor (PDGFR) and vascular endothelial growth factor receptor (VEGFR) are elevated (Engedal and Mills, 2014; Rodahl et al., 2009; Wegner et al., 2011), indicating that MVB sorting is involved in timely silencing of these receptors. Further studies need



to use these receptor tyrosine kinases as the model molecules to examine whether ALG-2 is also involved in MVB sorting of other receptor tyrosine kinases.

Activated receptor tyrosine kinases stimulate cell proliferation and survival, thus their signaling should be tightly controlled. ALG-2/ALIX-supported MVB sorting is an important negative regulator of the signaling of these receptors. If MVB sorting pathway has defects, the signaling of the activated receptors cannot be timely terminated. That may induce uncontrolled cell proliferation and tumorigenesis (Bache et al., 2004; Rodahl et al., 2009; Wegner et al., 2011).

My studies provide a novel insight into the over-activation of receptor tyrosine kinases in cancer cells and suggest that ALG-2/ALIX axis may be a potential target for cancer therapy.

#### **5.4. The switch of ALIX between its ESCRT-dependent function and ESCRT-independent function**

Besides the widespread roles of ALIX in ESCRT-mediated processes, ALIX also performs diverse ESCRT-independent cellular processes. ALIX was shown to regulate cell adhesion, cell morphology and migration (Pan et al., 2008; Pan et al., 2006; Schmidt et al., 2003). These studies indicate that cytosolic ALIX is able to perform these functions. My studies demonstrate that cytosolic ALIX is in closed conformation and that ALIX in open conformation will associate with membrane. Thus, the possible scenario is that ESCRT-dependent functions of ALIX require open conformation of ALIX, while ESCRT-independent functions of ALIX need closed conformation of ALIX. Then, how ALIX is switched between these two types of functions and its implication in cancer is an important and interesting question.

The evidence from the studies in our group indicates that the ESCRT-independent functions of ALIX may promote tumor cell migration. However, if ALIX is induced to open conformation, opened ALIX may exert malignancy inhibitory effects through promoting MVB sorting and silencing of activated receptor tyrosine kinases. In this context, ALG-2 may be an essential factor to regulate the switch of ALIX between pro-malignant function and anti-malignant function.

### **5.5. A potential new strategy to target activated receptor tyrosine kinases**

Current therapeutic strategies to target receptor tyrosine kinases in cancer cells are either targeting a specific type of receptors by using antibody, inhibiting the activity of a specific type of receptors by small-molecule inhibitors or inhibiting the downstream signaling of activated receptors by small-molecule inhibitors. The limitation of these strategies is that we can only target specific type of receptor tyrosine kinases. Then, other receptor tyrosine kinases may play redundant roles to induce drug-resistance.

If we can develop a compound that can mimic ALG-2/ALIX interaction to induce open conformation of ALIX, this compound will promote ALIX-supported MVB sorting and silencing of activated receptor tyrosine kinases. The advantage of this strategy is that it can target multiple receptor tyrosine kinases simultaneously.

### **5.6. Future directions**

Our current studies also raise multiple new problems that deserve further investigations.

- 1. To examine whether the regulatory mechanisms identified in the current studies also apply to other ESCRT-mediated processes.**

Besides the three classical ESCRT-mediated processes studied in the current research, there are many new identified ESCRT-mediated processes. How these ESCRT-mediated processes are regulated is an important and interesting question. By using three classical ESCRT-mediated processes, our current studies identified two regulatory mechanisms: calcium-dependent ALG-2 interaction and phosphorylation. Future studies would test whether either of them applies to new identified ESCRT-mediated processes. There is possible that some of the ESCRT-mediated processes use neither of these two mechanisms. In this case, further studies may be performed to explore the novel mechanisms that activate ALIX.

**2. To examine whether ALG-2/ALIX-supported MVB sorting applies to other receptor tyrosine kinases.**

EGFR is the model molecule for study of MVB sorting of ubiquitinated receptor tyrosine kinases. ALG-2 was identified as apoptosis inducing protein and shown to have dysregulation in many types of cancer. ALIX was also initially found to have apoptosis inducing effects. Moreover, ALG-2 and ALIX interaction is required for them to be involved in inducing apoptosis. However, the underlining mechanism is still not clear. The potential role of ALG-2/ALIX-supported MVB sorting in silencing of receptor tyrosine kinases is a possible underline mechanism. Thus, in future studies, we need to examine the effects of ALIX or ALG-2 knockdown on downstream signaling and degradation of insulin receptor, PDGFR and VEGFR. If positive results are obtained, further studies may be performed to examine the role of ALG-2/ALIX-supported MVB sorting in cell proliferation, apoptosis and migration.

**3. To identify the kinases responsible for catalyzing the phosphorylation at S718 and S721 residues of ALIX.**

Based on our current studies showing that even combination of PLK1 and PKD inhibitors cannot completely inhibit S718-S721 phosphorylation, there are two possibilities: one is that PLK1 and PKD are among the multiple kinases that play redundant roles in phosphorylating S718-S721 residues; the other possibility is that the major kinase(s) that is/are responsible for this activating phosphorylation is still unidentified. To test these possibilities, we can use GST-ALIX<sub>nPRD</sub> to pull down proteins from MEE or ME and wash off the binding proteins. These proteins will be analyzed by mass spectrometry, which may identify all kinases binding to ALIX<sub>nPRD</sub>. Then, the kinase inhibitors will be used to further test the involvement of these kinases. Identifying the responsible kinases will lead to a better understanding for the phosphorylation-dependent regulation of ESCRT-mediated processes.

#### **4. To examine the mechanisms that switch ALIX between non-ESCRT function and ESCRT function.**

Our current studies as well as the studies from previous graduate student in our group indicated that ESCRT function of ALIX may be involved in malignancy inhibition while non-ESCRT function of ALIX may be involved in promoting cell migration. Thus, investigating the potential mechanisms that switch ALIX between ESCRT function and non-ESCRT function will lead to a better understanding for the role of ALIX in cancer biology. We hypothesize that conformational change of ALIX may be the switch. To test the hypothesis, we will examine the role of ALIX in cell migration. We will also examine the effects of constitutive opened ALIX on cell proliferation, cell morphology and apoptosis. Further studies may develop a compound that can induce the open conformation of ALIX and examine the malignancy inhibitory effects of the compound.

## Chapter 6: Experimental procedures

### Cell culture, transfection, EGF stimulation and cell synchronization

HEK293 and HeLa cells were maintained in Dulbecco's Modification of Eagle's Medium (DMEM) (Mediatech Inc) supplemented with 2 mM L-glutamine and 10% fetal bovine serum (Atlanta Biologicals). Subconfluent cultures of cells in 60-mm or 35-mm culture dishes were transfected with siRNAs or expression vectors using GenMute™ siRNA Transfection Reagent or PolyJet™ DNA In Vitro Transfection Reagent (SignaGen Laboratories) according to manufacturer's instructions. Transfected cells were cultured for additional 24 to 48 h before experimental analyses. Transfection with ALIX-specific siRNAs was done twice (at 0 and 24 h) as performed in multiple previous studies, due to high abundance of ALIX. siRNAs used in this study are summarized in Table 2. Mammalian expression vectors used in this study are summarized in Table 3, and PCR primers used for site-directed mutagenesis and making vectors are summarized in Table 4.

The calcium ionophore A23187 (Sigma) was solubilized in 0.1% DMSO, and was added to the culture medium at a final concentration of 10  $\mu$ M 15 min before cell collection. Cell permeable calcium chelator BAPTA-AM (Toronto Research Chemicals) was solubilized in DMSO and added to the culture medium at a final concentration of 10  $\mu$ M 1 h before EGF stimulation.

Subconfluent cells in 35-mm dishes were switched to serum free DMEM medium and cultured for ~12 h for serum starvation. For continuous EGF stimulation, recombinant EGF (Sigma) was added to the serum free DMEM medium at a final concentration of 100 ng/ml, and cells were cultured further for indicated lengths of time.

For pulse-chase EGF stimulation, recombinant EGF was added to the serum free DMEM medium at a final concentration of 100 ng/ml. Serum-starved cells were first incubated with EGF at 4°C for 30 min (pulse), and then changed to EGF- and serum-free medium and cultured at 37°C for indicated lengths of time (chase). The lysosome inhibitor chloroquine (CQ) (Sigma) was added to the medium at a final concentration of 25 mM, whenever indicated.

To synchronize cells in mitosis, HEK293 cells were first cultured in DMEM containing 2.5 mM thymidine (Sigma) for 16 h and cultured in fresh DMEM for 3 h to release the cells. Then, 100 ng/mL nocodazole (NC) (Sigma) was added to DMEM for mitotic block. To prevent cells into mitosis, HEK293 cells were cultured in DMEM containing 2.5 mM thymidine (Sigma) for 16-24 hr to be arrested in S phase.

**Table 2. Sequences of siRNAs used in this study**

Target	Name	Sequence	Source
ALIX	si-ALIX(1)	5'-GAGAAGAAAUUGCAAGGUUdTdT-3'	Sigma-Genosys
ALIX	si-ALIX(2)	5'-GAAGGAUGCUUUCGAUAAAdTdT-3'	Sigma-Genosys
ALG-2	si-ALG-2(1)	5'-GGUCGAUCAUAUCCAUGUUdTdT-3'	Sigma-Genosys
ALG-2	si-ALG-2(2)	5'-GACAGGAGUGGAGUGAUUAUdTdT-3'	Sigma-Genosys
Firefly GL3 luciferase	si-NC	5'-CUUACGCUGAGUACUUCGAdTdT-3'	Sigma-Genosys
CHMP4B	si-CHMP4B	5'-AGAAGAGUUUGACGAGGAUdTdT-3'	Sigma-Genosys
CHMP4B	si-CHMP4B	5'-CGGAAGAGAUGUUAACGAAdTdT-3'	Sigma-Genosys

**Table 3. Mammalian expression vectors used in this study**

Vector	Source
pEGFP-C3-based expression vector for GFP-ALIX	A gift from Dr. Masatoshi Maki (Nagoya, Japan) (Shibata et al., 2004)
pEGFP-C3-based expression vector for ALIX-siRNA(1)-insensitive GFP-ALIX	Made in this study
pEGFP-C3-based expression vector for I212D GFP-ALIX	Made in this study
pEGFP-C3-based expression vector for ALIX-siRNA(1)-insensitive I212D GFP-ALIX	Made in this study
pEGFP-C3-based mammalian expression vector for $\Delta$ PxY GFP-ALIX	A gift from Dr. Masatoshi Maki (Nagoya, Japan) (Shibata et al., 2004)
pEGFP-C3-based expression vector for ALIX-siRNA(1)-insensitive DM GFP-ALIX	Made in this study
pEGFP-C3-based mammalian expression vector for S718A GFP-ALIX	Made in this study
pEGFP-C3-based mammalian expression vector for S721A GFP-ALIX	Made in this study
pEGFP-C3-based mammalian expression vector for S718A-S721A GFP-ALIX	Made in this study
pEGFP-C3-based mammalian expression vector for S712A-S729A GFP-ALIX	Made in this study
pEGFP-C3-based mammalian expression vector for S718A-S721A ALIX-siRNA-insensitive GFP-ALIX (S2A GFP-ALIX*)	Made in this study
pEGFP-C3-based mammalian expression vector for S712A-S729A ALIX-siRNA-insensitive GFP-ALIX (S2A-GFP-ALIX*)	Made in this study
pEGFP-C3-based mammalian expression vector for S718D-S721D GFP-ALIX	Made in this study



pCMV-based expression vector for FLAG-CHMP4b	A gift from Dr. Masatoshi Maki (Nagoya, Japan) (Kato et al., 2003)
pCMV-Tag2C-based mammalian expression vector for FLAG-ALG-2	A gift from Dr. Changmin Chen (Boston, MA) (Chen and Sytkowski, 2005)
pCMV-Tag2C-based mammalian expression vector for siRNA(1)-insensitive FLAG-ALG-2 (FLAG-ALG-2*)	Made in this study
pCMV-Tag2C-based mammalian expression vector for E47A FLAG-ALG-2	Made in this study
pCMV-Tag2C-based mammalian expression vector for E47A/E114A FLAG-ALG-2	Made in this study
pCMV-Tag2C-based mammalian expression vector for E47A/E114A FLAG-ALG-2*	Made in this study
The pIRES2-based mammalian expression vector for FLAG-TSG101	A gift from Dr. Wesley I. Sundquist (Salt Lake City, UT) (von Schwedler et al., 2003)
pEGFP-C3-based mammalian expression vector for GFP-Rab5 (Q79L)	A gift from Jean Gruenberg (Geneva, Switzerland) (Brankatschk et al., 2012)
pEV53B-based mammalian expression vector for infection defective EIAV	A gift from Dr. John Olsen (Chapel Hill, NC) (Olsen, 1998)
pGEX-4T3 based bacterial expression vector for WT GST-ALG-2	Made in this study
pGEX-4T3 based bacterial expression vector for E47A/E114A GST-ALG-2	Made in this study
pGEX-4T3 based bacterial expression vector for E47A/E114A GST-ALG-2	Made in this study
pGEX-4T3 based bacterial expression vector for GST-p6 <sup>HIV-Gag</sup>	A gift from Dr. Wesley I. Sundquist (Salt Lake City, UT) (Fisher et al., 2007)

pGEX-4T3 based vector bacterial expression for GST- p9 <sup>EIAV-Gag</sup>	A gift from Dr. Wesley I. Sundquist (Salt Lake City, UT) (Fisher et al., 2007)
pmCherry-C1-based expression vector for mCherry-CHMP4b	Made in this study
pmCherry-C1-based expression vector for mCherry-TSG101	Made in this study
pCS2-MT based TNT expression vector for myc- ALIX <sub>nPRD</sub>	Made in this study
pCS2-MT based TNT expression vector for S718A- S721A myc-ALIX <sub>nPRD</sub>	Made in this study
pCS2-MT based TNT expression vector for S712A- S729A myc-ALIX <sub>nPRD</sub>	Made in this study
pCS2-MT based TNT expression vector for S718D- S721D myc-ALIX <sub>nPRD</sub>	Made in this study
pCS2-MT based TNT expression vector for myc- TSG101	Made in this study
pCS2-HA based expression vector for HA-Plx1 (Xenopus)	Made in this study
pCS2-HA based expression vector for HA-K82R Plx1 (Xenopus)	Made in this study
pGEX-4T3 based bacterial expression vector GST- ALIX <sub>nPRD</sub>	Made in this study
pGEX-4T3 based bacterial expression vector for GST- ALIX <sub>Bro1</sub>	Generated in our previous studies (Zhou et al., 2009)
pGEX-4T3 based bacterial expression vector for GST- ALIX <sub>1-746</sub>	Generated in our previous studies (Zhou et al., 2009)
pGEX-4T3 based bacterial expression vector for GST- CHMP4b	Made in this study

**Table 4. PCR primers used in this study**

Product	Primers (Forward/Reverse)
ALIX-siRNA(1) insensitive GFP-ALIX	5'GAAGAAATTTGGAGAGGAAATTGCAAGGTTAC3' 5'GTAACCTTGCAATTCCTCTCCAAATTTCTTC3'
$\Delta$ PxY GFP- ALIX*	5'GAAGAAATTTGGAGAGGAAATTGCAAGGTTAC3' 5'GTAACCTTGCAATTCCTCTCCAAATTTCTTC3'
S718A GFP- ALIX	5'CATTGCCAGAGAACCTGCTGCTCCTTCAATTCCTACAC3' 5'GTGTAGGAATTGAAGGAGCAGCAGGTTCTCTGGCAATG3'
S721A GFP- ALIX	5'GAACCTAGTGCTCCTGCAATTCCTACACCTGC3' 5'-GCAGGTGTAGGAATTGCAGGAGCACTAGGTTC3'
S718A-S721A GFP-ALIX	5'CATTGCCAGAGAACCTGCTGCTCCTGCAATTCCTACACCTG 3' 5'CAGGTGTAGGAATTGCAGGAGCAGCAGGTTCTCTGGCAAT G3'
S712A-S729A GFP-ALIX	WT to S712A: 5'CTTAAAGGACTTGCAACAAGCCATTGCCAGAGAACCTAGTG 3' 5'CACTAGGTTCTCTGGCAATGGCTTGTTGCAAGTCCTTTAAG 3' S712A to S712A-S729A: 5'CTACACCTGCGTATCAGGCCTCACCAGCAGGAGGAC3' 5'GTCCTCCTGCTGGTGAGGCCTGATACGCAGGTGTAG3'
S718A-S721A ALIX-siRNA- insensitive GFP-ALIX	5'CATTGCCAGAGAACCTGCTGCTCCTGCAATTCCTACACCTG 3' 5'CAGGTGTAGGAATTGCAGGAGCAGCAGGTTCTCTGGCAAT G3'
S712A-S729A ALIX-siRNA- insensitive	5'GAAGAAATTTGGGGAGGAGATCGCGAGATTACAGCATGCA GCA3'

GFP-ALIX	5'CTGCTGCATGCTGTAATCTCGCGATCTCCTCCCCAAATTTC TTC3'
S718D-S721D GFP-ALIX	5'GCATTGCCAGAGAACCTGATGCTCCTGATATTCCTACACCT GCG3'  5'CGCAGGTGTAGGAATATCAGGAGCATCAGGTTCTCTGGCAA TGC3
Y319F-I212D FLAG-ALIX <sub>Bro1</sub>	5'GAGATAAAATGAAAGATGCCGACATAGCTAAATTGGCTAAT CAG3'  5'CCTGATTAGCCAATTTAGCTATGTCGGCATCTTTCATTTTAT CTC3'
FLAG-ALIX <sub>V</sub>	5'GAGGAATTCGCGTGTCTCAGTACAGTCT3'  5'TGTTGCGGCCGCGAGTCCTTTAAGAGTTCAT3'
<sup>638</sup> KMK <sub>640</sub> to <sup>638</sup> EEA <sub>640</sub> mutation in ALIX	5'CTCACATCAGGAATTTTCAGAAGCGGCGCAATCTAATAATG AAG3'  5'GCTTCATTATTAGATTGCGCCGCTTCTGAAAATTCCTGATGT GAG3'
<sup>643</sup> NNE <sub>645</sub> to <sup>643</sup> YKK <sub>645</sub> mutation in ALIX V domain	5'CAGAAGCGGCGCAATCTTATAAGAAAGCTAACTTAAGAGAA G3'  5'CTTCTCTTAAGTTAGCTTTCTTATAAGATTGCGCCGCTTCTG 3'
WT FLAG-ALG-2*	5'GTGACTGTCAGGTCCATCATATCCATGTTTG3'  5'CAAACATGGATATGATGGACCTGACAGTCAC3'
E47A FLAG-ALG-2	5'GAGTGATATCAGACACCGCGCTTCAGCAAGCTCTCTC3'  5'GAGAGAGCTTGCTGAAGCGCGGTGTCTGATATCACTC3'
E47A/E114A FLAG-ALG-2	5'GATGATCGATAAGAACGCGCTGAAGCAGGCCCTCTCAG3'  5'CTGAGAGGGCCTGCTTCAGCGCGTTCTTATCGATCATC3'
E47A/E114A FLAG-ALG-2*	5'GTGACTGTCAGGTCCATCATATCCATGTTTG3'  5'CAAACATGGATATGATGGACCTGACAGTCAC3'

WT GST-ALG-2	5'TAAGAATTCCATGGCCGCCTACTCTTAC3' (EcoR1) 5'TAACTCGAGTCATACGATACTGAAGACCATG3' (Xho1)
E47A/E114A GST-ALG-2	5'TAAGAATTCCATGGCCGCCTACTCTTAC3' (EcoR1) 5'TAACTCGAGTCATACGATACTGAAGACCATG3' (Xho1)
mCherry-TSG101	5'TAACTCGAGCT ATGGCGGTGTCTGGAGAG3' (Xho I) 5'TAAGAATTCTCAGTAGAGGTCACTGAGACCG3' (EcoRI)
pCS2-MT-ALIX <sub>nPRD</sub>	5'TAAGAATTCATTAAAGGACTTGCAACAAAGCATTG3' (EcoRI) 5'TAACTCGAGTGGCGCAGCAGTCCC3' (Xho I)
pCS2-MT-S718A-S721A ALIX <sub>nPRD</sub>	5'TAAGAATTCATTAAAGGACTTGCAACAAAGCATTG3' (EcoRI) 5'TAACTCGAGTGGCGCAGCAGTCCC3' (Xho I)
pCS2-MT-S712A-S729A ALIX <sub>nPRD</sub>	5'TAAGAATTCATTAAAGGACTTGCAACAAGCCATTG3' (EcoRI) 5'TAACTCGAGTGGCGCAGCAGTCCC3' (Xho I)
pCS2-MT-S718D-S721D myc-ALIX <sub>nPRD</sub>	5'TAAGAATTCATTAAAGGACTTGCAACAAAGCATTG3' (EcoRI) 5'TAACTCGAGTGGCGCAGCAGTCCC3' (Xho I)
pCS2-MT-TSG101	5'TAAGAATTCAATGGCGGTGTCTGGAGAG3' (EcoRI) 5'TAACTCGAGTCAGTAGAGGTCACTGAGACCG3' (Xho I)
pCS2-HA-Plx1 ( <i>Xenopus</i> )	5'AATGGGCCCTCAAGTGGCCGGTAAGAAAC3' (Apa I) 5'GCCTCTAGAGCCGAGGCCTTTACGTGTGC3' (Xba I)
pCS2-HA-Plx1 K82R ( <i>Xenopus</i> )	5'AATGGGCCCTCAAGTGGCCGGTAAGAAAC3' (Apa I) 5'GCCTCTAGAGCCGAGGCCTTTACGTGTGC3' (Xba I)
pGEX-4T3-ALIX <sub>nPRD</sub>	5'TAAGAATTCCTTAAAGGACTTGCAACAAAGCATTG3' (EcoRI) 5'TAACTCGAGTGGCGCAGCAGTCCC3' (Xho I)
pGEX-4T3-CHMP4b	5'TAAGAATTCCATGTCGGTGTTCGGGAAG3' (EcoRI) 5'TAACTCGAGTTACATGGATCCAGCCCAG3' (Xho I)

### **Protein extraction, immunoblotting and immunoprecipitation**

To prepare crude cell lysates for immunoblotting, cells scraped from culture plates or dishes were pelleted and extracted with cell lysis buffer consisting of 50 mM Tris-HCl, 150 mM NaCl, 1% Triton X-100, 0.1% SDS, 0.5 mM EDTA, 100  $\mu$ M sodium orthovanadate 100  $\mu$ M sodium fluoride, 100  $\mu$ M sodium pyrophosphate, 1 mM Dithiothreitol (DTT) and proteinase inhibitor cocktail (Sigma); 100-200  $\mu$ l of cell lysis buffer was used to extract cells from one 60-mm dish. Cell lysates were cleared by centrifugation at 16,000 *g* for 10 min at 4°C.

To prepare membrane solubilized cell lysates for immunoprecipitation, pelleted cells were extracted by sonication in 50-100  $\mu$ l of cell lysis buffer that omits 0.1% SDS and includes 10 mM N-Ethylmaleimide (NEM) (Sigma) whenever indicated. Cell lysates were cleared by centrifugation at 16,000 *g* for 10 min at 4°C and diluted 10 fold before immunoprecipitation.

To prepare cytosolic proteins from asynchronously growing cells or mitotically arrested cells for immunoprecipitation or GST pull-down, pelleted cells were sonicated with 10 volumes of extraction buffer (EB), consisting of 80mM  $\beta$ -glycerophosphate, 20 mM EGTA, 15 mM MgCl<sub>2</sub>, 150 mM NaCl, 1 mM DTT, and proteinase inhibitor cocktail (Sigma) (pH 7.4). For extraction of mitotically arrested cells and occasionally also asynchronously growing cells whenever indicated, EB was freshly supplemented with 1 mM microcystin (Sigma) and 1 mM ATP (Sigma). Cell lysates were cleared by centrifugation at 16,000 *g* for 10 min at 4°C. CIP (New England Biolabs) was added to MEE at a final concentration of 1 unit/mg substrate proteins according to the manufacture's instruction.

To prepare cell lysates for dIP, pelleted cells were re-suspended with 10 volumes of denaturing buffer consisting of 50mM Tris-HCl (pH 7.5), 1% SDS, and 5mM DTT, and sonicated. After the samples were boiled for 5 min and cleared by centrifugation at 16,000 g for 5 min, they were diluted 10-fold with an SDS neutralizing immunoprecipitation buffer consisting of 50 mM Tris-HCl (pH 7.5), 250 mM NaCl, 5 mM EDTA, 0.5% NP-40, 1 mM DTT (Tansey, 2007), and proteinase inhibitor cocktail (Sigma).

The immunoprecipitation was performed by incubating indicated antibodies with the cell lysates by rotating at 4°C overnight followed by adding Protein A or Protein G resin (Genscript) to the cell lysates and incubating by rotating at 4°C for 1 h. The immuocomplex was washed five times with the same buffer used for immunoprecipitation.

The protein samples were mixed with SDS sample buffer and boiled for 10 min before being subject to SDS-PAGE. The protein samples on the SDS-PAGE gel were then transferred onto nitrocellulose (NC) membrane, which was blocked by 5% non-fat milk in TBST (TBS (50 mM Tris-HCl, 150mM NaCl, PH7.4) plus 0.02% Tween 20) at room temperature for 1 h. Then, the NC membrane was incubated with primary antibodies diluted in 3% BSA in TBST at 4°C overnight and HRP (horseradish peroxidase)-conjugated secondary antibodies diluted in 5% non-fat milk in TBST at room temperature for 2 h. The signal was detected by ECL (enhanced chemiluminescence) solution. Antibodies used in this study are summarized in Table 5.

**Table 5. Antibodies used in this study**

Recognition	Type	Source
Actin	Mouse monoclonal	Sigma-Aldrich. Cat#: A5441
1A3 anti-ALIX	Mouse monoclonal	Made in our previous studies (Pan et al., 2006)
1A12 anti-ALIX	Mouse monoclonal	Made in our previous studies (Pan et al., 2006)
1F7 anti-ALIX	Mouse monoclonal	Made in our previous studies (Pan et al., 2006)
2H12 anti-ALIX	Mouse monoclonal	Made in our previous studies (Pan et al., 2006)
3A9 anti-ALIX	Mouse monoclonal	Made in our previous studies (Pan et al., 2006)
ALG-2	Rabbit monoclonal	Epitomics. Cat#: 3846-1
Tubulin	Rabbit monoclonal	Cell Signaling. Cat#: 2125S
CHMP4b	Rabbit polyclonal	Santa Cruz. Cat#: sc-134946
*CHMP4A	Rabbit polyclonal	Santa Cruz. Cat#: sc-67229
*CHMP4B/C	Rabbit polyclonal	Abcam. Cat#: ab76334-100
EIAV capsid antigen (CA)	Mouse monoclonal	A gift from Dr. Robert Mealey (Pullman, WA) (McGuire et al., 1994; Mealey et al., 2009)
EEA1	Rabbit monoclonal	Epitomics. Cat#: 3704-1
EGFR	Rabbit monoclonal	Epitomics. Cat#: 1902-1
ERK1	Rabbit polyclonal	Santa Cruz. Cat#:sc-94



ERK2	Rabbit polyclonal	Santa Cruz. Cat#:sc-154
FLAG	Mouse monoclonal	Pierce .Cat#: MA1-918781
FLAG	Rabbit polyclonal	Sigma-Aldrich.Cat#: F7425-.2MG
GFP	Mouse monoclonal	Santa Cruz. Cat#: sc-9996
GST	Rabbit polyclonal	Santa Cruz. Cat#: sc-459
HA	Rabbit polyclonal	Santa Cruz. Cat#: sc-805
HA	Mouse monoclonal	Pierce. Cat#: 26183
IgG	Mouse	Sigma-Aldrich. Cat#: I5381-10MG
IgG	Rabbit	Sigma-Aldrich. Cat#: I5006-10MG
myc	Rabbit polyclonal	Santa Cruz. Cat#: sc-789
MPM2	Mouse monoclonal	Lab reserve
#4381 antibody	Rabbit polyclonal	Cell Signaling. Cat#: 4381
pS2 antibody	Rabbit polyclonal	Made in this study
p-ERK	Mouse monoclonal	Santa Cruz Cat#: sc7383
p-Tyr	Mouse monoclonal	Cell Signaling. Cat#: 9416
ubiquitin	Mouse monoclonal	Santa Cruz. Cat#: sc8017
TSG101	Rabbit monoclonal	Epitomics. Cat#: 5377-1

### **Membrane floatation centrifugation**

The PNS of HEK293 cell lysates was prepared by re-suspending cell pellets in 100  $\mu$ l of 10% (w/v) sucrose in TE buffer (TBS plus 1 mM EDTA) supplemented with proteinase inhibitor cocktail. Cells were lysed by sonication followed by centrifugation at 1800  $g$  for 5 min at 4°C. 0.1 ml of aliquot from each PNS was mixed with 0.4 ml of 85.5% (w/v) sucrose in TE buffer to generate a final concentration of 73% (w/v) sucrose. This 73% (w/v) sucrose was placed at the bottom of a 4-ml ultracentrifuge tube, above which 2.3 ml of 65% (w/v) sucrose and 1.2 ml of 10% (w/v) sucrose in TE buffer were sequentially overlaid. The step sucrose gradients were ultracentrifuged at 100,000  $g$  for 18 h at 4°C in a Beckman SW55-Ti rotor. After centrifugation, ten 0.4-ml fractions were collected by pipetting, and equivalent aliquots were taken from collected fractions for immunoblotting. In a typical execution of this protocol, fractions 3 and 4 contained membrane vesicles floating to the boundary of the 10% (w/v) and 65% (w/v) sucrose layers, whereas fractions 9 and 10 contained soluble proteins unable to float up.

### **Proteinase K protection assay**

Mock treated or EGF stimulated cells were collected and pelleted by centrifugation at 1,800  $g$  for 5 min. Pelleted cells were re-suspended in 10 volumes of 6.5  $\mu$ g/mL digitonin (Sigma) in PBS, followed by incubation first at room temperature for 5 min and at 4°C for 30 min. Samples were then centrifuged at 16,000  $g$  at 4°C for 5 min, and pellets were re-suspended in 10 volumes of homogenization buffer containing 100 mM  $K_2HPO_4/KH_2PO_4$ , 5 mM  $MgCl_2$  and 250 mM sucrose. Three aliquots with the same volume were taken equally from each sample, which were treated either with ddH<sub>2</sub>O, 4 ng proteinase K/ $\mu$ g sample protein or 4 ng proteinase K/ $\mu$ g sample protein plus 0.1% Triton X-100 at room temperature for 10 min. Proteinase K digestion was

stopped by adding SDS-PAGE sample buffer followed by being boiled for 10 min, and proteins were subject to SDS-PAGE and immunoblotting. Proteinase K should digest all EGFR in the presence of 0.1% Triton X-100, which solubilizes the membrane vesicles. Thus, the percentage of proteinase K-resistant EGFR in the absence of 0.1% Triton X-100 relative to total EGFR in ddH<sub>2</sub>O-treated sample was taken as the percentage of EGFR sorted into MVBs.

### **GST pull-down**

GST and GST tagged proteins were produced and purified by the transformation of BL21 Competent *E. coli* strains (Thermo Fisher Scientific) with pGEX-4T3 based vectors for GST or GST tagged proteins. The transformed BL21 Competent *E. coli* strains were incubated with 0.1 mM IPTG (Sigma) to stimulate the expression of GST or GST tagged proteins. The *E. coli* strains were lysed with PBS containing lysozyme (Sigma), 1 mM DTT, proteinase inhibitor cocktail (PH 7.4) at 4°C for 30 min. Then, Triton X-100 was added with the final concentration of 0.5%. The lysates were sonicated and cleared by centrifugation at 12,000 rpm at 4°C for 40 min. The supernatant was incubated with Glutathione beads (GenScript) at 4°C overnight. The beads were washed with buffer I, buffer II and buffer III, sequentially. The GST or GST tagged proteins were eluted by incubating the beads with elution buffer containing 50 mM Tris-HCl, 150 mM NaCl, 1 mM DTT, proteinase inhibitor cocktail and 50 mM Glutathione (Sigma) at room temperature for 15 min. The elution step was repeated twice.

For GST pull-down, the GST or GST-tagged proteins, either untreated or treated, were first immobilized onto Glutathione beads by rotating at 4°C for 2 h. The immobilized beads were then incubated with either cell lysates or in-vitro translated

proteins at 4°C for 2 h. In vitro transcription and linked translation was performed by using the TNT QuickCoupled Transcription/Translation System (Promega) according to the manufacturer's instruction. The beads were washed five times with the same buffer used during pull-down. The samples were then mixed with SDS-sample buffer and subject to SDS-PAGE.

### **Biotinylation of cell surface proteins and affinity absorption of biotinylated proteins**

Serum-starved HEK293 cells cultured in 6-well plates were stimulated with 100 ng/ml EGF for indicated lengths of time followed by rinse with ice-cold PBS (pH 7.4) supplemented with 1.5 mM MgCl<sub>2</sub> and 0.2 mM CaCl<sub>2</sub>. The cells were then incubated twice (15 min each time) on a shaker with 200 mg/ml freshly prepared cold sulfo-NHS-SS-biotin solution (0.75 ml/well) (bioWORLD) at 4°C, and quenched by wash with quenching solution (PBS supplemented with 1.5 mM MgCl<sub>2</sub>, 0.2 mM CaCl<sub>2</sub> and 100 mM glycine, pH 7.4) and further incubation in this solution at 4°C for 30 min. Cell lysates were prepared with cell lysis buffer consisting of 50 mM Tris-HCl, 150 mM NaCl, 1% Triton X-100, 0.5 mM EDTA, 100 µM sodium orthovanadate, 100 µM sodium fluoride, 100 µM sodium pyrophosphate, 1 mM DTT and proteinase inhibitor cocktail and incubated with Streptavidin Separopore (Agarose) 4B (bioWORLD) at 4°C overnight. Pelleted beads were then washed five times with the same buffer used in incubation and proteins were eluted with SDS sample buffer for immunoblotting.

### **In Vitro Phosphorylation of ALIX Fragments with *Xenopus* Extracts**

MEE and IOE were prepared in the previous studies in our laboratory (Wu et al., 2010).

The in vitro phosphorylation reaction was performed by mixing one volume of substrate proteins and three volumes of IOE or MEE at room temperature for 2 h unless otherwise indicated, and terminated by adding SDS sample buffer. PLK1 inhibitor BI-2536, PKD inhibitor CID755673, and pan-kinase inhibitor staurosporine were dissolved in DMSO and added to MEE at 4°C 15 min prior to the phosphorylation reaction to reach a final concentration of 2 mM, 5 mM, and 5 mM, respectively.

### **The EIAV VLP release assay**

HEK293 cells were transfected with pEV53B EIAV vector and cultured for 48 h. Conditioned medium was collected and loaded onto a 2-ml 20% sucrose cushion in a 4-ml tube. After ultracentrifugation of the sample in an SW55-Ti rotor at 26,000 rpm for 2 h, pelleted proteins were extracted by using SDS sample buffer and immunoblotted with anti-EIAV capsid antigen (CA) antibodies.

### **Immunostaining and fluorescence microscopy**

Transfected HeLa cells were subcultured into chamber slides (Nunc Lab-Tek) coated with poly-D-Lysine (Cultrex) and cultured for 48 h before being fixed with 4% (w/v) of Paraformaldehyde at room temperature for 20 min. Fixed cells were permeabilized with 0.2% Triton X-100 in PBS followed by blocking with 1x blocking buffer (1% BSA, 0.25% horse serum, 0.2% Triton X-100 in PBS). Blocked cells were first stained with primary antibodies in 0.1x blocking buffer at 4°C overnight, and then with Alexa Fluor 568, Alexa Fluor 488 or Alexa Fluor 647 conjugated secondary antibodies in TBST (0.1% Triton X-100 in TBS) at room temperature for 1 h. Nuclei were stained with DAPI (Sigma). Images were acquired using MetaMorph software (7.7.5.0) on ZEISS Axioplan2 image system (Objective: plan-NEOFLUAR 20x/0.50 or plan-NEOFLUAR 100x/1.30 oil).

## **Generation of rabbit polyclonal antibodies for phosphorylated ALIX at S718 and S721**

To prepare antigen, a synthetic phosphopeptide consisting of the residues 711 to 724 of ALIX and phosphorylated at both S718 and S721 (CSIAREP(pS)AP(pS)IPT) was conjugated to keyhole limpet hemocyanin (KLH). To generate rabbit polyclonal antibodies, rabbits were immunized with the conjugated phosphopeptide for 42 days, and immunesera were collected. The IgG fraction of the antibodies was purified by protein G affinity chromatography. The phosphospecificity of the purified antibodies were evaluated with the enzyme-linked immune sorbent assay (ELISA).

### **Statistical analysis**

Statistical analyses were performed using Student's *t*-test. The *p*-value of  $\geq 0.01$  and  $< 0.05$  was considered significant (\*). The *p*-value of  $\geq 0.001$  and  $< 0.01$  was considered highly significant (\*\*). The *p*-value of  $< 0.001$  was considered very highly significant (\*\*\*)).

## REFERENCES

- Abrami, L., Lindsay, M., Parton, R.G., Leppla, S.H., and van der Goot, F.G. (2004). Membrane insertion of anthrax protective antigen and cytoplasmic delivery of lethal factor occur at different stages of the endocytic pathway. *The Journal of cell biology* 166, 645-651.
- Agromayor, M., and Martin-Serrano, J. (2013). Knowing when to cut and run: mechanisms that control cytokinetic abscission. *Trends in cell biology* 23, 433-441.
- Babst, M., Katzmann, D.J., Estepa-Sabal, E.J., Meerloo, T., and Emr, S.D. (2002a). Escrt-III: an endosome-associated heterooligomeric protein complex required for mvb sorting. *Developmental cell* 3, 271-282.
- Babst, M., Katzmann, D.J., Snyder, W.B., Wendland, B., and Emr, S.D. (2002b). Endosome-associated complex, ESCRT-II, recruits transport machinery for protein sorting at the multivesicular body. *Developmental cell* 3, 283-289.
- Babst, M., Wendland, B., Estepa, E.J., and Emr, S.D. (1998). The Vps4p AAA ATPase regulates membrane association of a Vps protein complex required for normal endosome function. *The EMBO journal* 17, 2982-2993.
- Bache, K.G., Slagsvold, T., and Stenmark, H. (2004). Defective downregulation of receptor tyrosine kinases in cancer. *The EMBO journal* 23, 2707-2712.
- Baietti, M.F., Zhang, Z., Mortier, E., Melchior, A., Degeest, G., Geeraerts, A., Ivarsson, Y., Depoortere, F., Coomans, C., Vermeiren, E., *et al.* (2012). Syndecan-syntenin-ALIX regulates the biogenesis of exosomes. *Nature cell biology* 14, 677-685.
- Banta, L.M., Robinson, J.S., Klionsky, D.J., and Emr, S.D. (1988). Organelle assembly in yeast: characterization of yeast mutants defective in vacuolar biogenesis and protein sorting. *The Journal of cell biology* 107, 1369-1383.

Bastos, R.N., and Barr, F.A. (2010). Plk1 negatively regulates Cep55 recruitment to the midbody to ensure orderly abscission. *The Journal of cell biology* 191, 751-760.

Beata MierzwaVotteler, J., and Sundquist, W.I. (2013). Virus budding and the ESCRT pathway. *Cell host & microbe* 14, 232-241.

Bilodeau, P.S., Urbanowski, J.L., Winistorfer, S.C., and Piper, R.C. (2002). The Vps27p Hse1p complex binds ubiquitin and mediates endosomal protein sorting. *Nature cell biology* 4, 534-539.

Bissig, C., and Gruenberg, J. (2014). ALIX and the multivesicular endosome: ALIX in Wonderland. *Trends in cell biology* 24, 19-25.

Boura, E., Rozycki, B., Chung, H.S., Herrick, D.Z., Canagarajah, B., Cafiso, D.S., Eaton, W.A., Hummer, G., and Hurley, J.H. (2012). Solution structure of the ESCRT-I and -II supercomplex: implications for membrane budding and scission. *Structure* 20, 874-886.

Bowers, K., Piper, S.C., Edeling, M.A., Gray, S.R., Owen, D.J., Lehner, P.J., and Luzio, J.P. (2006). Degradation of endocytosed epidermal growth factor and virally ubiquitinated major histocompatibility complex class I is independent of mammalian ESCRTII. *The Journal of biological chemistry* 281, 5094-5105.

Brankatschk, B., Wichert, S.P., Johnson, S.D., Schaad, O., Rossner, M.J., and Gruenberg, J. (2012). Regulation of the EGF transcriptional response by endocytic sorting. *Science signaling* 5, ra21.

Caballe, A., Wenzel, D.M., Agromayor, M., Alam, S.L., Skalicky, J.J., Kloc, M., Carlton, J.G., Labrador, L., Sundquist, W.I., and Martin-Serrano, J. (2015). ULK3 regulates cytokinetic abscission by phosphorylating ESCRT-III proteins. *eLife* 4, e06547.



Cabezas, A., Bache, K.G., Brech, A., and Stenmark, H. (2005). Alix regulates cortical actin and the spatial distribution of endosomes. *Journal of cell science* 118, 2625-2635.

Caillat, C., Macheboeuf, P., Wu, Y., McCarthy, A.A., Boeri-Erba, E., Effantin, G., Gottlinger, H.G., Weissenhorn, W., and Renesto, P. (2015). Asymmetric ring structure of Vps4 required for ESCRT-III disassembly. *Nature communications* 6, 8781.

Carlton, J.G., Agromayor, M., and Martin-Serrano, J. (2008). Differential requirements for Alix and ESCRT-III in cytokinesis and HIV-1 release. *Proceedings of the National Academy of Sciences of the United States of America* 105, 10541-10546.

Carlton, J.G., Caballe, A., Agromayor, M., Kloc, M., and Martin-Serrano, J. (2012). ESCRT-III governs the Aurora B-mediated abscission checkpoint through CHMP4C. *Science* 336, 220-225.

Carlton, J.G., and Martin-Serrano, J. (2007). Parallels between cytokinesis and retroviral budding: a role for the ESCRT machinery. *Science* 316, 1908-1912.

Chen, C., and Sytkowski, A.J. (2005). Apoptosis-linked gene-2 connects the Raf-1 and ASK1 signalings. *Biochemical and biophysical research communications* 333, 51-57.

Crosio, C., Fimia, G.M., Loury, R., Kimura, M., Okano, Y., Zhou, H., Sen, S., Allis, C.D., and Sassone-Corsi, P. (2002). Mitotic phosphorylation of histone H3: spatio-temporal regulation by mammalian Aurora kinases. *Molecular and cellular biology* 22, 874-885.

Dejournett, R.E., Kobayashi, R., Pan, S., Wu, C., Etkin, L.D., Clark, R.B., Bogler, O., and Kuang, J. (2007). Phosphorylation of the proline-rich domain of Xp95 modulates Xp95 interaction with partner proteins. *The Biochemical journal* 401, 521-531.

Dores, M.R., Chen, B., Lin, H., Soh, U.J., Paing, M.M., Montagne, W.A., Meerloo, T., and Trejo, J. (2012a). ALIX binds a YPX(3)L motif of the GPCR PAR1 and mediates ubiquitin-independent ESCRT-III/MVB sorting. *The Journal of cell biology* 197, 407-419.

Dores, M.R., Paing, M.M., Lin, H., Montagne, W.A., Marchese, A., and Trejo, J. (2012b). AP-3 regulates PAR1 ubiquitin-independent MVB/lysosomal sorting via an ALIX-mediated pathway. *Molecular biology of the cell* 23, 3612-3623.

Dowlatshahi, D.P., Sandrin, V., Vivona, S., Shaler, T.A., Kaiser, S.E., Melandri, F., Sundquist, W.I., and Kopito, R.R. (2012). ALIX is a Lys63-specific polyubiquitin binding protein that functions in retrovirus budding. *Developmental cell* 23, 1247-1254.

Doyotte, A., Mironov, A., McKenzie, E., and Woodman, P. (2008). The Bro1-related protein HD-PTP/PTPN23 is required for endosomal cargo sorting and multivesicular body morphogenesis. *Proceedings of the National Academy of Sciences of the United States of America* 105, 6308-6313.

Engedal, N., and Mills, I.G. (2014). Endosomal signaling and oncogenesis. *Methods in enzymology* 535, 179-200.

Feyder, S., De Craene, J.O., Bar, S., Bertazzi, D.L., and Friant, S. (2015). Membrane trafficking in the yeast *Saccharomyces cerevisiae* model. *International journal of molecular sciences* 16, 1509-1525.

Fisher, R.D., Chung, H.Y., Zhai, Q., Robinson, H., Sundquist, W.I., and Hill, C.P. (2007). Structural and biochemical studies of ALIX/AIP1 and its role in retrovirus budding. *Cell* 128, 841-852.

Forsburg, S.L. (2001). The art and design of genetic screens: yeast. *Nature reviews. Genetics* 2, 659-668.

Futter, C.E., Collinson, L.M., Backer, J.M., and Hopkins, C.R. (2001). Human VPS34 is required for internal vesicle formation within multivesicular endosomes. *The Journal of cell biology* 155, 1251-1264.

Gerasimenko, J.V., Tepikin, A.V., Petersen, O.H., and Gerasimenko, O.V. (1998). Calcium uptake via endocytosis with rapid release from acidifying endosomes. *Current biology : CB* 8, 1335-1338.

Gerasimenko, O., and Tepikin, A. (2005). How to measure  $\text{Ca}^{2+}$  in cellular organelles? *Cell calcium* 38, 201-211.

Goh, L.K., and Sorkin, A. (2013). Endocytosis of receptor tyrosine kinases. *Cold Spring Harbor perspectives in biology* 5, a017459.

Golsteyn, R.M., Mundt, K.E., Fry, A.M., and Nigg, E.A. (1995). Cell cycle regulation of the activity and subcellular localization of Plk1, a human protein kinase implicated in mitotic spindle function. *The Journal of cell biology* 129, 1617-1628.

Gruenberg, J., and Stenmark, H. (2004). The biogenesis of multivesicular endosomes. *Nature reviews. Molecular cell biology* 5, 317-323.

Guizetti, J., Schermelleh, L., Mantler, J., Maar, S., Poser, I., Leonhardt, H., Muller-Reichert, T., and Gerlich, D.W. (2011). Cortical constriction during abscission involves helices of ESCRT-III-dependent filaments. *Science* 331, 1616-1620.

Henne, W.M., Buchkovich, N.J., and Emr, S.D. (2011). The ESCRT pathway. *Developmental cell* 21, 77-91.

Henne, W.M., Buchkovich, N.J., Zhao, Y., and Emr, S.D. (2012). The endosomal sorting complex ESCRT-II mediates the assembly and architecture of ESCRT-III helices. *Cell* 151, 356-371.

Henne, W.M., Stenmark, H., and Emr, S.D. (2013). Molecular mechanisms of the membrane sculpting ESCRT pathway. *Cold Spring Harbor perspectives in biology* 5.

Hoffman, L., Stein, R.A., Colbran, R.J., and McHaourab, H.S. (2011). Conformational changes underlying calcium/calmodulin-dependent protein kinase II activation. *The EMBO journal* 30, 1251-1262.

Huang, F., Zeng, X., Kim, W., Balasubramani, M., Fortian, A., Gygi, S.P., Yates, N.A., and Sorkin, A. (2013). Lysine 63-linked polyubiquitination is required for EGF receptor degradation. *Proceedings of the National Academy of Sciences of the United States of America* 110, 15722-15727.

Hurley, J.H. (2010). The ESCRT complexes. *Critical reviews in biochemistry and molecular biology* 45, 463-487.

Hurley, J.H. (2015). ESCRTs are everywhere. *The EMBO journal* 34, 2398-2407.

Hurley, J.H., and Hanson, P.I. (2010). Membrane budding and scission by the ESCRT machinery: it's all in the neck. *Nature reviews. Molecular cell biology* 11, 556-566.

Jimenez, A.J., Maiuri, P., Lafaurie-Janvore, J., Divoux, S., Piel, M., and Perez, F. (2014). ESCRT machinery is required for plasma membrane repair. *Science* 343, 1247136.

Katoh, K., Shibata, H., Suzuki, H., Nara, A., Ishidoh, K., Kominami, E., Yoshimori, T., and Maki, M. (2003). The ALG-2-interacting protein Alix associates with CHMP4b, a human homologue of yeast Snf7 that is involved in multivesicular body sorting. *The Journal of biological chemistry* 278, 39104-39113.

Katzmann, D.J., Babst, M., and Emr, S.D. (2001). Ubiquitin-dependent sorting into the multivesicular body pathway requires the function of a conserved endosomal protein sorting complex, ESCRT-I. *Cell* 106, 145-155.

Katzmann, D.J., Odorizzi, G., and Emr, S.D. (2002). Receptor downregulation and multivesicular-body sorting. *Nature reviews. Molecular cell biology* 3, 893-905.

Katzmann, D.J., Stefan, C.J., Babst, M., and Emr, S.D. (2003). Vps27 recruits ESCRT machinery to endosomes during MVB sorting. *The Journal of cell biology* 162, 413-423.

Keren-Kaplan, T., Attali, I., Estrin, M., Kuo, L.S., Farkash, E., Jerabek-Willemsen, M., Blutraich, N., Artzi, S., Peri, A., Freed, E.O., *et al.* (2013). Structure-based in silico identification of ubiquitin-binding domains provides insights into the ALIX-V:ubiquitin complex and retrovirus budding. *The EMBO journal* 32, 538-551.

Kienzle, C., Eisler, S.A., Villeneuve, J., Brummer, T., Olayioye, M.A., and Hausser, A. (2013). PKD controls mitotic Golgi complex fragmentation through a Raf-MEK1 pathway. *Molecular biology of the cell* 24, 222-233.

Kim, J., Sitaraman, S., Hierro, A., Beach, B.M., Odorizzi, G., and Hurley, J.H. (2005). Structural basis for endosomal targeting by the Bro1 domain. *Developmental cell* 8, 937-947.

Lata, S., Schoehn, G., Solomons, J., Pires, R., Gottlinger, H.G., and Weissenhorn, W. (2009). Structure and function of ESCRT-III. *Biochemical Society transactions* 37, 156-160.

Lee, S., Joshi, A., Nagashima, K., Freed, E.O., and Hurley, J.H. (2007). Structural basis for viral late-domain binding to Alix. *Nature structural & molecular biology* 14, 194-199.

Lo, K.W., Zhang, Q., Li, M., and Zhang, M. (1999). Apoptosis-linked gene product ALG-2 is a new member of the calpain small subunit subfamily of Ca<sup>2+</sup>-binding proteins. *Biochemistry* 38, 7498-7508.

Madaule, P., Eda, M., Watanabe, N., Fujisawa, K., Matsuoka, T., Bito, H., Ishizaki, T., and Narumiya, S. (1998). Role of citron kinase as a target of the small GTPase Rho in cytokinesis. *Nature* 394, 491-494.

Mahul-Mellier, A.L., Hemming, F.J., Blot, B., Fraboulet, S., and Sadoul, R. (2006). Alix, making a link between apoptosis-linked gene-2, the endosomal sorting complexes required for transport, and neuronal death in vivo. *The Journal of neuroscience : the official journal of the Society for Neuroscience* 26, 542-549.

Mahul-Mellier, A.L., Strappazzon, F., Petiot, A., Chatellard-Causse, C., Torch, S., Blot, B., Freeman, K., Kuhn, L., Garin, J., Verna, J.M., *et al.* (2008). Alix and ALG-2 are involved in tumor necrosis factor receptor 1-induced cell death. *The Journal of biological chemistry* 283, 34954-34965.

Malerod, L., Stuffers, S., Brech, A., and Stenmark, H. (2007). Vps22/EAP30 in ESCRT-II mediates endosomal sorting of growth factor and chemokine receptors destined for lysosomal degradation. *Traffic* 8, 1617-1629.

Marsh, M., and McMahon, H.T. (1999). The Structural Era of Endocytosis. *Science* 285, 215-220.

Martin-Serrano, J., and Neil, S.J. (2011). Host factors involved in retroviral budding and release. *Nature reviews. Microbiology* 9, 519-531.

McCullough, J., Clippinger, A.K., Talledge, N., Skowrya, M.L., Saunders, M.G., Naismith, T.V., Colf, L.A., Afonine, P., Arthur, C., Sundquist, W.I., *et al.* (2015). Structure and membrane remodeling activity of ESCRT-III helical polymers. *Science* 350, 1548-1551.

McCullough, J., Fisher, R.D., Whitby, F.G., Sundquist, W.I., and Hill, C.P. (2008). ALIX-CHMP4 interactions in the human ESCRT pathway. *Proceedings of the National Academy of Sciences of the United States of America* 105, 7687-7691.

McGuire, T.C., O'Rourke, K.I., Baszler, T.V., Leib, S.R., Brassfield, A.L., and Davis, W.C. (1994). Expression of functional protease and subviral particles by vaccinia virus

containing equine infectious anaemia virus gag and 5' pol genes. The Journal of general virology 75 ( Pt 4), 895-900.

Mealey, R.H., Leib, S.R., Littke, M.H., Wagner, B., Horohov, D.W., and McGuire, T.C. (2009). Viral load and clinical disease enhancement associated with a lentivirus cytotoxic T lymphocyte vaccine regimen. Vaccine 27, 2453-2468.

Mellman, I. (1996). Endocytosis and molecular sorting. Annual review of cell and developmental biology 12, 575-625.

Mierzwa, B., and Gerlich, D.W. (2014). Cytokinetic abscission: molecular mechanisms and temporal control. Developmental cell 31, 525-538.

Missotten, M., Nichols, A., Rieger, K., and Sadoul, R. (1999). Alix, a novel mouse protein undergoing calcium-dependent interaction with the apoptosis-linked-gene 2 (ALG-2) protein. Cell death and differentiation 6, 124-129.

Missotten MTrioulier, Y., Torch, S., Blot, B., Cristina, N., Chatellard-Causse, C., Verna, J.M., and Sadoul, R. (2004). Alix, a protein regulating endosomal trafficking, is involved in neuronal death. The Journal of biological chemistry 279, 2046-2052.

Morita, E., Sandrin, V., Chung, H.Y., Morham, S.G., Gygi, S.P., Rodesch, C.K., and Sundquist, W.I. (2007). Human ESCRT and ALIX proteins interact with proteins of the midbody and function in cytokinesis. The EMBO journal 26, 4215-4227.

Murrow, L., Malhotra, R., and Debnath, J. (2015). ATG12-ATG3 interacts with Alix to promote basal autophagic flux and late endosome function. Nature cell biology 17, 300-310.

Odorizzi, G. (2006). The multiple personalities of Alix. Journal of cell science 119, 3025-3032.

Odorizzi, G., Katzmann, D.J., Babst, M., Audhya, A., and Emr, S.D. (2003). Bro1 is an endosome-associated protein that functions in the MVB pathway in *Saccharomyces cerevisiae*. *Journal of cell science* 116, 1893-1903.

Olmos, Y., Hodgson, L., Mantell, J., Verkade, P., and Carlton, J.G. (2015). ESCRT-III controls nuclear envelope reformation. *Nature* 522, 236-239.

Olsen, J.C. (1998). Gene transfer vectors derived from equine infectious anemia virus. *Gene therapy* 5, 1481-1487.

Ono, A., and Freed, E.O. (1999). Binding of human immunodeficiency virus type 1 Gag to membrane: role of the matrix amino terminus. *Journal of virology* 73, 4136-4144.

Pan, S., Wang, R., Zhou, X., Corvera, J., Kloc, M., Sifers, R., Gallick, G.E., Lin, S.H., and Kuang, J. (2008). Extracellular Alix regulates integrin-mediated cell adhesions and extracellular matrix assembly. *The EMBO journal* 27, 2077-2090.

Pan, S., Wang, R., Zhou, X., He, G., Koomen, J., Kobayashi, R., Sun, L., Corvera, J., Gallick, G.E., and Kuang, J. (2006). Involvement of the conserved adaptor protein Alix in actin cytoskeleton assembly. *The Journal of biological chemistry* 281, 34640-34650.

Pashkova, N., Gakhar, L., Winistorfer, S.C., Sunshine, A.B., Rich, M., Dunham, M.J., Yu, L., and Piper, R.C. (2013). The yeast Alix homolog Bro1 functions as a ubiquitin receptor for protein sorting into multivesicular endosomes. *Developmental cell* 25, 520-533.

Pires, R., Hartlieb, B., Signor, L., Schoehn, G., Lata, S., Roessle, M., Moriscot, C., Popov, S., Hinz, A., Jamin, M., *et al.* (2009). A crescent-shaped ALIX dimer targets ESCRT-III CHMP4 filaments. *Structure* 17, 843-856.



Raiborg, C., Bache, K.G., Gillooly, D.J., Madhus, I.H., Stang, E., and Stenmark, H. (2002). Hrs sorts ubiquitinated proteins into clathrin-coated microdomains of early endosomes. *Nature cell biology* 4, 394-398.

Raymond, C.K., Howald-Stevenson, I., Vater, C.A., and Stevens, T.H. (1992). Morphological classification of the yeast vacuolar protein sorting mutants: evidence for a prevacuolar compartment in class E vps mutants. *Molecular biology of the cell* 3, 1389-1402.

Robinson, J.S., Klionsky, D.J., Banta, L.M., and Emr, S.D. (1988). Protein sorting in *Saccharomyces cerevisiae*: isolation of mutants defective in the delivery and processing of multiple vacuolar hydrolases. *Molecular and cellular biology* 8, 4936-4948.

Rodahl, L.M., Stuffers, S., Lobert, V.H., and Stenmark, H. (2009). The role of ESCRT proteins in attenuation of cell signalling. *Biochemical Society transactions* 37, 137-142.

Sandrin, V., and Sundquist, W.I. (2013). ESCRT requirements for EIAV budding. *Retrovirology* 10, 104.

Scheffer, L.L., Sreetama, S.C., Sharma, N., Medikayala, S., Brown, K.J., Defour, A., and Jaiswal, J.K. (2014). Mechanism of Ca<sup>2+</sup>(+)-triggered ESCRT assembly and regulation of cell membrane repair. *Nature communications* 5, 5646.

Schiel, J.A., Simon, G.C., Zaharris, C., Weisz, J., Castle, D., Wu, C.C., and Prekeris, R. (2012). FIP3-endosome-dependent formation of the secondary ingression mediates ESCRT-III recruitment during cytokinesis. *Nature cell biology* 14, 1068-1078.

Schmidt, M.H., Chen, B., Randazzo, L.M., and Bogler, O. (2003). SETA/CIN85/Ruk and its binding partner AIP1 associate with diverse cytoskeletal elements, including FAKs, and modulate cell adhesion. *Journal of cell science* 116, 2845-2855.

Schmidt, M.H., Dikic, I., and Bogler, O. (2005). Src phosphorylation of Alix/AIP1 modulates its interaction with binding partners and antagonizes its activities. *The Journal of biological chemistry* 280, 3414-3425.

Schmidt, M.H., Hoeller, D., Yu, J., Furnari, F.B., Cavenee, W.K., Dikic, I., and Bogler, O. (2004). Alix/AIP1 antagonizes epidermal growth factor receptor downregulation by the Cbl-SETA/CIN85 complex. *Molecular and cellular biology* 24, 8981-8993.

Scott, C.C., Vacca, F., and Gruenberg, J. (2014). Endosome maturation, transport and functions. *Seminars in cell & developmental biology* 31, 2-10.

Shibata, H., Yamada, K., Mizuno, T., Yorikawa, C., Takahashi, H., Satoh, H., Kitaura, Y., and Maki, M. (2004). The penta-EF-hand protein ALG-2 interacts with a region containing PxY repeats in Alix/AIP1, which is required for the subcellular punctate distribution of the amino-terminal truncation form of Alix/AIP1. *Journal of biochemistry* 135, 117-128.

Sorkin, A., and Goh, L.K. (2009). Endocytosis and intracellular trafficking of ErbBs. *Experimental cell research* 315, 683-696.

Spearman, P., Horton, R., Ratner, L., and Kuli-Zade, I. (1997). Membrane binding of human immunodeficiency virus type 1 matrix protein in vivo supports a conformational myristyl switch mechanism. *Journal of virology* 71, 6582-6592.

Strack, B., Calistri, A., Craig, S., Popova, E., and Gottlinger, H.G. (2003). AIP1/ALIX is a binding partner for HIV-1 p6 and EIAV p9 functioning in virus budding. *Cell* 114, 689-699.

Sun, S., Sun, L., Zhou, X., Wu, C., Wang, R., Lin, S.H., and Kuang, J. (2016). Phosphorylation-Dependent Activation of the ESCRT Function of ALIX in Cytokinetic Abscission and Retroviral Budding. *Developmental cell* 36, 331-343.

Teis, D., Saksena, S., and Emr, S.D. (2008). Ordered assembly of the ESCRT-III complex on endosomes is required to sequester cargo during MVB formation. *Developmental cell* 15, 578-589.

Vandre, D.D., Davis, F.M., Rao, P.N., and Borisy, G.G. (1986). Distribution of cytoskeletal proteins sharing a conserved phosphorylated epitope. *European journal of cell biology* 41, 72-81.

Vietri, M., Schink, K.O., Campsteijn, C., Wegner, C.S., Schultz, S.W., Christ, L., Thoresen, S.B., Brech, A., Raiborg, C., and Stenmark, H. (2015). Spastin and ESCRT-III coordinate mitotic spindle disassembly and nuclear envelope sealing. *Nature* 522, 231-235.

Vito, P., Lacana, E., and D'Adamio, L. (1996). Interfering with apoptosis: Ca(2+)-binding protein ALG-2 and Alzheimer's disease gene ALG-3. *Science* 271, 521-525.

Vito, P., Pellegrini, L., Guet, C., and D'Adamio, L. (1999). Cloning of AIP1, a novel protein that associates with the apoptosis-linked gene ALG-2 in a Ca<sup>2+</sup>-dependent reaction. *The Journal of biological chemistry* 274, 1533-1540.

von Schwedler, U.K., Stuchell, M., Muller, B., Ward, D.M., Chung, H.Y., Morita, E., Wang, H.E., Davis, T., He, G.P., Cimbara, D.M., *et al.* (2003). The protein network of HIV budding. *Cell* 114, 701-713.

Votteler, J., and Sundquist, W.I. (2013). Virus budding and the ESCRT pathway. *Cell host & microbe* 14, 232-241.

Wegner, C.S., Rodahl, L.M., and Stenmark, H. (2011). ESCRT proteins and cell signalling. *Traffic* 12, 1291-1297.

Wemmer, M., Azmi, I., West, M., Davies, B., Katzmann, D., and Odorizzi, G. (2011). Bro1 binding to Snf7 regulates ESCRT-III membrane scission activity in yeast. *The Journal of cell biology* 192, 295-306.

White, I.J., Bailey, L.M., Aghakhani, M.R., Moss, S.E., and Futter, C.E. (2006). EGF stimulates annexin 1-dependent inward vesiculation in a multivesicular endosome subpopulation. *The EMBO journal* 25, 1-12.

Willard, F.S., and Crouch, M.F. (2001). MEK, ERK, and p90RSK are present on mitotic tubulin in Swiss 3T3 cells: a role for the MAP kinase pathway in regulating mitotic exit. *Cellular signalling* 13, 653-664.

Wu, C.F., Wang, R., Liang, Q., Liang, J., Li, W., Jung, S.Y., Qin, J., Lin, S.H., and Kuang, J. (2010). Dissecting the M phase-specific phosphorylation of serine-proline or threonine-proline motifs. *Molecular biology of the cell* 21, 1470-1481.

Xu, T.R., Lu, R.F., Romano, D., Pitt, A., Houslay, M.D., Milligan, G., and Kolch, W. (2012). Eukaryotic translation initiation factor 3, subunit a, regulates the extracellular signal-regulated kinase pathway. *Molecular and cellular biology* 32, 88-95.

Yang, B., Stjepanovic, G., Shen, Q., Martin, A., and Hurley, J.H. (2015). Vps4 disassembles an ESCRT-III filament by global unfolding and processive translocation. *Nature structural & molecular biology* 22, 492-498.

Zhai, Q., Fisher, R.D., Chung, H.Y., Myszka, D.G., Sundquist, W.I., and Hill, C.P. (2008). Structural and functional studies of ALIX interactions with YPX(n)L late domains of HIV-1 and EIAV. *Nature structural & molecular biology* 15, 43-49.

Zhou, X., Pan, S., Sun, L., Corvera, J., Lee, Y.C., Lin, S.H., and Kuang, J. (2009). The CHMP4b- and Src-docking sites in the Bro1 domain are autoinhibited in the native state of Alix. *The Biochemical journal* 418, 277-284.

Zhou, X., Pan, S., Sun, L., Corvera, J., Lin, S.H., and Kuang, J. (2008). The HIV-1 p6/EIAV p9 docking site in Alix is autoinhibited as revealed by a conformation-sensitive anti-Alix monoclonal antibody. *The Biochemical journal* 414, 215-220.

Zhou, X., Si, J., Corvera, J., Gallick, G.E., and Kuang, J. (2010). Decoding the intrinsic mechanism that prohibits ALIX interaction with ESCRT and viral proteins. *The Biochemical journal* 432, 525-534.

## **Vita**

Sheng Sun was born in the City of Anqing, Anhui Province in China on July 17, 1985, the son of Jing Sun and Jin Zhou. After completing his work at No.6 High School, Hefei, Anhui Province, China in 2003, he entered Anhui Normal University in Wuhu, Anhui Province, China. He received the degree of Bachelor of Sciences with a major in Biology from Anhui Normal University in June, 2007. For the next three years, he studied as graduate student at Beijing Normal University in Beijing, China. He received the degree of Master of Sciences in June, 2010. In September of 2010, he entered The University of Texas Graduate School of Biomedical Sciences at Houston.

Permanent address:

157 Wangjiang West Road

Hefei, Anhui, China, 230001